Functional Studies of the *Arabidopsis thaliana* Ubc13-Uev Complex

A Thesis Submitted to the College of

Graduate Studies and Research

In Partial Fulfillment of the Requirements

For the Degree of Doctor of Philosophy

In the Department of Microbiology and Immunology

University of Saskatchewan

Saskatoon

By

Rui Wen

Canadä

PERMISSION TO USE

ABSTRACT

Ubiquitination is an important biochemical reaction found in all eukaryotic organisms and is involved in a wide range of cellular processes. Conventional ubiquitination requires the formation of polyubiquitin chains linked through Lys48 of the ubiquitin, which targets proteins for degradation, while the noncanonical Lys63-linked polyubiquitination of the proliferating cell nuclear antigen is required for error-free DNA damage tolerance (DDT or postreplication repair) in yeast. The ubiquitin-conjugating enzyme Ubc13 and a cognate Ubc enzyme variant (Uev or Mms2) are involved in this process. Because there is less information available on either Lys63-linked ubiquitination or error-free DDT in plants, the goal of my research was to study the functions of Ubc13 and Uev in plants using *Arabidopsis thaliana* as the model organism.

Four *UEV1* genes from *Arabidopsis thaliana* were isolated and characterized. All four Uev1 proteins can form a stable complex with AtUbc13 and can promote Ubc13 mediated Lys63 polyubiquitination. All four *UEV1* genes can replace yeast *MMS2* in DDT function *in vivo*. Although these genes are ubiquitously expressed in most tissues, *UEV1D* appears to be expressed at a much higher level in germinating seeds and pollen. We obtained and characterized two *uev1d* null mutant T-DNA insertion lines. Compared with wild-type plants, seeds from *uev1d* null plants germinated poorly when treated with a DNA-damaging agent. Seeds that germinated grew slow and the majority ceased growth within 2 weeks. Pollen from *uev1d* plants also displayed a moderate but significant decrease in germination in the presence of DNA damage agent. These results indicate that Ubc13-Uev complex functions in DNA damage response in *Arabidopsis thaliana*.

Arabidopsis thaliana contains two *UBC13* genes, *AtUBC13A* and *AtUBC13B*, that are highly conserved with respect to DNA sequence, protein sequence and genomic organization, suggesting that they are derived from a recent gene duplication event. Both AtUbc13 proteins are able to physically interact with human and yeast Mms2, implying that plants also employ a Lys63-linked polyubiquitination reaction. Furthermore, Both *AtUBC13* genes were able to functionally complement the yeast *ubc13* null mutants, suggesting the existence of an error-free DNA damage tolerance pathway in plants. The *AtUBC13* genes appear to be expressed ubiquitously and were not induced by various conditions tested.

The *ubc13a/b* double mutant lines were created and displayed strong phenotypic changes. The double mutant plants were delayed in seed germination as well as cotyledon and true leaf development. When seedlings were grown vertically on plates, the roots of the double mutant were shorter and grew in a zig-zag manner, compared to the straight growth of wild type roots. Root length and number of lateral roots on wild type and *ubc13a* and *ubc13b* single mutant plants were about 3 times longer than those of double mutant plants after 9 and 12 days of growth. When double mutant seeds were sown directly into soil, many did not germinate and those that germinated grew much slower than wild type. At 35 days, double mutant plants were smaller with thinner, flatter, and lighter coloured rosette leaves compared to wild type plants. These phenotypes indicate that AtUbc13 not only plays a role in DDT to protect genome integrity but also is involved in plant development. Hence, this study set a cornerstone for future investigations into the roles of Ubc13 and Uev1 in plant development.

ACKNOWLEDGEMENTS

My special thanks would go to my beloved family: my husband Jinghe Wang and my son Zheng Wang, for their loving considerations, constant help, and great patience during my studies.

TABLE OF CONTENTS

CHAPTER THREE– *ARABIDOPSIS THALIANA UEV1D* PROMOTES LYS63 – LINKED POLYUBIQUITINATION AND IS INVOVLED IN DNA DAMAGE RESPONSE

CHAPTER FOUR– ISOLATION AND FUNCTION CHARACTERIZATION OF
***ARABIDOPSIS THALIANA UBC13* GENES**

CHAPTER FIVE – CONCLUSIONS AND FUTURE DIRECTIONS

LIST OF TABLES

LIST OF FIGURES

LIST OF ABBREVIATIONS

At	*Arabidopsis thaliana*
3-AT	3-aminotriazole
a.a.	amino acids
AD	activation domain
Ade	adenine
amp	ampicillin
ATP	Adenosine 5'-Triphosphate
BD	binding domain
BLAST	basic local alignment search tool
bp	base pair
Da	Dalton
dd	double-distilled
DDT	DNA damage tolerance
DMSO	dimethyl sulfoxide
E	glutamate
E1	ubiquitin activating enzyme
E2	ubiquitin conjugating enzyme
E3	ubiquitin ligating enzyme
EDTA	Ethylenediaminetetraacetic acid
F	phenylalanine
Gln	glutamine
Glu	glutamate
Gly	glycine
GST	Gluthathione-S-Transferase
HRP	Horseradish Peroxidase
HECT	homology to the E6-AP carboxyl terminus
His	histidine
I	isoleucine

Ile	isoleucine
IκB	Inhibitor of κB protein kinase
IKK	IκB kinase
IPTG	isopropyl-β-D-thiogalactopyranoside
K	lysine
LB	Luria broth
Leu	leucine
MMS	methylmethane sulfonate
MW	Molecular Weight
nt	nucleotide
NEMO	NF-κB Essential Modulator
NF-κB	Nuclear factor kappa B
OD	optical density
ORF	Open Reading Frame
PBS	Phosphate Buffered Saline
PRR	postreplication repair
PEG	Polyethylene Glycol
PCNA	Proliferating Cell Nuclear Antigen
PCR	Polymerase Chain Reaction
PVDF	Polyvinylidene Difluoride
RING	really interesting new gene
RT	Room Temperature
SD	synthetic dextrose
SDS-PAGE	sodium dodecyl sulfate-polyacrylamide gel electrophoresis
ss	single strand
TLS	translesion synthesis
UV	ultraviolet
Wt	wild-type
y	yeast (budding)
YPD	yeast extract-peptone-dextrose

TNFα	Tumour necrosis factor alpha
TNFR	Tumor necrosis factor receptor
TRAF2	Tumor necrosis factor receptor-associated factor 2
TRAF6	Tumor necrosis factor receptor-associated factor 6
Ub	Ubiquitin
Ubc	Ubiquitin-conjugating enzyme
Uev	Ubiquitin-conjugating enzyme variants

CHAPTER ONE – INTRODUCTION

1.1 Ubiquitin and ubiquitination

Ubiquitin (Ub) is a small protein consisting of 76 amino acids (a.a.) and a molecular mass of about 8.5 kilodalton (kDa) (Figure 1-1). It is ubiquitously expressed in eukaryotic cells and highly conserved from yeast to human. Sequence alignment reveals only three amino acid differences between yeast and human and two amino acid differences between yeast and the plant *Arabidopsis thaliana*. The 76 amino acid Ub polypeptide is critical for many cellular processes such as stress response, cell cycle progression, oncogenesis and antigen presentation (Hofmann and Pickart, 1999). Ub has two key features. One is that the carboxyl group of the last C-terminal glycine residue (Gly76) can form an isopeptide bond with a substrate lysine residue. Another is that seven lysine residues in Ub, i.e. Lys6, Lys11, Lys27, Lys29, Lys33, Lys48 and Lys63 can be potentially used to form distinct types of poly-Ub chains, at least five of which have been observed *in vitro* or *in vivo* (Volk, Wang et al. 2005).

Ubiquitin is encoded by a multigene family which includes monomeric and multimeric Ub genes. The former is that the ubiquitin gene is fused to a ribosomal protein gene giving rise to a translation product of Ub-ribosomal fusion protein (Callis et al, 1995). The latter encodes several repeats of Ub moieties within a protein (or polypeptide) (Ozkaynak et al., 1987). Ub can exist as a free cellular monomer or covalently attach to other

proteins. Ub proteins are generated either from newly-synthesized polyproteins by proteolysis or by recycling Ub molecules linked to other proteins (Kalderon, 1996).
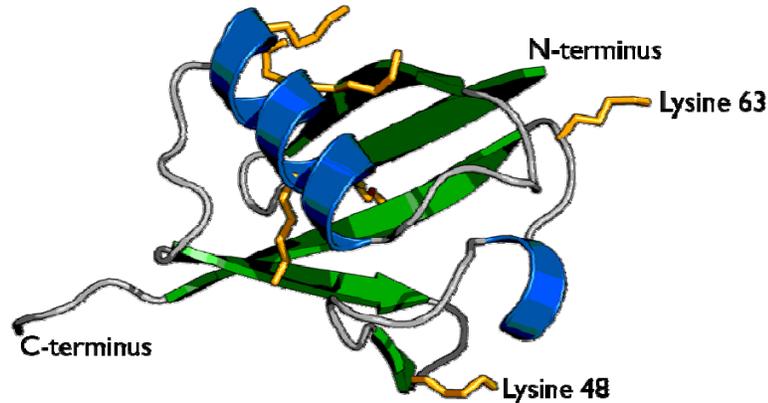
Figure 1-1 The structure of ubiquitin protein**.** Alpha-helices are coloured in blue and β-strands in green. The orange sticks indicate seven lysine residues. The two best-characterized lysine residues lysine 48 and 63 in polyubiquitin chain formation are marked. The image was taken from http://en.wikipedia.org/wiki/Ubiquitin.

Ubiquitination, the attachment of Ub to a protein, is an essential process found in all eukaryotic cells from unicellular yeast to human. Ub conjugated in the target protein can alter the protein stability, localization or activity (Dorval and Fraser 2007). Ubiquitination is involved in many cellular processes including ribosomal biogenesis (Finley, Bartel et al. 1989), cell cycle progression (Harper 2002), apoptosis (Zhang, Wang et al. 2004), mitochondrial inheritance (Fisk and Yaffe 1999), transcriptional regulation

(Kao, Chen et al. 2004) and DNA repair (Jentsch, McGrath et al. 1987; Pastushok and Xiao 2004). Ubiquitination requires the formation of an isopeptide bond between the C-terminal Gly76 on a Ub and a Lys residue on the target protein via a series of steps (Jentsch 1992; Hochstrasser 1996). In this process, Ub is first activated by a Ub-activating enzyme (Uba or E1) in the presence of ATP, forming a high-energy E1-Ub thiolester bond. The activated Ub is then transferred from E1 to a specific thiol group of a Ub-conjugating enzyme (Ubc or E2) to form an E2-Ub thiolester. The Ub of E2-Ub is further donated to the target protein either alone or in conjunction with a Ub ligase (E3). Substrate specificity of ubiquitination is mainly determined by the interaction of E2 and E3. Formation of poly-Ub chains is thought to be essential for targeting the Ub-tagged protein to the 26S proteasome (Eytan, Ganoth et al. 1989).

Most organisms have only one E1 enzyme and deletion of E1 in yeast is lethal (McGrath, Jentsch et al. 1991). In human E1 has two isoforms resulting from alternative translation initiation sites (Cook and Chock 1992; Handley-Gearhart, Stephen et al. 1994). However, there are multiple E2s and even more E3s in all organisms. All the known E2s belong to a single family and share a conserved catalytic core domain of 150 amino acids which possess the active site cysteine residue for forming a thiolester bond with Ub (Pickart 2001). Eleven different E2s in yeast, fifty in human and thirty-eight in *Arabidopsis thaliana* were identified. Individual E2s can interact with different E3s, and a single E3 might interact with more than one E2. The diversity of relationship between E2s and E3s may increase the opportunity for the target protein to be recognized by the ubiquitination system. E3s are important for substrate recognition and therefore, there are diverse classes of E3s that differ in size and functional domains. All known E3s belong to

two main subfamilies, namely the HECT (homologous to the E6-AP carboxyl terminus) domain and RING (really interesting new gene) domain families (Pickart 2001). For HECT E3s, Ub is transferred from E2 to a highly conserved cysteine residue in the HECT domain, and then the Ub is conjugated to a lysine of the substrate bound to an E3. E3s of the RING domain subfamily do not appear to form the thioester intermediate with Ub. They directly transfer Ub from the E2 to the target protein.

The C-terminal domain of HECT E3s, about 150 amino acid long, contains the conserved cysteine residue that is the Ub receptor and N-terminal domain-of the HECT E3s that is substrate recognition (Scheffner, Huibregtse et al. 1993). The RING finger domain is about 50 amino acids long and characterized by a conserved Zn^{+2} chelating His/Cys-rich motif which mediates E3-E2 binding.

A family of proteins called U-box domain is also involved in poly-Ub chain formation. The U-box domain is a modified version of the RING finger motif which lacks the important Zn^{+2} chelating residue (Hatakeyama and Nakayama 2003). The best characterized U-box domain protein is yeast Ub fusion degradation protein 2 (Ufd2) and C-terminus of the Hsc70 interacting protein (Chip). These E3 proteins play a role in Ub chain elongation (Kuhlbrodt, Mouysset et al. 2005).

1.2 Multiple functions of ubiquitin and ubiquitin chains

Ubiquitination is an ATP dependent reversible process in which a Ub molecule or a chain of Ub molecules is attached to a substrate protein. Ubiquitination can be divided into three types: mono-ubiquitination, multiple mono-ubiquitination, and poly-ubiquitination. The attachment of a single Ub to a substrate is called mono-ubiquitination (Hicke 2001). When two or more lysine residues in a substrate are appended with single Ub molecules, it is called multiple mono-ubiquitination (Haglund, Sigismund et al. 2003; Mosesson, Shtiegman et al. 2003), while poly-ubiquitination means that a substrate is attached to a chain of Ub, formed by a repeat process (Pickart 2001). Ubiquitin has seven lysine residues. In theory, each residue can be potentially poly-ubiquitinated to form poly-ubiquitin chain. Indeed, all seven ubiquitin–ubiquitin linkages have been observed in budding yeast (Peng, Schwartz et al. 2003).

Different Ub modifications can play different roles in the regulation of cellular processes (Weissman 2001). Histone H2B mono-ubiquitination regulates chromatin structure and transcription leading to methylations on another core histone H3 (Briggs, Xiao et al. 2002). Membrane receptor mono-ubiquitination promotes receptor endocytosis and degradation in vacuole of yeast (Bonifacino and Traub 2003). In addition, protein mono-ubiquitination is also involved in endocytosis of plasma membrane proteins, sorting of proteins to multivesicular bodies (MVB), DNA repair, histone activity, and transcriptional regulation (Gupta-Rossi et al., 2004). Recently, it has been shown that the epidermal growth factor receptor (EGFR) and platelet-derived growth factor receptor (PDGFR) are modified by Casitas b-lineage lymphoma (Cbl)-mediated mono-ubiquitination at several sites (multi-ubiquitinated), this multiple mono-ubiquitination

appears to be necessary and sufficient for endocytosis and degradation of the receptors (Bakowska, Jupille et al. 2007). Similarly, different poly-Ub chains can have different functions. Polyubiquitin chains formed via the C-terminal glycine and Lys48 of ubiquitins play a role in targeting proteins for degradation by the 26S proteasom. Lys6-linked polyubiquitin chain on E3 enzyme Brca1 is implicated in nuclear focus formation during DNA repair (Morris and Solomon 2004). Lys27 linked polyubiquitin chain is involved in protein kinase activation and lysosomal localization of ubiquitinated Jun (Ikeda and Kerppola, 2008; Okumura et al., 2004), Lys11-linked chains have been implicated in proteasomal targeting and protein turnover (Johnson, Ma et al. 1995; Baboshina and Haas 1996); and Lys63-linked chains are involved in DNA repair and NF-κB activation (Zhang, Johnston et al. 2001).

It is unclear how the ubiquitination machinery decides if the substrate should be mono-ubiquitinated or poly-ubiquitinated. There are several possible explanations. Firstly, E3 ubiquitin ligase has specificities in terms of the type of ubiquitination. For example, the E3 Rad18 mediates PCNA mono-ubiquitinaton at the Lys164 residue, whereas the E3 Rad5 promotes PCNA poly-ubiquitination at the same site (Hoege, Pfander et al. 2002). As another example, p53 is mono-ubquitinated by the E3 Mdms2 and poly-ubiquitinated by p300 (Grossman, Deato et al. 2003). Secondly, Ub-binding proteins may specify the type of Ub modifications. For instance, Ub-interacting motif (UIM) and the Cue1-homologous (CUE) domain in the endocytic proteins control their mono-ubiquitination (Di Fiore, Polo et al. 2003). Thirdly, Ub conjugationg enzymes may play a role in deciding if a substrate should be monoubiquitinated or polyubiquitinated. Up to now, Ubc13 is the only known E2 enzyme capable of catalyzing Lys63-linked

polyubiquitin chains, which is believed to play an important role in cell signalling. Other

E2 enzymes such as Ubc4 and Ubc5 in yeast and Ubc8, Ubc9 and Ubc10 in *Arabidopsis*

thaliana function in Lys48-linked poly-ubiquitination for protein degradation (Kraft,

Stone et al. 2005). In addition, ubiquitination is a dynamic and reversible process, and

de-ubiquitinating enzymes mediate rapid removal of ubiquitin from substrates (Wilkinson

2000). It is possible that a balance between activity and subcellular localization of de-

ubiquitinating enzymes and Ub ligases determines whether a specific protein becomes

mono- or poly-ubiquitinated (Haglund, Di Fiore et al. 2003). Various ubiquitin

modifications and their function are shown in Figure 1-2.
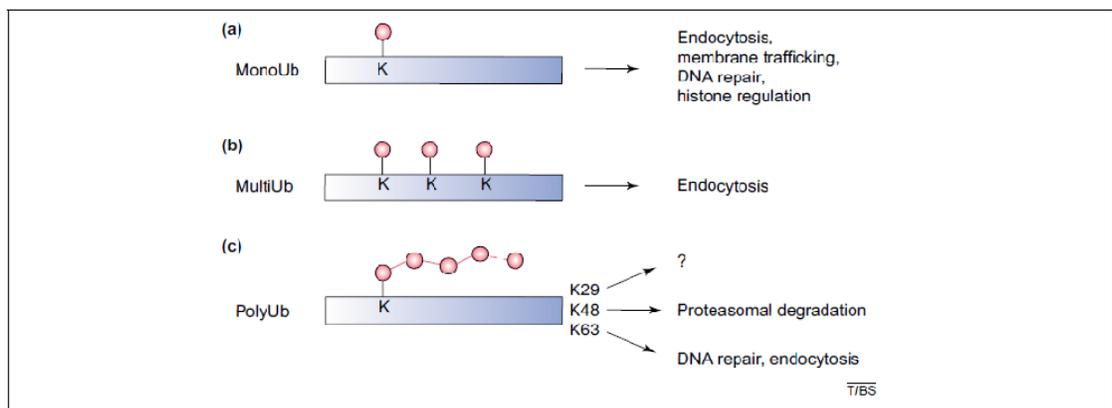
Figure 1-2 Various ubiquitin modifications and their functions. (a) Monoubiquitination

(b) Multiubiquitination (MultiUb), (c) Polyubiquitination (PolyUb). Pink circle: ubiquitin;

K: lysine residue (Dikic 2003).

1.3   Functions of Lys48-linked polyubiquitination in plants

It is well known that polyubiquitin chains with different linkages transmit distinct structural and functional information. A well accepted concept in the field of ubiquitination is that ubiquitin chains were linked by Lys48 to target proteins for degradation. Protein degradation through ubiquitination was discovered by Aaron Ciechanover, Avram Hershko, and Irwin Rose who were awarded the Nobel Prize in chemistry in 2004 (Li and Ye 2008). Since this discovery, remarkable advances have been made on the mechanisms for protein turnover. Nowadays, it is known that protein degradation mediated by Lys48-linked polyubiquitination plays a pivotal role in almost every cellular process. For example, proteins with synthetic errors and free-radical-induced damage must be removed (Hershko and Ciechanover 1998). Almost 30% of initial translation products are non-functional and need rapid degradation (Schubert, Anton et al. 2000). In addition, protein degradation through Lys48 polyubiquitination also functions in responses to hormones (Hellmann and Estelle 2002; Vierstra 2003), abiotic and biotic stresses (Schrammeijer, Risseeuw et al. 2001; Hardtke, Okamoto et al. 2002) and in plant development (Zhao, Yu et al. 2001). Below, I will focus on some of the functions mediated by Lys48 poly-Ub in plants.

1.3.1 Preventing self-pollination in plants

Most flowering plants produce perfect flowers containing both male and female reproductive organs, therefore self pollination will occur (Kao and Tsukamoto 2004). Because self pollination leads to a gradual decline in genetic diversity, plants have

evolved reproductive strategies, called self-incompatibility by which plants prevent self-pollination and promote outcrossing (Gaudeul and Till-Bottraud 2004). Plants use the Lys48 poly-Ub chain mediated protein degradation pathway to reject self pollen and promote cross fertilization. It has been shown that in plant *Antirrhinum majus*, one protein encoded by a self-incompatibility gene interacts with another protein, a S-RNases that would be polyubiquitinated through the Lys48 poly-Ub chain and degradated by the 26S proteasome in compatible pollination rather than incompatible pollination. Growth of pollen from the same plant is inhibited in this self-incompatible response in *Antirrhinum majus* (Qiao, Wang et al. 2004).

1.3.2 Regulation of the cell cycle

A typical eukaryotic cell cycle consists of five distinct phases: G0, G1, S, G2, and M. In the S phase, DNA replication occurs, while in the M phase, mitosis occurs and one cell divides into two daughter cells (Bicknell and Brooks 2008). Transitions from one cell cycle phase to the next are tightly regulated by a set of protein kinases called cyclin-dependent kinases (CDKs). The activity of CDKs in turn is regulated positively by cyclins and negatively by CDK inihibitors, as well as other factors (Hochegger, Takeda et al. 2008). Cyclins and CDK inhibitors are ubiquitinated through the Lys48 poly-Ub chain and degraded by protesomes to ensure the unidirectional and irreversible progression of the cell cycle (Santopietro, Shabalova et al. 2006). Two ubiquitin E3 ligases important for the cell cycle are SCF whose name comes from three central components (Skip1, Culin, and F-box) of the E3 enzyme complex and APC (Anaphase Promoting Complex). In general, the SCF complex mediates G1/S transition SCF-Skp2

mainly ubiquitinates and degrades cyclin-dependent-kinase inhibitors (CKIs) such as p27 and p21 as well as G1/S cyclin and CyclinE to promote cell cycle progression and cell growth (Nakayama and Nakayama 2005). APC controls metaphase-anaphase transition with the activator Cdc 20 to boost sister chromatid separation. APC with another activator, Cdh1, is also active in the G1 phase and controls levels of mitosis regulating proteins (Vodermaier 2004). In addition, many other important cell cycle regulators, such as Cyclin B or Plk1, are degraded through Lys48 poly-Ub chain mediated protein degradation pathway (Stegmeier, Sowa et al. 2007)

1.3.3 Involvement in auxin-mediated lateral root formation

Lys48 poly-Ub chain mediated protein degradation also plays an important role in auxin-mediated lateral root formation. The first piece of evidence for the involvement of protein ubiquitination came from the studies of *Arabidopsis thaliana* E3, SCF^{TIR1} protein complex. TRANSPORT INHIBITOR RESPONSE 1 (TIR1) is a key component of SCF and encodes a protein containing leucine-rich repeats and an F-box motif. Auxin signals captured by *TIR1* promote degradation of the Aux/IAA (Auxin/Indole-3-Acetic Acid) proteins, the repressors of auxin-responsive transcription, through Lys48 poly-Ub chain mediated protesome pathway (Gray, Kepinski et al. 2001; Dharmasiri and Estelle 2004). The Aux/IAA degradation allows ARF (Auxin Response Factor) proteins to bind to the promoters of the many auxin responsive genes, activating transcription of these target genes leading to lateral root development (Guilfoyle, Hagen et al. 1998; Tiwari, Hagen et al. 2003).

1.4 Functions of Lys63-linked polyubiquitination

The most common type of polyubiquitin chain link is to link through Lys48 of Ub. Lys48-linked polyubiquitination is known to target specific proteins for degradation and functions in cell division, hormone responses, and responses to the abiotic/biotic environments. In contrast, polyubiquitin chains linked through the Lys63 of Ub is believed to play signalling roles. So far, Ubc13 is the only known Ub conjugating enzyme capable of catalyzing Lys63-linked polyubiquitination reaction and this function requires an interaction with a Ubc variant Mms2 or Uev1 (Hofmann and Pickart 1999). Ubc13-Uev1 (or Ubc13-Mms2) mediated Lys63 poly-Ub chains have been found to be important for error-free DNA damage tolerance (Hofmann and Pickart 1999) and nuclear factor kappa-light-chain-enhancer of activated B cells (NF-κB) (Deng et al., 2000) pathways. Since little is known about the Ubc13-mediated pathway in plants, the following results from yeast and mammalian systems will be reviewed.

1.4.1 Role of Ubc13-Mms2 mediated Lys63 poly-Ubiquitination in DNA repair

The *RAD6* pathway is central to DNA postreplication repair (PRR) in yeast and mammalian cells (Saffran, Ahmed et al. 2004). Two Ubcs, Rad6 and the heteromeric Ubc13-Mms2 complex, have been implicated in PRR in yeast (Broomfield, Chow et al. 1998; Xiao, Chow et al. 2000). Mms2 is a Uev initially discovered in yeast (Broomfield, Chow et al. 1998). Two RING-finger type E3s, Rad18 and Rad5, play a central role in mediating physical contacts between the members of the *RAD6* pathway. Rad5 recruits the Ubc13–Mms2 complex to DNA through its RING finger domain. Moreover, Rad5 associated with Rad18 brings Ubc13-Mms2 into contact with the Rad6–Rad18 complex

(Ulrich and Jentsch 2000). Interaction between the two RING-finger proteins thus promotes the formation of a heteromeric complex in which the two E2 enzymes, Rad6 and Ubc13–Mms2, can be closely coordinated to enhance the Lys63 poly-Ub chain formation. Interestingly, Ubc13 and Mms2 are largely cytosolic proteins, and DNA damage triggers their redistribution to the nucleus (Ulrich and Jentsch 2000).

The *RAD6* pathway has been divided into three sub-pathways: one error-prone sub-pathway represented by *REV3* and two error-free sub-pathways represented by *RAD5* and *POL30* (Xiao, Chow et al. 2000). The two independent error-free PRR pathways are both under the control of *RAD6/RAD18* (Xiao, Chow et al. 2000). Ubc13-Mms2 promotes one (Ulrich and Jentsch 2000) or both (Xiao, Chow et al. 2000) of the error-free pathways.

In the *RAD6* pathway, PCNA (proliferating cell nuclear antigen) is a component of PRR. A critical residue Lys164 in PCNA can be modified in three ways: monoubiquitination by the E2 and E3 enzyme of Rad6 and Rad18, Lys63-linked polyubiquitination by Ubc13-Mms2 in complex with Rad5, and conjugation of SUMO (small ubiquitin-related modifier) by Ubc9 (Hoege, Pfander et al. 2002). It has been demonstrated that these modifications have different implications in DNA damage tolerance and repair. The same lysine residue can also be modified by E2 Ubc9 and E3 Siz1 through conjugation of SUMO (S) (small ubiquitin-related modifier), which functions antagonistically with Ubc13-mediated polyliuquitination since ubiquitination and sumolation compete for the same residue. The roles of Ubc13-Uev mediated Lys63 poly-Ub chain in DNA repair are shown in Figure 1-3.
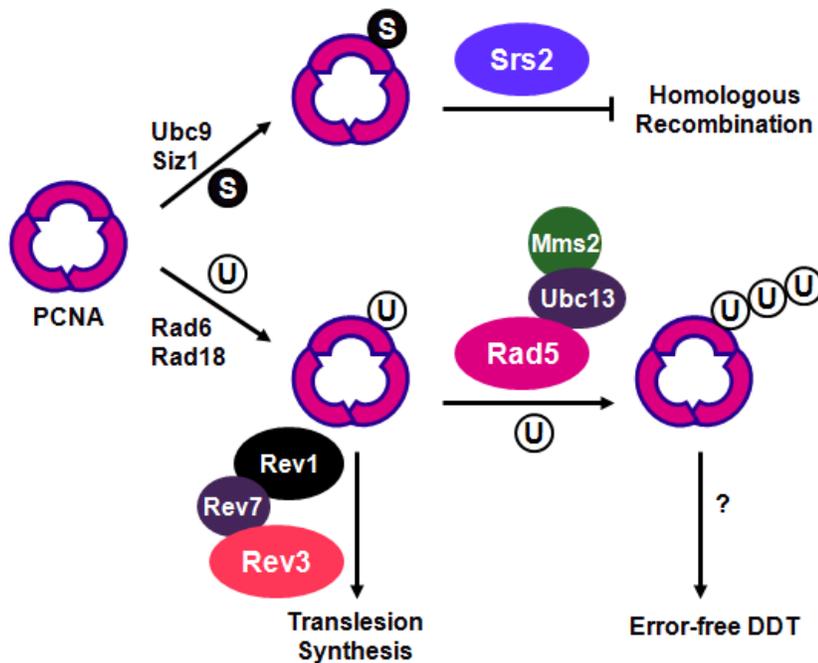
Figure 1-3 The roles of yeast Ubc13-Uev mediated Lys63 poly-Ub chain in PRR. The Lys164 residue of PCNA is firstly mono-ubiquitinated by Rad6 and Rad18, and further poly-ubquitinated by Ubc13-Mms2 complex with Rad5. The poly-ubiquitinated PCNA then functions in the error-free post replication DNA repair pathway (Pickart 2002). The same lysine residue of PCNA can also be modified through conjugation of SUMO (S) (small ubiquitin-related modifier), SUMO-modified PCNA recruits Srs2 to prevent recombination.

1.4.2 Role of Ubc13-Mms2 mediated Lys63-linked polyubiquitination in the NF-κB pathway

In mammals, the transcription factor Nuclear Factor kappa-lighter-chain-enhancer of activated B cells (NF-κB) consists of homo- or hetero-dimers of different subunits which are members of a family related protein called Rel/NF-kB proteins. Five different Rel/NF-κB proteins (also called Rel proteins) p50, p52, p65, RelB, and c-Rel have been identified, and they all contain a conserved N-terminal region called the Rel Homology Domain (RHD). The RHD contains the DNA-binding and dimerization domains as well as the nuclear localization signal (Muller and Harrison, 1995; Sullivan et al., 2007).

The NF-κB family of transcription factors is involved in a number of processes, mainly stress-induced immunity, cell cycle progression, inflammatory response, oncogenesis, viral replication, and various autoimmune diseases (Zhang, Johnston et al. 2001).

In normal cells, NF-κB proteins in the form of dimers are sequestered in the cytosol via non-covalent interactions with a class of inhibitor proteins, called IκBs. Various stimuli that activate NF-κB cause phosphorylation of IκBs, which is followed by ubiquitination of the IκBs and subsequent degradation through the ubiquitin–proteasome pathway (Wegener and Krappmann 2008) (Figure 1-4). IκB proteins are phosphorylated by an IκB kinase (IKK) complex consisting of IKKα, IKKß, and IKKγ/NEMO (NF-κB essential modulator). NEMO is not a kinase, but considered as a regulatory subunit of IKK essential for NF-κB activation. The phosphorylation of IκB by IKK and the degradation of IκB result in the exposure of the nuclear localization

14
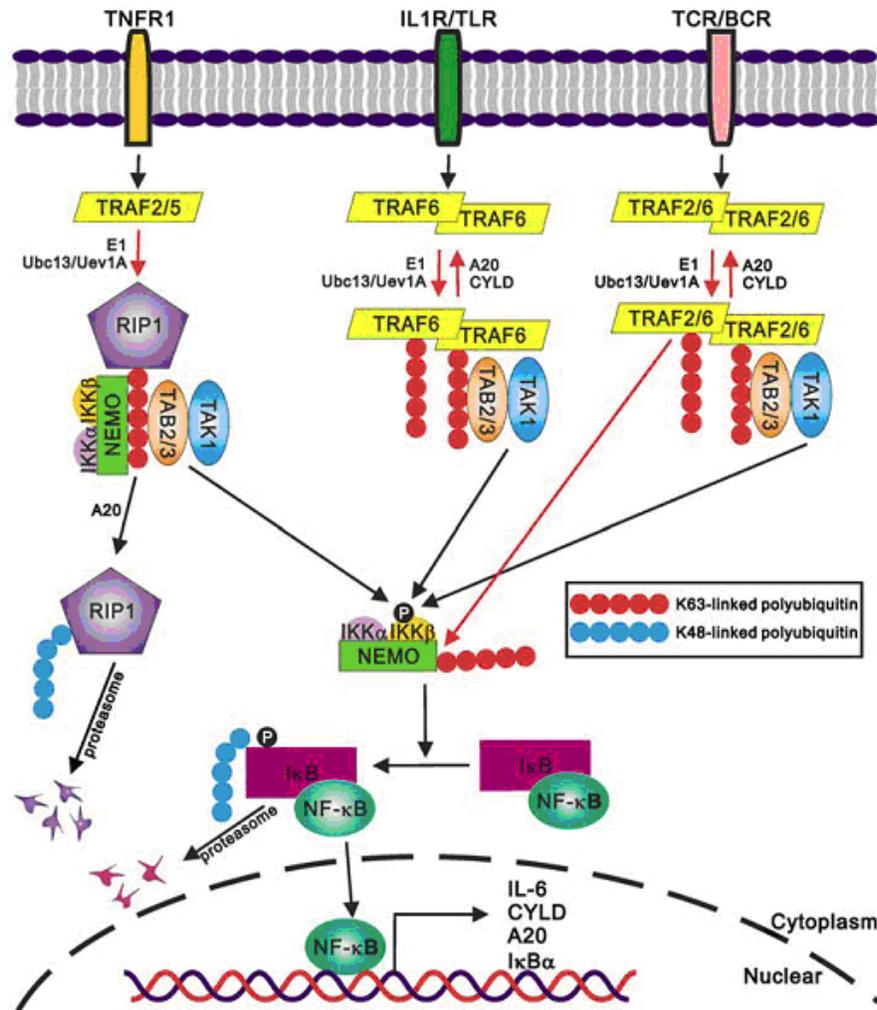
Figure 1-4 The Ubc13-Uev1A mediated Lys63-linked polyubiquitination promotes activation of the NF-κB transcription factor (Adhikari, Xu et al. 2007). Ubc 13 and Uev1A complex together with TRAF 2/5 or TRAF6 catalyzes the formation of a Lys63-linked polyubiquitin chain on substrate NEMO which leads to phosphorylation and degradation of IκBs, then freed NF-κB subunits enter to the nucleus and activate the transcription of the corresponding genes.

signals (NLS) on the NF-κB subunits and the subsequent translocation of NF-κB to the nucleus. In the nucleus, NF-κB binds with a consensus sequence (5'-GGGACTTTCC-3') in various promoters, activating the transcription of corresponding genes.

TRAF6 (Tumor-necrosis factor (TNF)-receptor associated factor 6) is a signal transducer that activates IKK and the Jun amino-terminal kinase (JNK). TRAF6 is a RING-finger protein and physically interacts with Ubc13 through its RING-finger domain (Wooff, Pastushok et al. 2004). This Ubc 13 and Uev1A complex together with TRAF6 catalyzes the formation of a Lys63-linked polyubiquitin chain that mediates IKK activation through a unique proteasome-independent mechanism (Deng, Wang et al. 2000; Wang, Deng et al. 2001). Subsequently, it was reported that NF-κB activation by TRAF2, another RING-finger protein, also requires Ubc13-Uev for Lys63-linked poly-Ub (Shi and Kehrl 2003). It appears that the cellular target of the above Lys63 poly-Ub is NEMO in T- and B-cells and possibly in other cells as well (Zhou, Wertz et al. 2004).

1.5 The structure of Lys48 and Lys63-linked polyubiquitin chain

Lys48-linked polyubiquitin mainly functions in protein degradation by the 26S proteasome. In contrast, Lys63-linked polyubiquitin is involved in a variety of cellular events that are independent of degradative signalling (Weissman 2001). Obviously the linkage-specificity of polyubiquitin chains is crucial for different cellular functions. Why do Lys63-linked and Lys48-linked polyubiquitin chains have very different functions?

Structural and modeling analyses reveal that these two polyubiquitin chains have very different conformations, which are probably responsible for their distinct functions. The crystal structure of Lys48-linked di- and tetra-ubiquitin shows that there is a hydrophobic patch, which is composed of Leu8, Ile44, and Val70 in each ubiquitin molecule at the interface between two subunits (Cook, Jeffrey et al. 1992). Studies with NMR also indicate that the Lys48-linked diubiquitin forms a closed conformation in which the hydrophobic patch is stacked at the interface at neutral pH, but the conformation is open at lower pH (Varadan, Walker et al. 2002). The topology of the Lys48 poly-Ub chain likes zigzag.

Lys63-linked di- and tetra-ubiquitin chains however lack the covalent hydrophobic interface. The conformation of Lys63-linked chain is likean array of beads on a string (Tenno, Fujiwara et al. 2004). The hydrophobic patch of ubiquitin is not present at the inter subunit interface of Lys63-linked chains and this patch is a major contact surface for the proteasome to contact with ubiquitin (Tenno, Fujiwara et al. 2004). The topology of the poly-Ub chain is shown in Figure 1-5.
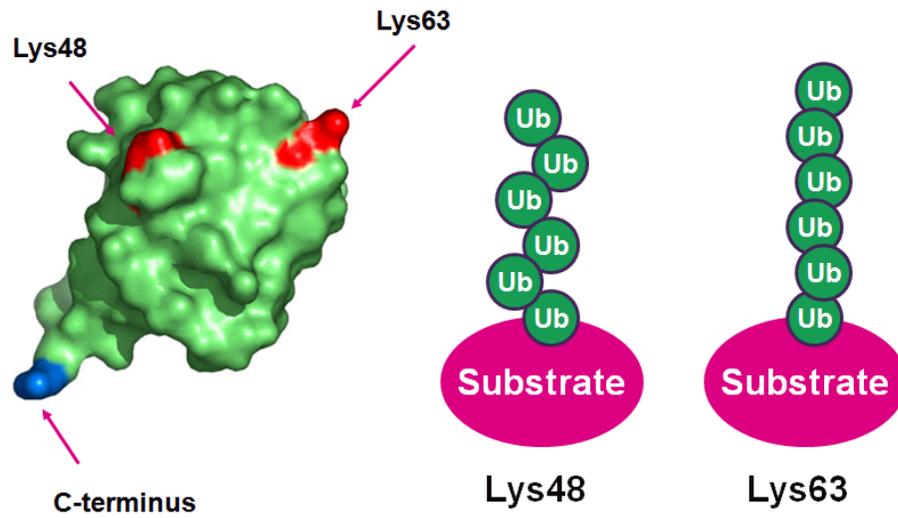
Figure 1-5 Ubiquitin structure and its topology. The sites of Lys48 and Lys63 are shown in red colour, and the c-terminus of ubiquitin shown in blue. The topology of the Lys48 likes zigzag, while Lys63 likes a string.

1.6 DNA damage and repair

Cellular DNA is subject to alterations caused by exogenous environmental factors and the factors inside the cell. The alteration of genetic information encoded in the DNA can lead to cell death or tumorigenesis. To maintain the cellular DNA integrity, DNA repair must be carried out to correct damaged DNA molecules in the genome of an organism.

1.6.1 Sources of DNA damage

The sources of DNA damage can be divided into two main types: endogenous and exogenous. Endogenous DNA damage includes that caused by reactive oxygen species resulting from normal metabolic processes as well as replication errors (Sekiguchi and Tsuzuki 2002). Exogenous DNA damage is caused by external agents including:

Ultraviolet (UV) radiation: UV is an electromagnetic radiation and with a wave length of UVA at 400 nm–315 nm, UVB 320 nm – 280 nm, and UVC 280 nm –100 nm. UV from sun light is the external of DNA damage agent (Wester, Boldemann et al. 1999).

X rays and gamma rays: Both X rays and gamma rays are electromagnetic radiation and their wavelengths are 10 to 0.01 nm and less than 10 picometers, separately (Phillips, Gebow et al. 1997).

Mutagenic chemicals: Mutagenic chemicals thatcan damage DNA and cause mutations include MMS and Cisplatin (Myung and Kolodner 2003).

Viruses: Some viruses can infect all kinds of organisms from plants and animals to bacteria and archaea (Koonin, Senkevich et al. 2006). The infected cells of the organism will die because of cell lysis or suppression of virus-specific proteins (Kim, Liu et al. 2003).

The majority of DNA damage caused by above the external agents affects the primary structure of the double helix. The bases of the double helix are chemically modified by induced non-native chemical bonds or bulky adducts, and these modifications disrupt the DNA regular structure.

1.6.2 Types of DNA damage

DNA is composed of two long polymers of four nucleotides adenine (A), thymine (T), guanine (G) and cytosine (C). The backbone of the DNA molecule is comprised of phosphate and sugar residues joined by ester bonds. The types of DNA damage can be divided into two classes: spontaneous and environmental DNA damage.

Spontaneous DNA damage is caused by endogenous cellular processes such as oxidation of bases by the reactive oxygen species, alkylation of bases caused by methylation, and hydrolysis of bases by deamination and mismatch of bases due to errors in DNA replication. Environmental DNA damage comes in different ways. For example, the main type of DNA damage caused by the UV-B is formation of the cyclobutylpyrimidine dimer (CPD) and the pyrimidine pyrimidone (6-4) dimers. In addition, UV light can also cause base damage and DNA strand breaks (Britt 1996). The DNA damage caused by ionizing radiation (IR) directly induces strand breaks, and 100

Rads of IR can trigger 600-1000 single strand and 16-40 double strand breaks (Ward 1988). DNA alkylating agents covalently bind the nucleophilic sites of DNA such as N7 of Guanine and result in DNA-alkyl adducts. Alkylating reagents can be divided into S_N1 and S_N2 subgroups based on the mechanism of the alkylation attack. The S_N1 reagents quickly transfer the alkyl group to attack the DNA, while the S_N2 alkylating agents react to produce intermediates to attack the DNA. *N*-methyl-*N*-nitrosourea (MNU) and *N*-methyl-*N'*-nitro-*N*-nitrosoguanidine (MNNG) are S_N1 reagents, that use a monomolecular mechanism, while methyl methanesulfonate (MMS) and methyliodide (MeI) are S_N2 reagents using a bimolecular mechanism (Nieminuszczy and Grzesiuk 2007).

1.6.3 DNA repair pathways

To maintain genome integrity, all living organisms have evolved a variety of DNA repair mechanisms to protect cells from DNA damage. Up to now, five major multi-step DNA repair mechanisms are known, i.e. nucleotide base excision repair (NER) and base excision repairs (BER), mismatch repair (MMR), recombination repair and post replication repair (PRR). Some of these are specific for a particular type of damage, while others can handle more than one DNA damage type.

1.6.3.1 Direct reversal of damage

The Direct reversal mechanism is the simplest way to repair special types of DNA damage that do not involve breakage of the DNA backbone. This mechanism does not need any template and often only one single step enzyme catalysed reaction is needed For example, thymidine dimers caused by UV light and methylation of an O^6-guanine base by

alkylating agents are all repaired by the direct reversal mechanism (Friedberg, Aguilera et al. 2006). The photolyase enzyme recognizes and directly binds to the damaged DNA site, absorbs a photon of sun light, separates the pyrimidine dimers and restores them to their monomeric forms. After the damaged site is repaired, the photolyase is dissociated from the substrate. This repair mechanism is found in bacterium, yeast and plants. The strategy used by O^6-alkylguanine-DNA alkyltransferase (AGT or MGMT) to directly repair alkylation damage of O^6-alkylguanine and O^4-alkylthymine is to irreversibly transfer the alkyl groups to nucleophilic Cys residues in the repair protein. A nucleophilic Cys residue is utilized to receive the alkyl lesion in a SN_2 manner and the alkylated protein is degraded after the repair (Goosen and Moolenaar 2008).

1.6.3.2 Base excision repair (BER)

BER removes damaged bases caused by both endogenous and exogenous factors such as oxidative and alkylating agents from the DNA and replaces them with pristine bases. The molecular mechanism of the BER pathway consists of five sequential steps: removing the incorrect base to create an apurinic/apyrimidinic (AP) site, the most common form of DNA damage; nicking the damaged DNA strand upstream of the AP site by AP endonuclease to create a 3'-OH terminus adjacent to the AP site; excising the incised AP site; extending the 3'-OH terminus by a DNA polymerase and ligating.

The initiation of the base excision repair is the recognition and removal of damaged bases by DNA glycosylases. A large number of DNA N-glycosylases such as uracil DNA N-glycosylase (UNG), thymine DNA glycosylase (TDG) and methyl purine DNA glycosylase (MPG) have been identified in human and other organisms. The crystal

structures of different DNA glycosylases have been determined. They are similar to each other, indicating that a common mode of action is employed by a variety of DNA glycosylases. So far, 11 DNA glycosylases are known for human and eight for *Escherichia coli* (Sidorenko and Zharkov 2008). DNA glycosylases remove a variety of damaged bases by cleavage of the N-glycosylic bonds between the bases and the deoxyribose moieties of the nucleotide residues (Krokan, Standal et al. 1997). After glycosylase action, the apurinic/apyrimidinic (AP) site is further processed by an incision step and an excision step. DNA polymerase B independent of PCNA or a DNA polymerase dependent on PCNA can efficiently fill the short gap in DNA (Randahl, Elliott et al. 1988). DNA synthesis and ligation are through two alternative pathways, i.e. short-patch BER (1-nucleotide patch size) and long-patch BER (2-6-nucleotide patch size), which need AP endonuclease to generate a 3'-hydroxyl group (Klungland and Lindahl 1997; Wilson and Thompson 1997; Fortini, Parlanti et al. 1999).

BER is an important pathway for the repair of DNA base damage such as oxidized, alkylated, deaminated or absent bases that causes only minor disturbance to the helical structure of DNA. It differs from the NER which is required for the removal of a large variety of long DNA lesions.

1.6.3.3 Nucleotide excision repair (NER)

NER is one of the DNA repair mechanisms employed by cells to repair the distorted DNA helix damaged by UV light, bulky adducts and DNA intra- and inter-strand crosslink. NER is characterized by the incision of the damaged DNA strand on both sides of the lesion. NER is initiated with the recognition of helical distortion lesions,

followed by the removal of 24-32 oligonucleotides from the DNA strand containing the lesion. The resulting single stranded DNA gap is filled by DNA polymerase and followed by ligation. NER can be divided into two classes: globe genome NER (GG-NER) and transcription coupled NER (TC-NER). Different sets of proteins are involved in the two classes of NER.

GG-NER repairs the damage including both transcribed and untranscribed DNA strands in active and inactive genes throughout the genome. The proteins involved in this pathway are the DNA-damage binding (DDB) and components of XPC-Rad23B complexes. These proteins continuously scan the entire genome to find helix distortions. Once the damaged site is detected, corresponding repair proteins are recruited to the damaged DNA to confirm the presence of DNA damage. Once the damage is verified, incision of the damaged DNA strand will occur on both sides of the lesion and the gap is filled. GG-NERR is a random process that occurs slowly (Balajee and Bohr 2000).

TC-NER repairs lesions occurring in transcriptionally silent and transcriptionally active regions of the genome. However, the repair efficiency is different between these two regions. Studies carried out with mammalian cells demonstrate that the transcriptionally active genes of the transcribed strands are repaired faster by TC-NER than the genes on the nontranscribed strands as well as the genes that are transcriptionally silent (Bohr et al., 1985; Madhani et al., 1986). A similar phenomenon has been demonstrated in *E. coli* (Mellon and Hanawalt 1989) and *S. cerevisiae* (Smerdon and Thoma 1990; Sweder and Hanawalt 1992). TC-NER and GG-NERR are two subpathways of NER which differ only in the initial steps of DNA damage recognition. TC-NER is initiated by RNA polymerase which stalls at a lesion in DNA and the following steps such

as remove the lesion need NER factors XPA, TFIIH and RPA as well as the nucleases ECC1-XPF and XPG for dual incisions at a lesion.

1.6.3.4 DNA mismatch repair (MMR)

MMR repairs the insertions, deletions and mismatched bases that arise during DNA replication and recombination (Iyer, Pluciennik et al. 2006). The major pathway for cells to repair the mismatches is the MutHLS pathway which comes from the work performed on the methyl directed MMR system on *E. coli* (Modrich and Lahue 1996). Proteins including MutS, MutL, MutH, UvrD and Dam (Marinus and Morris 1975; Robson, Hall et al. 1988; Grilley, Welsh et al. 1989) are essential in detecting mismatch repair machinery. MutS forms a dimer (MutS$_2$) which recognizes the mismatched base on the daughter strand and can bind to a variety of mispaired bases and short base-paired loops (Marinus and Morris 1975; Parker and Marinus 1992). MutL also forms a dimer (MutL$_2$) to bind the MutS-DNA complex and act as a mediator to activate MutH. Once activated by the MutS-DNA complex, MutH nicks the daughter strand at the GATC methylation site closest to the mismatch and recruits a UvrD helicase (DNA Helicase II) to separate the two strands with a specific 3' to 5' polarity (Grilley, Holmes et al. 1990). UvrD is a DNA helicase responsible for unwinding DNA in an ATP-dependent manner (Hickson, Arthur et al. 1983). The entire MutSHL complex then slides along the DNA in the direction of the mismatch and MutH, and both the mismatched site and its surrounding nucleotides are excised by the exonuclease ExoVII and RecJ. The resulting single-stranded gap is repaired by DNA polymerase III and sealed by DNA ligase.

Homologs of the bacterial MutS have been identified in eukaryotes. They form two major heterodimers: Msh2/Msh6 (MutSα) and Msh2/Msh3 (MutSβ). The former is involved in base substitution and small loop mismatch repair, and the latter is implicated in both small loop repair and large loop (~10 nucleotides) repair. However, MutSβ does not repair base substitutions (Tian, Gu et al. 2009).

MutL homologs *PMS1* and *MLH* in eukaryotes are involved in post meiotic segregation (Prolla, Pang et al. 1994). In yeast, mutations in either *MLH1* or *PMS1* lead to an increased mutation rate, and the *mlh1 pms1* double mutant showed identical phenotypes as their corresponding single mutants, suggesting that *MLH1* and *PMS1* function in the same MMR pathway (Prolla, Pang et al. 1994). The mutant, yeast *mutS homolog 2* (*MSH2*) gene, showed similar phenotypes to disruption of *PMS1* and *MLH1* (Reenan and Kolodner 1992). Two additional *S. cerevisiae* MMR homologs, *MSH3* and *MSH6*, displayed a weak mutantr phenotype, but strains deleted for both *MSH3* and *MSH6* had a mutation rate similar to that observed in *msh2* strains, indicating that *S. cerevisiae* has different independent mismatch repair pathways. No MutH homologs have been identified in eukaryotes, suggesting that strand discrimination in eukaryotes is different from that of *E. coli* (Kolodner and Marsischky 1999).

Except for the above proteins, there are some additional factors with a possible function in eukaryotic MMR. For example, PCNA, EXO1 and DNA polymerases δ and ε are implicated in the MutSL pathway (Kadyrov, Genschel et al. 2009). There also appears to be a pathway identified in both *S. cerevisiae* and human that corrects loops with about 16 to several hundred of unpaired nucleotides; such large loops cannot be processed by MMR (Marti, Kunz et al. 2002)

1.6.3.5 Recombination repair

Both single and double-strand DNA can be broken by endogenous or environmental factors. Double-strand breaks (DSBs) and single-strand break (SSBs) are the most deleterious lesions in damaged DNA. Unrepaired DSBs can result in cell cycle arrest and cell death (Bonura and Smith 1975). If the DSB is not repaired correctly, mutation will accumulate and genome integrity will be impaired. DSBs cannot be repaired by DNA repair pathways such as BER, MMR and NER. To protect genome integrity, cells utilize recombination repair mechanism to repair this type of DNA damage. There are two different pathways including homologous recombination (HR) and non-homologous end joining (NHEJ) to accomplish the DSB repair task.

1.6.3.5.1 DSB repair by homologous recombination (HR)

Homologous recombination is genetic recombination in which two similar or identical strands of DNA are exchanged. HR occurs not only in chromosomal crossover during meiosis to adapt to a changed environment (Alberts 2002) but also mostly in repairing double-strand DNA breaks. HR is highly conserved among archaea, bacteria and eukaryotes and most of the knowledge regarding the HR repair pathway has been obtained from bacteriophage, bacteria and yeast.

There are two types of HR: conservative and non-conservative; both types of HR are dependent on Rad52 and Rad51 (Shinohara and Ogawa 1995; Paques and Haber 1999). Conservative HR rebuilds the broken chromosomes by copying sequence information from the sister chromatid during mitosis or the homologous chromosome

during meiosis to achieve its accuracy. Both reciprocal and nonreciprocal genetic information can be exchanged during HR, and are defined as crossing over and gene conversion, respectively. Crossing over does not change the content of the genome, but alters the rearrangement of genetic linkage patterns. On the other hand, gene conversion transfers the genetic information from a donor locus to a recipient locus, resulting in a set of genes gained or lost (Paques and Haber 1999). Conservative HR can be divided into three pathways including the DSB repair model of Szostak, synthesis dependent strand annealing (SDSA) and break induced replication (BIR) (Pfeiffer, Goedecke et al. 2000). Non-conservative HR is performed by the single stranded annealing (SSA) pathway, in which single stranded regions that extend to the repeated sequences are created adjacent to the break so that complementary strands can anneal to each other (Haber and Heyer 2001).

1.6.3.5.2. Non-homologous end joining

Non-homologous end joining (NHEJ) is one of the mechanisms to repair DSBs in DNA. "Non-homologous" means no homologous template being used in repairing the damage. By NHEJ the DSB ends can directly ligate without the homologous template but does not mean that homology is never involved (Pfeiffer 1998). NHEJ was first observed in mammalian cells (Pellicer, Robins et al. 1980; Perucho, Hanahan et al. 1980) and later also found in yeast (Orr-Weaver and Szostak 1983). NHEJ not only ligates the compatible ends, but also rejoins non-complementary ends irrespective of their sequence and structure (Pfeiffer, Goedecke et al. 2000). In budding yeast, the NHEJ pathway is dependent on a Ku70-Ku80 heterodimer (Doherty and Jackson 2001; Jones, Gellert et al.

28

2001). Ku70 and Ku80 bind the ends of broken DNA protecting them from degradation, stabilizing them for processing and re-ligation (Liang and Jasin 1996; Feldmann, Schmiemann et al. 2000).

1.6.3.6 DNA damage tolerance

DNA damage-tolerance (DDT), also named DNA postreplication repair (PRR), is a damage tolerance process that permits DNA synthesis over a damaged template. The PRR pathway is highly conserved from yeast to human, and the proteins involved in PRR are biochemically diverse. The DDT pathway includes two sub-pathways: the error-prone and the error-free.

1.6.3.6.1 Error-prone translesion synthesis

The mechanism of translesion synthesis (TLS) is to use specialized damage-tolerant DNA polymerases to bypass the DNA lesion. As a consequence, TLS result in damage-induced mutations (Friedberg 2005; Andersen, Xu et al. 2008). In eukaryotes, TLS is initiated by monoubiquitination of PCNA, with this modification of the PCNA resulting in the recruitment of damage-tolerant polymerases including Polζ (Rev3 and Rev7), Polδ, and Rev1, which are required for TLS to be recruited to stall replication forks (Kannouche, Wing et al. 2004; Bienko, Green et al. 2005) and stimulate their ability to polymerize across lesions (Garg and Burgers 2005). It is now clear that yeast TLS is accomplished by stepwise covalent modifications of the PCNA encoded by *POL30*. In response to DNA damage, the E2 and E3 complex, Rad6-Rad18, monoubiquitinate PCNA at the Lys164 residue to promote TLS.

1.6.3.6.2 Error free lesion bypass

Error-free lesion bypass is one branch of PR mediated by the Ubc13-Mms2 complex in yeast, which acts to prevent spontaneous and DNA damage–induced mutagenesis (Barbour and Xiao, 2003; Broomfield et al., 2001). The mechanism of error-free lesion bypass is that Rad6-Rad18 ubiquitination complex monoubiquitinates PCNA at the Lys164 residue, and Mms2-Ubc13-Rad5 complex further polyubiquitinates PCNA through Lys63–linked chains (Hoege, Pfander et al. 2002). It is thus assumed that monoubiquitinated PCNA promotes error-prone TLS, whereas polyubiquitinated PCNA promotes error-free bypass of damaged templates (Pastushok and Xiao, 2004; Stelter and Ulrich, 2003). During normal replication, the same Lys164 residue could also be covalently modified by SUMO (for small ubiquitin-related modifier), which requires the Siz1-Ubc9 complex; sumoylated PCNA recruites the DNA helicase Srs2 to stalled replication forks to prevent inappropriate recombination (Papouli et al., 2005; Pfander et al., 2005).

1.7 DNA repair in plants

Plants, being sessile, have to tolerate and sometimes thrive in a wide range of environmentally harmful conditions such as excessive sunlight radiation, chemical mutagens, fungal toxins, high and low temperatures, and water stress. Under such conditions, it is essential for plant survival that an efficient system exists to maintain genome stability. This system may consist of different mechanisms to prevent damage to DNAand when damage to DNA occurs, to remove or repair the damage. Although

pathways involved in DNA repair have been extensively investigated in yeast and animal, much less is known in plants.

Sunlight, which is used by plants for photosynthesis, is stressful under different conditions. Strong sunlight can damage the photosystems in the chloroplasts by overproduction of reactive oxygen species (Asada 1999). UV light, a subcomponent of the sunlight, exerts serious effects on plants. UV light not only damages various cellular compounds, membranes, and phytohormones, but also induces various DNA lesions. The major lesions are cyclobutane pyrimidine dimers (CPDs) and pyrimidine (6-4) pyrimidinone dimers [(6-4) photoproducts], and the minor lesion includes oxidized or hydrated bases, single-strand breaks, and others (Ballare et al., 2001; Rousseaux et al., 1999). Through evolution, plants have acquired two main protective strategies to avoid the adverse effects of UV light. One is the shielding by flavonoids and phenolic compounds (Schmitz-Hoerner and Weissenbock 2003) and the other is DNA repair mechnisms such as photoreactivation and dark repair (Britt, 1999; Hays, 2002; Tuteja et al., 2001). Photoreactivation, which is mediated by a photolyase, is thought to be the major DNA repair pathway for CPDs in higher plants (Dany, Douki et al. 2001). Photolyases absorb light in the 300-600 nm range (Pang and Hays 1991) to monomerize UV-induced CPD.

The dark repair mechanism includes NER, BER, MMR and other DNA repair pathways. Dark repair has been observed in several plant species. The completed plant genome full sequences of *Arabidopsis thaliana* and rice revealed that most of the genes involved in NER and BER are present in higher plants (Kimura, Tahira et al. 2004),

suggesting that these DNA repair mechanisms are highly conserved in yeast, human and plants.

Arabidopsis thaliana contains homologs of *RAD6* genes (Sullivan et al., 1994; Zwirn et al., 1997), indicating the existence of a plant DNA damage tolerance pathway. Plant genes involved in the error-prone damage tolerance pathway have been reported. For example, *AtPOLH* (Santiago et al., 2006), *AtPOLK* (Rodriguez-Rojas, Garcia-Cruz et al. 2004), *AtREV3* (Sakamoto et al., 2003), *AtREV1* and *AtREV7* (Takahashi, Sakamoto et al. 2005) have been isolated and characterized; while error-free damage tolerance have not been reported in plants.

Despite a constant threat of oxidative damage, the DNA genome sequence of mitochondria and chloroplasts in plants usually has a very low rate of changes compared to the DNA in nucleus, indicating there are efficient DNA repair mechanisms existing in these organelles. Recent work demonstrates that plant mitochondria possess BER pathway. The mitochondrial DNA is replicated, proofread, and repaired in inner membrane-associated nucleoids, and DNA repair occurs through single nucleotide insertion, indicating the short-patch BER mechanism is involved (Boesch, Ibrahim et al. 2009).

The expression patterns of DNA repair genes encoding CPD photolyase, UV-DDB1, CSB, PCNA, RPA32, and FEN-1 were investigated using Northern and *in situ* hybridization in rice (*Oryza sativa* L. cv. Nipponbare) (Kimura, Tahira et al. 2004). The results showed that all of the genes tested were expressed in tissues rich in proliferating cells, but only CPD photolyase was expressed in non-proliferating tissue such as the mature leaves and elongation zone of the root. These results imply that photoreactivation

might be a major DNA repair pathway for UV-induced damage in non-proliferating cells, while both photoreactivation and excision repair are active in proliferating cells. Interestingly, most of the MMR genes were expressed more in mature leaves than the shoot apical meristem (SAM), indicating that MMR has important roles in DNA repair in mature leaves (Kimura, Tahira et al. 2004). The overview of DNA repair in plants is shown in Figure 1-6.
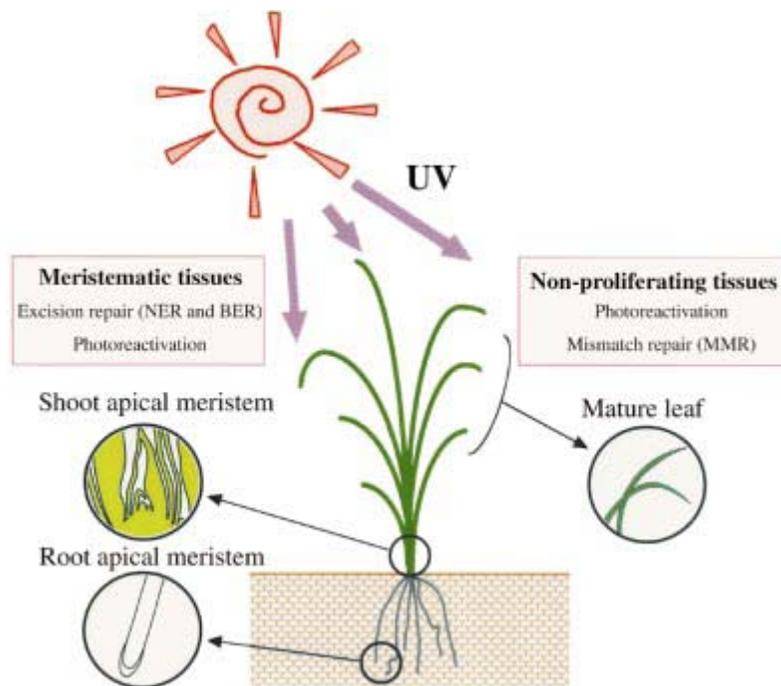
Figure 1-6 The overview of DNA repair in plants. Photoreactivation and mismatch repair are major DNA repair pathways in non-proliferating cells such as leaves, while both photoreactivation and excision repair are active in meristematic tissues (Kimura, Tahira et al. 2004).

1.8 *Arabidopsis thaliana* is an ideal model to study DNA repair and mutagenesis

Arabidopsis thaliana is a small flowering plant that has been widely used as a model organism in plant biology. *Arabidopsis thaliana* is a member of the mustard (*Brassicaceae*) family, which includes cultivated species such as cabbage and radish. it has important advantages for basic research in genetics and molecular biology, such as small size, rapid generation time (5-6 weeks under optimum growth conditions), ease of cross and self-fertilization, and a small genome (125 megabases) (Bowman, 1993).

The genome of *Arabidopsis thaliana* has been sequenced (Initiative, 2000). It is predicted that the genome contains 25,498 genes encoding 11,000 families of proteins. Most of the gene families are similar to those found in other eukaryotes, but several hundred gene families are unique to the plant kingdom. These include over 800 genes primarily involved in photosynthetic activities (Initiative, 2000). The genomic sequence provides valuable information and raw materials for comprehensive analyses of gene function in plants. It also provides opportunities for comparison with the genetic complements of animals, fungi, prokaryotes, and other plant species (Bennetzen, 2001).

Arabidopsis thaliana is a good model organism to study cellular and molecular processes because of the following features: 1) Extensive genetic and physical maps of all 5 chromosomes are available; 2) Transgenic plants can be obtained easily by using *Agrobacterium tumefaciens* as the vector to introduce foreign genes; 3) A large number of mutant lines and genomic resources are available from stock centers. In addition, *Arabidopsis thaliana* is an excellent multicellular model organism to study genes involved in genome maintenance. Firstly, the genome of *Arabidopsis thaliana* encodes orthologs of human genome-maintenance proteins (Hays, 2002). Secondly, plant genes

involved in DNA repair and mutation-prevention functions resemble more closely mammalian counterparts than counterparts of the microbial models. Thirdly, the plant genome is more tolerant to genome instability than mammalian models such as mice. In mice, embryonic lethality has been reported in many cases when DNA repair genes are deleted, including *Rev3* (Bemark et al., 2000; Esposito et al., 2000; Wittschieben et al., 2000), the function of which parallels the Ubc13-mediated error-free damage tolerance in yeast. In contrast, *Arabidopsis thaliana rev3* null mutants have been recently isolated and characterized (Sakamoto et al., 2003; Takahashi et al., 2005) with phenotypes similar to the yeast *rev3* mutant. Given the strong synergistic interactions between the Ubc13-Mms2-mediated error-free damage tolerance and Rev3/Rev7-mediated error-prone TLS in yeast (Broomfield et al., 2001; Xiao et al., 1999a), it would be of great interest to determine genetic interactions between plant *REV3* and *UBC13* genes.

1.9 Objective of this project

Among ubiquitin conjugating enzymes, Ubc13 is unique and can promote Lys63-linked polyubiquitination, unlike the conventional Lys48-linked polyubiquitination that leads to the target protein degradation, is thought to serve as a signal. In yeast and mammalian cells, Ubc13 has shown to function in DNA damage tolerance and NF-κB activation as well as some other less defined pathways. The essential role of Ubc13 in mammals is implied by the mouse embryonic lethality from *Ubc13* deletion, which hampers its further genetic analysis.

Arabidopsis thaliana genome sequence analysis showed the existence of genes similar to Ubc13 and Uev1A. However, there is no published information regarding

whether they play similar or different roles in plant cells, in comparison to mammalian cells. This project aims to understand the functions of AtUbc13, AtUev1, and AtUbc13-AtUev1 complexes in plants using *Arabidopsis thaliana* as a model organism.

CHAPTER TWO

MATERIALS AND METHODS

2.1 Plant materials and techniques involved in plant work

2.1.1 Plant materials

Arabidopsis thaliana ecotype ''Columbia'' was used in this study. Plants were grown in pots, in growth chambers (20 ºC constant, 16/8 h day/night photoperiod with a daylight fluence rate of 140 μmoles/m^2/min). The *Arabidopsis thaliana* cell suspension culture was from Dr. Gordon Gray, Department of Plant Sciences, University of Saskatchewan. The suspension was derived from a callus induced from a ''Columbia'' seedling. The cell suspension was grown in liquid MS (Murashige and Skoog) medium with minimal organics (Sigma M6899, 4.4 g/l), 20 g/l sucrose, 1 mg/l naphthalene acetic acid, 0.05 mg/l kinetin, 200–300 mg/l Timentin (filter-sterilized and added after autoclaving), and 0.5 g/l MES hydrate, pH 5.8. The flasks with the cell suspension were kept shaking at 22 ºC under moderate light (fluence rate of 5 μmoles/m^2/min). To maintain the cell culture, 3 ml cultured cells were taken from the existing culture and used to inoculate 30 ml of fresh medium in a 125-ml flask every week.

T-DNA insertion *AtUEV1D* lines SALK_064912, SALK_052144, *AtUBC13A and AtUBC13 lines* WISCDSLOX323H12 and SALK_043781 were obtained from the Arabidopsis Biological Resource Center (ABRC) (www.arabidopsis.org); while the *AtUEV1A* T-DNA insertion mutant line is not available from the (ABRC); instead, a line

(FLAG_128G02) with a T-DNA insertion at the fourth exon was obtained from the Institut Jean-Pierre Bourgin collection.,

2.1.2 Genomic DNA isolation

Genomic DNA was prepared as described (Edwards et al., 1991). A disc of *Arabidopsis thaliana* leave was pinched out by a lid of a sterile eppendorf tube into the tube. The tissue was macerated in the original eppendorf tube at room temperature without buffer for 15 second. Then 400 µl of extraction buffer (200 mM tris-HCI, pH7.5; 250 mM NaCI; 25 mM EDTA; 0.5% SDS) was added to the sample and votexed for 5 seconds. The mixture was left at room temperature until all samples were extracted. The tubes were centrifuged at 13000 rpm for 1 min and 300 µl of supernatant was transferred to a fresh eppendorf tube. This supernatant was mixed with 300 µl isopropanol and left at room temperature for 2 ml, followed by centrifugation at 13000 rpm for 5 min. The supernatant was discarded and the pellet dried for about 10 min at room temperature. The pellet was dissolved in 100 µl TE buffer or water. Two and a half microliters of the sample were used for a standard 50 µl PCR.

2.1.3 Total RNA extraction and RNA concentration

Total RNA was isolated from tissues such as leaves, floral, seedlings or cell culture using the TRIzol reagent (Invitrogen). The *Arabidopsis thaliana* tissues were homogenized with a motar and pestle in the presence of liquid nitrogen. The homogenized tissue (the mount of the tissue should be less than 100 mg per ml Trizol) were added to in 1 ml Trizol, incubated for 5 min at 15-30 ºC and spun down at 12000g

for 10 min at 4 ºC to remove proteins and polysaccharides. The aqueous phase was taken and 200 µl chloroform was added to the samples. After shaking vigorously by hand for 15 sec, the sample was incubated at 15-30 ºC for 2-3 min and centrifuged at no more than 12000g for 15 min at 4 ºC. The aqueous phase was transferred to a fresh tube and 0.5 ml isopropanol was added. The sample was incubated at RT for 10 min and centrifuged at 12000g for 10 min at 4 ºC to precipitate RNA. The supernatant was discarded and the pellet washed with 1 ml 70% ethanol. The RNA sample was centrifuged again at 7500 g for 5 min at 4 ºC, the pellet briefly dried (air dry for 5-10 min) and stored at -80 ºC. RNA concentration was measured with a spectrophotometer (Pharmacia Biotech, Ultrospec 3000) following the manufacturer's instructions.

2.1.4 Northern hybridization and RT-PCR

To study tissue distribution of *AtUBC13* and *AtUEV1*, tissue samples were taken from *Arabidopsis thaliana* plants, snap-frozen in liquid nitrogen and stored at 80 ºC until use. To determine the expression of *AtUBC13* and *AtUEV1* under different stress conditions, the cell suspension was maintained for 5 days following subculture, and then subjected to various treatments as specified. After a 24-h treatment, total RNA was isolated and the concentration of the RNA determined. For Northern hybridization, 15 mg of total RNA was loaded for each sample, transferred to a nitrocellulose membrane and hybridized as described (Wang et al., 1998). DNA fragments containing *AtUBC13A*, *AtUEV1C* or *UBQ11* ORF were isolated from an agarose gel after restriction enzyme digestion and electrophoresis, and used as templates for probes labeled with ^{32}P-dCTP

using a random primer labeling kit from Invitrogen. The membrane was hybridized with *AtUBC13A* or *AtUEV1C*, stripped and then hybridized with the *UBQ11* probe.

For RT-PCR analysis, total RNA from various tissues was isolated using TRIzol and treated with DNaseI (Promega). Total RNA from mature pollen was extracted as described (Fei et al., 2004), and total RNA from germinating seeds was extracted as described (Vicient and Delseny, 1999). Synthesis of first-strand cDNA by reverse transcriptase was performed using a SuperScript RT-PCR III system (Invitrogen) following the protocol as described (Karsai et al., 2002). Briefly, 2 mg of total RNA from each sample was treated with DNase I (Roche Diagnostics) and reverse-transcribed with Moloney murine leukemia virus reverse transcriptase (Invitrogen) and d(T)18. The final input amount of cDNA used for RT-PCR was adjusted by analyzing the expression of the At4g33380 control gene (Czechowski et al., 2005). Experiments were performed using *AtUEV1* gene-specific primer pairs with different cycle conditions (22, 28, and 35 cycles) to make sure that the amount of PCR product was not excessive and that the difference among different tissue samples was not a result of saturation of PCR amplification. Eight microliters of each reaction was used for agarose gel electrophoresis. All RT-PCR series were assayed at least twice

2.1.5 Protein extraction

Fourteen-day-old seedlings of wild type, single mutants and double mutants of *Atubc13* were homogenized with a motar and pestle in the presence of liquid nitrogen. The homogenized tissues were transferred into a tube with protein extraction buffer [50 mM Tris-HCl (pH8.0); 200 mM NaCI; 5 mM EDTA; 10 mM DTT; Sigma protease

inhibitor cocktail (Sigma # P9599)] as described (Wang et al., 1998). Cell extracts were centrifuged at 14000g for 15 min at 4 ºC and the supernatant transferred into fresh tubes and centrifuged again for 5 min. The protein samples were aliquoted into small volume (1.0, 0.5 and 0.1 ml) and stored at -80 ºC for further use.

2.1.5.1 Protein concentration

Bradford protein assay were used to measure the concentration of protein (Bradford, 1976). The steps of the Bradford protein assay are: dilute proteins and obtain between 1 and 20 µg protein to a final volume 800 µl in one assay tube; prepare standards containing a range of 2, 4, 6, 8, 10 µg proteins (albumin or gamma globulin are recommended) in 800 µl volume; add 200 µl dye reagent and incubate 20 min at RT; measure the absorbance at 595 nm; prepare a standard curve of absorbance versus the amount of protein in microgram and determine protein concentrations of original samples from the standard curve.

2.1.5.2 SDS-PAGE

Proteins were visualized using sodium dodecyl sulfate polyacrylamide gel electrophoresis (SDS-PAGE) in a Mini-Protean 3 gel apparatus. In general, samples for SDS-PAGE were made by the addition of 2X protein sample buffer (125 mM Tris pH 6.8, 4% SDS, 10% glycerol, 0.006% bromophenol blue, 1.8% β-mercaptoethanol) to the protein solution. The protein samples were placed in boiling water for 5 min, cooled, and then loaded onto the protein gel. Usually 12% discontinuous (5% stacking, 12% separating) Tris-glycine polyacrylamide (37:1 acrylamide:bisacrylamide) gels were used

(Maniatis et. al, 1989) and the gels were run at 180 V for 45 min. Gels were stained with Coomassie Blue staining solution (0.025% Coomassie Brilliant Blue R250, 40% methanol, 7% acetic acid) for at least 30 minutes, followed by incubation in a de-stain solution (40% methanol, 10% acetic acid) until appropriate protein bands could be visualized (after 30-60 min).

2.1.5.3 Western blotting analysis

Following SDS-PAGE, the resolving gel was equilibrated for 20 min in a transfer buffer along with equal-sized polyvinylidene difluoride (PVDF) membrane and 3M filter papers. The components were assembled as described in the manual for the Bio-Rad trans-blot semi-dry transfer cell, which was used for the transfer of proteins onto the PVDF membrane. Transfers were performed at a constant current of 1 mA/cm^2 for 2 hr. The membrane was then incubated in a blocking solution overnight at 4°C. The primary monoclonal antibody against the hUbc13 protein raised in Dr, Xiao's laboratory was diluted at 1:4000 in 10 ml phosphate buffered saline (PBS) with 0.1% Tween 20 (PBST) and incubated with the membrane at room temperature (RT) for 1 hr with gentle rocking. The membrane was washed 3 times for 5 min each with PBST. Subsequently, the horseradish peroxidase-conjugated secondary antibody was diluted at 1:10000 in 10 ml PBST and incubated with the membrane same as with the primary antibody. The membrane was then washed 3 times for 5 minutes each with PBST followed by 2 rinses each with PBS to prepare for the detection. The Western Lightening Chemiluminescence Reagent (Perkin-Elmer, #NEL101) was used as the substrate for the visualization of

horseradish peroxidase-conjugated secondary antibody. and the membrane were developed by using the

2.1.6 Seed germination assays

The homozygous *UEV1D* T-DNA insertion lines SALK_064912 (*uev1d-1*) and SALK_052144 (*uev1d-2*) were used in the sensitivity assay to the DNA-damaging agent MMS. To exclude any possible non-specific effect, we used three controls, the wild-type Arabidopsis Columbia, a T-DNA insertion line not related to *UEV1* genes (SALK_042050), and a homozygous wild-type segregant line (1d-1WT or 1d-2WT) derived from the initial mutant seeds received. For the *uev1a-1* mutant, the parental wild-type line Ws-4 and a homozygous wild-type (1a-1WT) segregant from FLAG_128G02 were used as controls. The identity of the wild-type and mutant segregants was determined by genomic PCR and RT-PCR. In addition, to minimize the effect of individual plants, seeds of three homozygous mutant plants were pooled and used for the assay. Seeds were surface-sterilized with 20% bleach and 0.1% Triton X-100 for 20 min, followed by three rinses in sterile water. After sterilization, seeds were suspended in 0.1% agarose and stored at 4 ºC in the dark for 3 d to synchronize germination. Three days later, the seeds were removed from the dark and sown on half-strength Murashige and Skoog agar plates supplemented with different concentrations of MMS. Each plate was planted with 50 seeds, and at least three plates (150 seeds) were used for each treatment. After 5-d incubation in a growth chamber, germination of the seeds was surveyed. After 13-d incubation, the color of cotyledons was rated (green versus non-green) while the first pair of true leaves was still small. Since seedlings with non-green cotyledons at this stage

were dead or dying, the percentage of seedlings with green cotyledons was an indicator of seedling viability. The fresh weight of seedlings was also determined and was used as an indicator of seedling growth.

2.1.7 In vitro pollen germination assay

To quantitatively measure pollen germination efficiency in the presence of MMS, 2 ml of the germination medium (Fan et al., 2001) containing 1% agar with or without 0.005% MMS was poured into a 35-mm Petri dish to form a thin layer. Freshly anther-dehisced flowers at stage 13 or 14 (Smyth et al., 1990) were randomly picked and used to carefully touch the central area of the agar plate in order to spread pollen grains. The Petri dishes were incubated in a humid chamber at 26 ºC for 8 h without light before counting pollen germination and photographing. For each plate more than 400 pollen grains were counted using a phase-contrast microscope for each plate, and three plates were used for each treatment.

2.2 Molecular biology techniques

2.2.1 Plasmids preparation

Cloning of the *Arabidopsis thaliana UBC13* and *UEV* genes was accomplished prior to my involvement with the project. Human Mms2 and Ubc13 protein sequences were used to search the *Arabidopsis thaliana* protein database available from the Arabidopsis Genome Initiative. For Ubc13, two *Arabidopsis thaliana* putative proteins with an E value better (lower) than 10^{-55} were found. For Mms2, four *Arabidopsis thaliana* putative proteins with an E value better (lower) than 10^{-38} were found. To clone the full-length

coding cDNAs of these genes, RNA was isolated from *Arabidopsis thaliana* seedlings using TRIzol reagent (Invitrogen). The total RNA was used to perform RT-PCR with the ThermoScript RT-PCR kit (Invitrogen) according to manufacturer's instructions. Gene-specific primers were designed and used to obtain amplicants of the putative *Arabidopsis thaliana UBC13* and *UEV1* homologs. All primers used in this study were listed in Table 2.1. Pfu DNA polymerase was used to reduce the frequency of errors in PCR. *AtUBC13* homologs were initially cloned in-frame into the yeast two hybrid pGBT9E vector, while *AtUEV1* homologs were cloned in-frame into the yeast two hybrid pGAD424E vector for determining interactions in the yeast two-hybrid system. Sequences of all the clones were verified by sequencing in the Plant Biotechnology Institute, National Research Council of Canada, Saskatoon. In consideration of the sequence relatedness, they are named: *AtUBC13A*, *AtUBC13B*, *AtUEV1A*, *AtUEV1B*, *AtUEV1C*, and *AtUEV1D*.

In order to over express these genes in *E. coli*, the ORFs of each DNA were isolated from pGBT9 or pGAD424 vector and cloned into pGEX6p-2 (Amersham Biosciences, Piscataway, NJ, USA) to form N-terminal gene fusions to GST.

Table 2-1 Oligonucleotide sequences

Primer	Sequence
AtUBC13A-1	5'cccgtcgacAATGGCCAACAGTAATTTGCCG-3'
AtUBC13A-2	5'cccgtcgacTCATGCGCCGCTTGCATAAAG-3'
AtUBC13A-3	TCA GCC TTT GGT AGC TTC GT
AtUBC13B-1	5'cccgtcgacAATGGCCAATAGTAATCATCCC-3'
AtUBC13B-2	5'cccgtcgac TTAAGCACCACTTGCGTAAAG-3'
AtUEV1A-1	5'-cccgtcgacaATGAGTTCGGAGGAAGCCAAG-3'
AtUEV1A-2	5'-cccgtcgacTCACATCACACAACATTTAGC-3'
AtUEV1B-1	5'-cccgtcgacaATGGGTTCGGAAGAAGAGAAG-3'
AtUEV1B-2	5'-cccgtcgacTCACATCACGCAACATTTCACCAC-3'
AtUEV1C-1	5'-cccgtcgacaATGACTCTTGGCTCAGGATCG-3'
AtUEV1C-2	5'-cccgtcgacTTAGAAGAAAGTTCCTTCGGG-3'
AtUEV1D-1	5'-cccgtcgacaATGACTCTTGGCTCAGGAGG-3'
AtUEV1D-2	5'-cccgtcgacCTAGAAGCAAGTACCTTCCGG-3'
UBQ11-1	5'-CAGATTTTTGTTAAAACCCTA-3'
UBQ11-2	5'-CTTCTGAATGTTGTAATCC-3'
LB1	5'-GCGTGGACCGCTTGCTGCAACT-3'
4g33380-F	5'-ATGAGAAGCTGGAGGAAGC-3'
4g33380-R	5'-TCAAGCCGTTACAACACC-3'

2.2.2 Bacterial strains, culture and storage

The bacterial strain used in this study for protein expression was BL21-CodonPlus (DE3)-RIL. This strain carries extra copies of the *argU*, *ileY* and *leuW* tRNA genes to help overcome codon bias, and was purchased from Stratagene (#230245). For typical DNA plasmid propagation and isolation, *Escherichia coli* DH10B (GibcoBRL, Grand Island, NY, USA) was used. Because all of the plasmids in this study contains the ampicillin- resistance gene β-lactamase (bla) as a selectable marker, transformed cells were cultured in LB liquid or agar media (1% Bacto-tryptone, 0.5% Bacto-yeast extract, 0.5% NaCl and 1.2% agar for plates) containing 50 μg/ml of ampicillin (Amp). For short-term storage (2 or 3 months), clones were stored on corresponding plates. For long-term storage, clones were grown overnight in 900 μl of LB plus Amp liquid medium, mixed with 100 μl of DMSO and immediately placed in a −70 ℃ freezer.

2.2.3. Preparation of competent cells

E. coli competent cells for electroporation were prepared as recommended in the Bio-Rad *E. coli* Pulser manual. One liter of culture was incubated until an OD_{600nm} reached 0.6. The culture was centrifuged at 3500 rpm for 15 min in a Beckman GSA rotor and the pellet was resuspended in 500 ml of 10% ice-colded sterile glycerol. The centrifugation was repeated 4 times, with each pellet resuspended in a reduced volume; the last pellet was resuspended in 4 ml of ice-colded, sterile 10% glycerol. The cells were aliquoted into 1.5 ml eppendorf tubes to a volume of 25 μl, and were quickly placed in the −70 ℃ freezer for storage.

2.2.4. Bacterial transformation

All bacterial transformations in this study were carried out by the electroporation method. The plasmids were added to *E. coli* competent cells and the cell mixture was transferred to a pre-chilled electroporation cuvette (BioRad). After a brief incubation on ice, the cells were exposed to a voltage of 1.8 kV (for cuvettes with 0.1 mm width) using the *E. coli* Pulser (BioRad). 500 μl of SOC medium was added to the cuvette after electroporation. The cells were transferred to a 1.5 ml eppendorf tube, incubated at 37 ºC for 45 min and spread on LB + Amp plates and incubated at 37 ºC overnight for single colonies.

2.2.5 Rapid preparation of plasmid DNA

Plasmid amplification and isolation was performed following the methods described in by (Maniatis, 1982). Single colonies were used to inoculate 2 ml LB + Amp liquid medium and grown overnight at 37 ºC. Cells were collected by centrifugation and the pellet was resuspended in 350 μl of STET (8% sucrose, 0.5% Triton X-100, 50 mM EDTA pH 8.0, 10 mM Tris-HCl pH 8.0). After mixing with 20 μl of lysozyme (10 mg/ml; Sigma, St Louis MI), the mixture was quickly placed in a boiling water-bath for 40 sec, followed by centrifugation for 10 min. The pellet was removed with a toothpick, and 8 μl of 5 M NaCl and 2 volumes of 95% ethanol were added to precipitate the DNA. After centrifugation, the pellet was resuspended in 30 μl double-distilled water (ddH$_2$O).

2.2.6 DNA gel electrophoresis

Plasmid DNA and DNA fragments were separated by agarose gel electrophoresis. The proper amount of agarose was added to the appropriate 1 x TAE buffer (40 mM Tris-acetate, 2 mM Na_2EDTA) to make a gel of 0.6-1% agarose. The gel was loaded into an electrophoresis apparatus filled with 1X TAE buffer and a current of <100 mA was allowed until the proper migration distance was attained. Gels were stained in 0.5 µg/ml ethidium bromide for 5-10 min and the DNA was viewed using a UV trans-illuminator.

2.2.7 DNA fragment isolation

DNA fragment isolation from an agarose gel was adapted from the Wang and Rossman method (Wang and Rossman,1994). After enzyme digestion, the sample was electrophoresed through 0.6% agarose gel and stained with EtBr. The band of interest was identified using an UV-illuminator and cut out of the gel. A 0.5 ml microcentrifuge tube was pierced at the bottom, and packed with chopped cheesecloth. The gel slice containing the DNA fragment was placed into the prepared tube, which was inserted into 1.5 ml tube, left it at −70 ºC for a minimum of 20 min and spun for 10 min at top speed. The flow through was extracted with an equal volume of phenol/chloroform (1:1) and then with chloroform. The DNA in the upper aqueous phase was precipitated by ethanol and resuspended in 50 ul ddH_2O.

2.2.8 Polymerase chain reaction

Polymerase chain reaction (PCR) was used to amplify DNA fragments for the purposes of cloning and other analyses. PCR mixtures were created using the recipe

guidelines in the instruction manual for Pfu Turbo DNA polymerase (Strategene, #600250), which was used in all reactions. A PTC-100 programmable thermocycle (MJ Research, Inc., Watertown, MA) was used to carry out the various amplifications. As a program guideline, a denaturing temperature of 94°C for one min was followed by an annealing temperature of 55°C for 45 sec, and primer extension was carried out at 72°C for 1 min per kilobase of DNA to be amplified. These three steps were repeated 29 times for a total of 30 cycles.

2.2.9 DNA sequencing

DNA sequencing was performed by the DNA sequencing laboratory in the Plant Biotechnology Institute, National Research Council of Canada, Saskatoon.

2.2.10 Recombinant protein over expression and purification

2.2.10.1 Induction of gene expression

pGEX6-*AtUBC13A*, pGEX-*AtUEV1A*, pGEX-*AtUEV1B*, pGEX-*AtUEV1C* and pGEX-*AtUEV1D* as well as pGEX-*hMms2* were used to transform in to the protein expressing BL21(DE3)-RIL cells and grown overnight at 37 °C in the LB + Amp medium, then sub-cultured 1:50 into pre-warmed LB + Amp the following day. Cells were allowed to grow continuously to OD 600 nm between 0.6 and 0.8, induced with 0.5 mM isopropyl-β-D-thiogalactopyranoside (IPTG) for 2 h, harvested by centrifugation at 8,000 rpm in an Avanti Beckman JA10.5 rotor and stored at -70 ºC.

2.2.10.2 Preparation of cell extract

The harvested cells were resuspended in phosphate-buffered saline (PBS, 140 mM NaCl, 2.7 mM KCl, 10 mM Na_2HPO_4, 1.8 mM KH_2PO_4, pH 7.3). Crude extracts were generated by passing the cells through a French Press at 10,000 psi. The soluble fraction was retained after centrifugation at 17,000 rpm in an Avanti Beckman JA17 rotor for 30 min. The soluble fraction was then run through a chromatography system for purification.

2.2.10.3 Chromatography

All following steps were carried out at 4 °C. Soluble extracts were passed through a pre-packed 5 ml GSTrap column (GE Healthcare, #17-5131-01), which was then washed with at least 5 column volumes of 1X PBS. GST-fusion proteins were eluted with reduced glutathione elution buffer (10 mM glutathione in 50 mM Tris-HCl, pH 8.0) and dialyzed extensively against cleavage buffer (50 mM Tris-HCl, 150 mM NaCl, 1 mM EDTA, 1 mM dithiothreitol, pH 7.0). If protein purity was not sufficient, the above purification steps were repeated. When needed, cleavage was performed by the addition of 2 units of Prescission Protease (GE Healthcare, #27-0843-01) per mg of fusion protein, followed by a16-h incubation at 4°C with gentle rocking. Cleaved proteins were applied to a GSTrap column in order to remove the GST component from the cleaved protein of interest. When necessary, proteins were concentrated in Amicon Ultra centrifugal 54 filter devices. Protein concentrations were determined using the BCA Protein Assay Kit (Pierce, #23227) according to the instruction manual. Purified proteins were kept at 4°C for short-term use, or placed into <500 μl aliquots, frozen quickly and kept at -70°C for long-term storage.

2.2.11 GST pull-down assays

GST pull-downs were performed using MicroSpin GST Purification Modules (GE Healthcare, #27-4570-03). The purpose of this assay was to test the interaction between AtUbc13 and AtUev1A, AtUev1B, AtUev1C, AtUev1D as well as human Mms2. Fifty microliters of purified GST and GST fusion proteins in 1X PBS were loaded and incubated in the purification module for 1 h at 4°C with gentle rocking. The module was then washed three times with 500 μl PBS. Subsequently, 50 μg of purified, non-fused AtUbc13 in 1X PBS was added to the module separately and the incubation was continued for another hour at 4°C. The module was washed again three times with 500 μl PBS and 80 μl of reduced glutathione elution buffer was then added to elute the affinity-purified proteins. Eluted samples were subjected to SDS-PAGE and visualized by Coomassie Blue staining.

2.2.12 Ub Conjugation Reaction

In vitro Ub conjugation reactions were performed using the purified Ubc13A and GST-Uev1 proteins as described above, and Ub thioester/conjugation initiation reagents were purchased from Boston Biochem. Unless noted otherwise, the 20-ml reaction mixture contained 225 nM E1 enzyme, 450 mM Ub, 1 mM MgATP, 1 mM Ubc13, and 1 mM Uev1 in the supplied reaction buffer. The K63R and K48R mutant Ub proteins were purchased from Boston Biochem (UM-K63R and UM-K48R). The conjugation reactions were performed at 37°C for 2 h. Samples were subjected to SDS-PAGE (12%), and Ub and poly-Ub were detected through protein gel blots using polyclonal rabbit anti-Ub antibodies (Sigma-Aldrich).

2.3 Yeast genetic analyses

2.3.1 Yeast strains and cell culture

The haploid yeast strains used in this study are listed in Table 2.2. Yeast cells were grown at 30 ºC in either rich YPD (1% Bacto-yeast extract, 2% Bacto-peptone and 2% glucose) or in a synthetic dextrose (SD) medium (0.67% Bacto-yeast nitrogen base without amino acids, 2% glucose) supplemented with necessary nutrients including 30 mg/L L-isoleucine, 150 mg/L L-valine, 20 mg/L adenine hemisulfate salt, 20 mg/L arginine HCl, 20 mg/L L-histidine HCl monohydrate, 100 mg/L L-leucine, 30 mg/L lysine HCl, 20 mg/L L-methionine, 50 mg/L L-phenylalanine, 200 mg/L L-threonine, 20 mg/L L-tryptophan, 30 mg/L L-tyrosine, 20 mg/L L-uracil as recommended (Sherman, 1983). Any of the above auxotrophic supplements can be omitted to provide a selection medium for yeast transformation. The auxotrophic supplements were made in 100 × stocks and added into culture media prior to autoclaving. To make plates, 2% agar was added to either YPD or SD medium prior to autoclaving. Yeast cells can be stored up to four months on plates sealed with parafilm at 4 ºC. For long-term storage, yeast cells were grown in an appropriate liquid medium (rich or minimal selective) at 30 ºC overnight. For storage, 0.7 ml of the culture was added into 0.3 ml of 50% sterile glycerol, mixed and stored at -70 ºC. For preparing MMS (Methyl methanesulfonate) special media, MMS (Aldrich, Milwaukee, USA) was added immediately before pouring the plates. In order to avoid MMS degradation, MMS plates were usually freshly made and never stored for more than one day before using.

Table 2-2 *Saccharomyces cerevisiae* strains

Strain	Genotype	Source
PJ69-4A	*MATa trp1-901 leu2-3,112 ura3-52 his3-200 gal4Δ gal80Δ Met2::GAL7-lacZ LYS2::GAL1-HIS3 GAL2-ADE2*	P. James University of Wisconsin
HK580-10D	*MATa ade2-1 can1-100 his3-11,15 leu2-3,112 trp1-1 ura3-1*	H. Klein New York University
WXY942	HK580-10D with *mms2 Δ::HIS3*	Lab stock
WXY955	HK580-10D with *mms2 Δ::HIS3 ubc13 Δ::hisG-URA3-hisG*	This study
DBY747	*MATa his3-1 leu2-3,112 trp1-289 ura3-52*	D. Botstein Preston University
WXY642	DBY747 with *mms2 Δ ::HIS3*	Lab stock
WXY904	HK578-10D with *ubc13 Δ::HIS3*	This study
WXY1233	HK578-10D with *rev3 Δ ::hisG-URA3-hisG*	This study
WXY921	HK578-10D with *ubc13 Δ::HIS3 rev3 Δ::hisG-URA3-hisG*	This study
WXY849	DBY747 with *ubc13 Δ::HIS3*	This study

2.3.2. Yeast transformation

Yeast cells were transformed using a dimethyl sulfoxide (DMSO)-enhanced method as described (Hill et al., 1991). A 2 ml culture of yeast cells was grown overnight at 30 ℃ in a rich YPD medium (or appropriate minimal media), and sub-cultured into 3 ml of fresh YPD and grown for 3-4 hs, yeast cells would reach a mid-logarithmic phase of growth. Yeast cells were precipitated by centrifugation, washed in 400 μl LiOAc solution (0.1 M lithium acetate, 10 mM Tris-HCl (PH 8.0), 1 mM EDTA), and resuspended in 100 μl of the same solution. 5 μl of denatured carrier DNA (single-stranded salmon sperm DNA) and 1-5 μl of transforming DNA were added and mixed well. After incubation at room temperature for 5 minutes, 280 μl of 50% PEG4000 (50% polyethylene glycol 4000 in LiOAc solution) was added and mixed by inverting the tube 4-6 times. After the transformation mixture was incubated for 30 minutes at 30 ℃, 40 μl of DMSO was added, followed by a 5-minute heat shock in a 42 ℃ water bath. Yeast cells were then washed with sterile ddH_2O and resuspended in 100 μl of ddH_2O. The resuspended cells were plated on an appropriate minimal medium and the plates were incubated at 30°C for 3 days to allow colony formation.

2.3.3 Yeast two-hybrid analysis

The yeast two-hybrid strain PJ69-4A (James et al., 1996), received from Dr. P. James (University of Wisconsin, Madison, USA), was co-transformed with different combinations of $Gal4_{BD}$ and $Gal4_{AD}$ constructs. The co-transformed colonies were initially selected on SD-Leu-Trp plates. For each transformation, at least five independent colonies were grown in SD-Leu-Trp plates and then replica plated onto either SD-Leu-

Trp-His alone or SD-Leu-Trp-His with various concentrations of 1,2,4-amino triazole (3-AT) to test the activation of the P_{GAL1}-*HIS3* reporter gene, or SD-Ade to test the activation of the P_{GAL1}-*ADE* reporter gene. Plates were incubated for 48 hours at 30°C unless otherwise indicated.

2.3.4 Functional complementation assays

Gradient plate assays were performed for the semi-quantitative measurement of yeast cell sensitivity to MMS. At least three independent colonies from different transformants for each strain were individually inoculated into 1 ml of SD minimal media. Following an overnight incubation, cell density was determined and equal numbers of cells from the transformants as well as untransformed controls were imprinted onto YPD alone or YPD gradient plates containing 0.025% MMS. An MMS gradient was formed by pouring 30 ml of YPD + MMS medium in a tilted square petri dish. The petri dish was placed flat after solidification and a top layer of 30 ml YPD was poured. 0.1 ml of overnight culture, mixed with 0.4 ml sterile water and 0.5 ml of molten YPD agar was printed onto the plates using a sterile microscope slide. Plates were incubated at 30 °C for the given time before taking photograph.

2.3.5 Spontaneous mutagenesis assay

Spontaneous Trp$^+$ reversion rates of DBY747 derivatives were measured by a modified Luria and Delbruck fluctuation test as described (Von Borstel, 1978). The *trp1-289* amber mutant can be reverted to Trp$^+$ by several different mutation events (Xiao and Samson, 1993). WXY849 was transformed with pGAD-*AtUBC13A*, pGAD-*AtUBC13B* or

the vector pGAD424E, and WXY642 was transformed with pGAD-*AtUEV1A*, pGAD-*AtUEV1B*, pGAD-*AtUEV1C*, pGAD-*AtUEV1D* or pGAD424E. Transformants were selected on SD-Leu plates. Each set of experiments contained five independent cultures of each strain. Overnight yeast cultures were counted using a hemocytometer and 5 ml of YPD liquid medium was inoculated to a final concentration of 20 cells/ml and incubated at 30 °C until the cell titer reached 2×10^7 cells/ml. Cells were spun down at 4000 rpm, resuspended in sterile ddH$_2$O and plated onto YPD in duplicate to score total survivors and onto SD-Trp plates to score Trp$^+$ revertants. Spontaneous mutation rates (number of revertants per cell per generation) were calculated as previously described (Williamson et al., 1985). The following formula was used to calculate the frequency of spontaneous mutagenesis:

Frequency (F) = total cell number of TRP$^+$ cells / total number of viable cells

To calculate the rate of spontaneous mutagenesis, the following formula was used:

Rate = 0.4343 x Frequency / log (total cell number) – log (initial cell number)

The formula was derived to determine mutation rate for a replication system, where 0.4343 is approximately log10 e.

CHAPTER THREE

ARABIDOPSIS THALIANA UEV1D PROMOTES LYS63–LINKED POLYUBIQUITINATION AND IS INVOVLED IN DNA DAMAGE RESPONSE

3.1 Introduction

Cellular DNA is subject to assaults by environmental factors and endogenous metabolites. The alteration of DNA can lead to mutations, genome rearrangements, and cell death (Friedberg et al., 2006a). To maintain genome integrity, all living organisms have evolved a variety of DNA repair mechanisms to protect cells from DNA damage. However, despite great advances made during the last decade in the field of DNA repair and mutagenesis, the molecular mechanisms of DNA damage tolerance (DDT) in eukaryotes, especially in multicellular eukaryotes, have not yet been well characterized. In the lower eukaryote *Saccharomyces cerevisiae*, a DDT process known as DNA postreplication repair (PRR) facilitates DNA synthesis in the presence of replication blocking lesions in the template. PRR consists of two branches: an error-prone (mutagenesis) branch and an error-free branch. The error-prone branch is mediated by specialized DNA polymerases, including Polz (Rev3 þ Rev7), Polh, and Rev1, which are required for translesion DNA synthesis (TLS). By contrast, the error-free branch is mediated by the ubiquitin (Ub)-conjugating enzyme (Ubc or E2)–Ubc variant (Uev) complex Ubc13-Mms2 (for methyl methanesulfonate2), which acts to prevent spontaneous and DNA damage–induced mutagenesis (Barbour and Xiao, 2003;

Broomfield et al., 2001). It is now clear that yeast PRR is accomplished by Mms2-Ubc13-Rad5 complex polyubiquitinates Pol30 through Lys63–linked chains (Hoege et al., 2002). Ubc13 and Uev homologs are found in all eukaryotes examined to date (Pastushok and Xiao, 2004; Villalobo et al., 2002), However, the functions of these proteins remain uncharacterized in a multicellular organism. It is reported that *Arabidopsis thaliana* genes such as REV3 (Sakamoto et al., 2003), REV1, REV7 (Takahashi et al., 2005), POLK (Garcia-Ortiz et al., 2004), and POLH (Curtis and Hays, 2007) are involved in TLS and TLS appears to play an important role in the tolerance of DNA damage in plants. In this chapter, we describe the molecular cloning and functional characterization of four *Arabidopsis thaliana UEV1* genes and report a case of mutant phenotypes in DNA damage response when one of the *UEV1* genes is inactivated.

3.2 Results

3.2.1 Isolation of *Arabidopsis thaliana UEV1* genes

To identify *Arabidopsis thaliana UEV1* genes, a human Mms2 sequence (Xiao et al., 1998) was used to search for homologs in the *Arabidopsis thaliana* protein database (through The Arabidopsis Information Resource [TAIR]: www.arabidopsis.org). Four hypothetical proteins with a high degree of similarity (E-values $< 2e^{-38}$) were found and named *AtUEV1A* (At1g23260), *AtUEV1B* (At1g70660), *AtUEV1C* (At2g36060), and *AtUEV1D* (At3g52560). The genomic structures of these four corresponding *UEV1* genes are shown in Figure 3-1A. At*UEV1A* and *AtUEV1B* have the same number of exons and introns, and their exon–intron junctions are identical. *AtUEV1B* has shorter intron sequences than *AtUEV1A*. Similarly, *AtUEV1C* and *AtUEV1D* have the same numbers of

exons and introns, the same exon–intron junctions, and all introns in *AtUEV1D* are longer than those in *AtUEV1C*. Nucleotide sequence alignment of *AtUEV1* open reading frames (ORFs) reveals 86% identity between *AtUEV1A* and *AtUEV1B* and 88% identity between *AtUEV1C* and *AtUEV1D*. Based on the above analyses, we predicted that the four *UEV1* genes resulted from two separate gene duplication events. This agrees with a duplication mapping analysis (http://wolfe.gen.tcd.ie.athal/dup)(Blanc et al., 2003). Further nucleotide sequence analysis of four *AtUEV1* promoter and downstream sequences do not reveal significant similarity between the two pairs of duplicated genes, indicating that they were derived from segmental duplications. This is consistent with database analysis (http://www.tigr.org/tdb/e2k1/athl/athl.shtml), suggesting that their expression profiles may be different. All four *AtUEV1* ORFs were cloned from *Arabidopsis thaliana* by RT-PCR using gene-specific primers (the work was done by Dr. Genyi Li in Dr. Wang's Lab). The nucleotide sequences were identical to the annotated complete coding sequences in the *Arabidopsis thaliana* database. The predicted AtUev1A, AtUev1B, AtUev1C, and AtUev1D proteins contain 158, 159, 145, and 146 amino acids, respectively, with differences in length primarily at the C terminus. AtUev1A and AtUev1B contain C-terminal tails not found in other Uevs (Figure 3-1B). Amino acid sequence alignment (Figure 3-1B) shows 86% identity between AtUev1A and AtUev1B and 92% identity between AtUev1C and AtUev1D, whereas amino acid sequence identity between AtUev1A and AtUev1C is 75%. The sequences of AtUev1 proteins were also aligned with those of Uev proteins from six other eukaryotic organisms, including human. As shown in Figure 3-1B, amino acid sequence identity between AtUev1s and those from other six species ranges from 47% to 56%, and similarity ranges from 65% to 75%.

Furthermore, several critical residues implicated in Uev activity are also conserved in AtUev1s. These residues include Phe-13 of HsMms2 required for physical interaction with Ubc13 (Pastushok et al., 2005) and Ser-32 and Ile-62 of HsMms2 (Pastushok et al., 2007) and the corresponding Ser-27 (Eddins et al., 2006) and Ile-57 (Tsui et al., 2005) of ScMms2 required for noncovalent interaction with Ub and polyubiquitin chain assembly. It is noted that mammals also contain two Uev proteins, Mms2 and Uev1A, with >91% amino acid sequence identity in their core domains (Franko et al., 2001; Xiao et al., 1998). Amino acid sequence comparison could not assign lineage between the two pairs of AtUev1 proteins and the mammalian Uevs, indicating that plant and animal Uevs evolved independently within their own kingdoms.
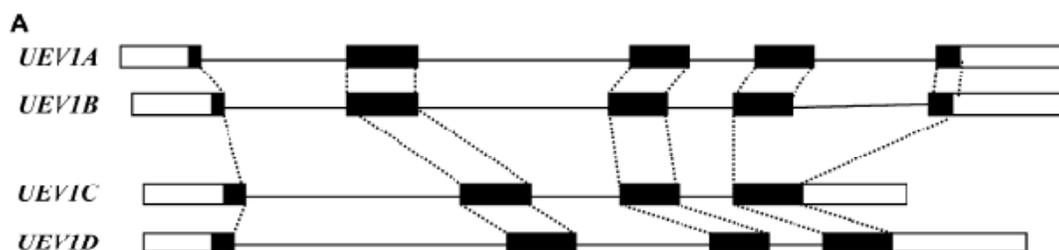
A

UEV1A

UEV1B

UEV1C

UEV1D

B

```
ScMms2   ..............................MSKVPRNFRLLEELEKGEKGFGPESCSYGLADSDDITMTK  40
SpMms2   ..............................MAKVPRNFRLLEELEKGEKGLGESSCSYGLTNADDITISD  40
CeMms2   ..............................MVDVPRNFRLLEELEGQKGKDGNISWGLEDDSDMTLTR   40
DmMms2   ....................MANTSSTGVVVVPRNFRLLEELDQGGVGDGTISWGLENDDDMTLTY    47
AtUev1A  ....................MSSEEAKVVVPRNFRLLEELERGEKGIGDGTVSYGMDDADDIYMQS   46
AtUev1B  ....................MGSEEEKVVVPRNFRLLEELERGEKGIGDGTVSYGMDDADDILMQS   46
AtUev1C  ....................MTLGSG.SSVVVPRNFRLLEELERGEKGIGDGTVSYGMDDGDDIYMRS  47
AtUev1D  ....................MTLGSGGSVVVPRNFRLLEELERGEKGIGDGTVSYGMDDGDDIYMRS  48
MmMms2   .....................MAVSTGVKVPRNFRLLEELEEGQKGVGDGTVSWGLEDDEDMTLTR   45
MmUev1   ....................MAATTGSGVKVPRNFRLLEELEEGQKGVGDGTVSWGLEDDEDMTLTR   47
HsMms2   .....................MAVSTGVKVPRNFRLLEELEEGQKGVGDGTVSWGLEDDEDMTLTR   45
HsUev1A  MPGEVQASYLKSQSKLSDEGRLEPRKFHCKGVKVPRNFRLLEELEEGQKGVGDGTVSWGLEDDEDMTLTR  70
                                   *                          *

ScMms2   WNGTILGPPHSHHENRIYSLSIDCGPNYPDSPPKVTFISKINLPCVIPTTGEVQ.TDFHTLRDYKRAYTM   109
SpMms2   WNATILGPAHSVHENRIYSLKIHCDANYPDAPPIVTFVSRINLPGVDGETGKVNPHKIDCLRHYKREYSM   110
CeMms2   WTASIIGPPRTPYESRIYRLQIQCGGNYPREPPTVRFTTKVHWVGVIQSNGVIDKRNLTTLRRYSNSYHI   110
DmMms2   WIGMIIGPPRTPFENRMYSLKIECGERYPDEPPTLRFITKVNIHCIHQNMGVVDHRSVQMLARYSREYHI   117
AtUev1A  WTGTILGPPNTAYEGKIFQLKLFCGKEYPESPPTVRFQTRINACVHPETGVVPSLFPMLTRWRREYTM    116
AtUev1B  WTGTIILGPHNTAYEGKIFQLKLFCGKDYPESPPTVRFQSRINACVPENGVVDPSHFPMLSRWRREFTM   116
AtUev1C  WTGTIIGPHNTVHEGRIYQLKLFCDKDYPEKPPTVRFHSRINMTCVHDTGVVDSKKFGVLARWQRQLTM   117
AtUev1D  WTGTIIGPHNTVHEGRIYQLKLFCDKDYPEKPPTVRFHSRVNMACVHHETGVVDPKKFGLLARWQREYTM   118
MmMms2   WTGMIIGPPRTRYENRIYSLEVECGSKYPEAPPSVRFVTKINMNGINNSSGAVDARSIPVLAKWQNSYSI   115
MmUev1   WTGMIIGPPRTIYENRIYSLKIECGPKYPEAPPSVRFVTRVNMSGVSSHGVVDPRATAVLAKYQNSHSI   117
HsMms2   WTGMIIGPPRTRYENRIYSLKVECGPKYPEAPPSVRFVTKINMNGINNSSGAVDARSIPVLAKWQNSYSI   115
HsUev1A  WTGMIIGPPRTIYENRIYSLKIECGPKYPEAPPSVRFVTKINMNGVNSSNGVVVDPRAISVLAKWQNSYSI   140
                                   *

ScMms2   ETLLLDLEK.EMATPANKKLPQPKEGETF..............   137
SpMms2   ETVLLDLEK.ELASSSNRKLPQPPEGSTFF.............   139
CeMms2   KTVLFDTRKNMMAKENLKLQQPAEGAMF................  139
DmMms2   KTMLQEIPR.DMTMKENLKLAQPPEGSCF...............  145
AtUev1A  EDILVKLEK.EMMTSHNRKLAQPPEGNEEARADPKGPAKCCVM.   158
AtUev1B  EDLLIQLEK.EMMSSQNRKLAQPLEGNEEGRTDPKGLVVKCCVM  159
AtUev1C  EDILTQLEK.EMAASHNRKLVQPPEGTFF...............  145
AtUev1D  EDILVQLEK.EMSTSHNRKLVQPPEGTCF...............  146
MmMms2   KVILQELPR.LMMSKENMKLPQPPEGQTYNN.............  145
MmUev1   KVILQELPR.LMMSKENMKLPQPPEGQCYSN.............  147
HsMms2   KVVLQELPR.LMMSKENMKLPQPPEGQTYNN.............  145
HsUev1A  KVVLQELPR.LMMSKENMKLPQPPEGQCYSN.............  170
```

62

Figure 3-1 Sequence analysis of *AtUEV1* genes and their products.

(A) Genomic organization of *UEV1*. Open boxes, untranslated region; closed boxes, coding regions; solid lines, introns; dotted lines, identical intron–exon alignment between different *UEV1* genes.

(B) Amino acid sequence alignment of AtUev1 and Uevs from six other organisms. The sequences were aligned and edited using a BioEdit program version 5.0.9 (Hall, 1999). Residues are highlighted when 50% of them are identical. Critical residues for Mms2/Uev functions are indicated with asterisks underneath the residue. The GenBank accession numbers for different organisms are: Sc, *S. cerevisiae* (NP_011428.1); Sp, *Schizosaccharomyces pombe* (NP_588162.1); Dm, *Drosophila melanogaster* (NP_647959.1); Mm, *Mus musculus* (NP_076074.2); At, *Arabidopsis thaliana*, AtUev1A=NP_565834.1, AtUev1B=NP_564994.1, AtUev1C=NP_850259.1, AtUev1D=NP_566968.1; Ce, *Caenorhabditis elegans* (NP_493578.1); Hs, *Homo sapiens*, hMms2=NP_003341.1, hUev1A= NP_068823.2.

In addition, phylogenetic analysis was performed on AtUev1s in relation to Uevs from model organisms (Figure 3-2) as well as with known genomic sequence from other plant species. This analysis revealed that plant *UEV1* genes evolved from a common *UEV1/MMS2* ancestor, which were duplicated and further evolved within each species. Hence, it would be of great interest to examine whether or how functions have evolved in the *UEV* family of genes.
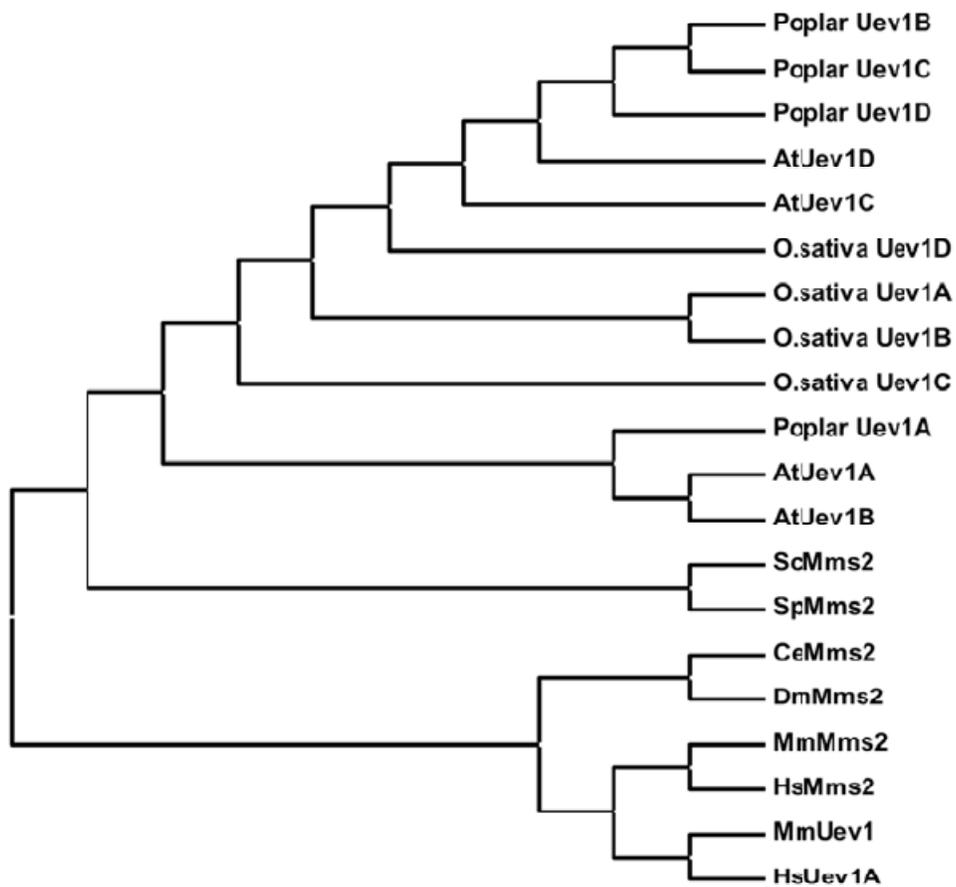
Figure 3-2 Phylogenetic analyses of hypothetical Uev family proteins from different organisms. The similarity clustering was conducted by using MEGA version 3 (Tamura et al., 2007). High similarity is indicated by the short branch length between any two sequences. Source of sequences: *O. sativa* Uev1A: NP_001054312.1; Uev1B: NP_001062804.1; Uev1C: NP_001051063.1 and Uev1D: NP_001067224.1. Poplar (*Populus trichocarpa*) Uev1A: CX655441; Uev1B: AJ767274, Uev1C: DT525203 and Uev4: BU894366. The above gene names are arbitrary for the purpose of comparison only.

3.2.2 Physical interaction of AtUev1 with Ubc13 from different species

Both yeast and human Uevs play an essential role in Ubc13-mediated Lys63–linked polyubiquitination, and the prerequisite of this activity is that the Uev has to form a stable complex with Ubc13 (Hofmann and Pickart, 1999, 2001; McKenna et al., 2001). In order to detect this interaction, a yeast two hybrid assay (Fields and Song, 1989) between the cloned *AtUEV1*s and *UBC13* genes from different species was carried out. This work was done by Dr. Xiaoqin Lai in Dr. Xiao's Lab. All four AtUev1 proteins were able to interact with either AtUbc13A or AtUbc13B; however, the strength of interaction appears to be different. AtUev1A and AtUev1B gave positive results with AtUbc13s under high stringency (SD-Ade for 3 d), but AtUev1C and AtUev1D gave weak and no interaction, respectively, under the same conditions (Figure 3-3A). Nevertheless, all of the above interactions are robust and deemed strong, as none of the negative controls reveals positive interactions under low stringency and many bona fide positive interactions may not survive as low as 1 mM 1, 2, 4-aminotriazole concentration under the same experimental conditions. The *AtUEV1D*-4 clone was identified among initial *AtUEV1D* clones; its ORF contains a three-nucleotide (GTA) insertion at position 175 that would encode the additional amino acid Val. This has been predicted to be a splicing variant of *AtUEV1D* (At3g52560.2) in the Arabidopsis genome database. AtUev1D-4 appears to be able to interact with Ubc13, albeit at a reduced affinity compared with Uev1D (Figure 3-3A). The physiological significance of this variant has yet to be investigated. In addition, the yeast two-hybrid analyses showed that all four AtUev1 proteins are able to physically interact with Ubc13 from yeast or human, and the strength of interaction follows the trend AtUev1A >AtUev1B > AtUev1C > AtUev1D (Figure 3-3B and Figure 3-3C).
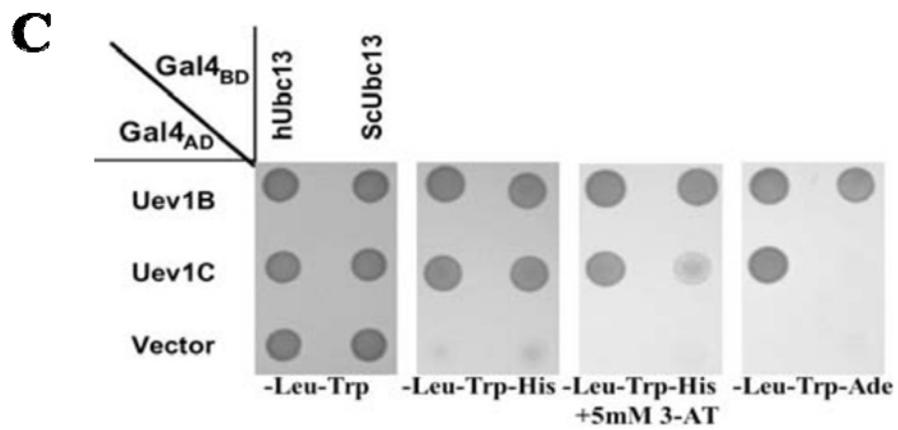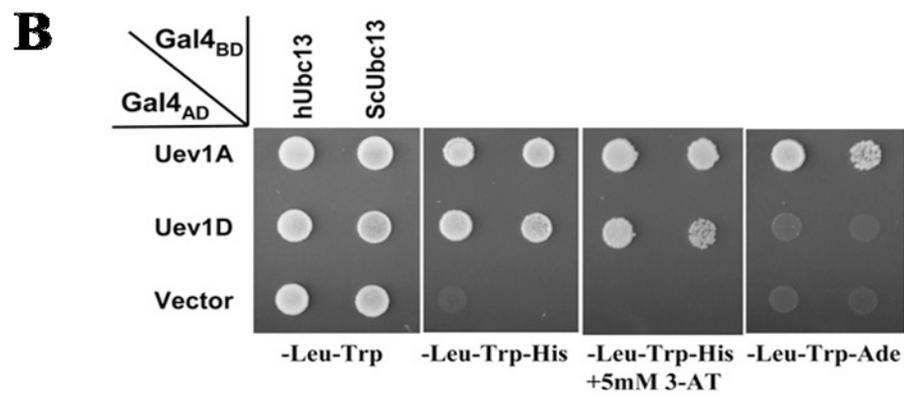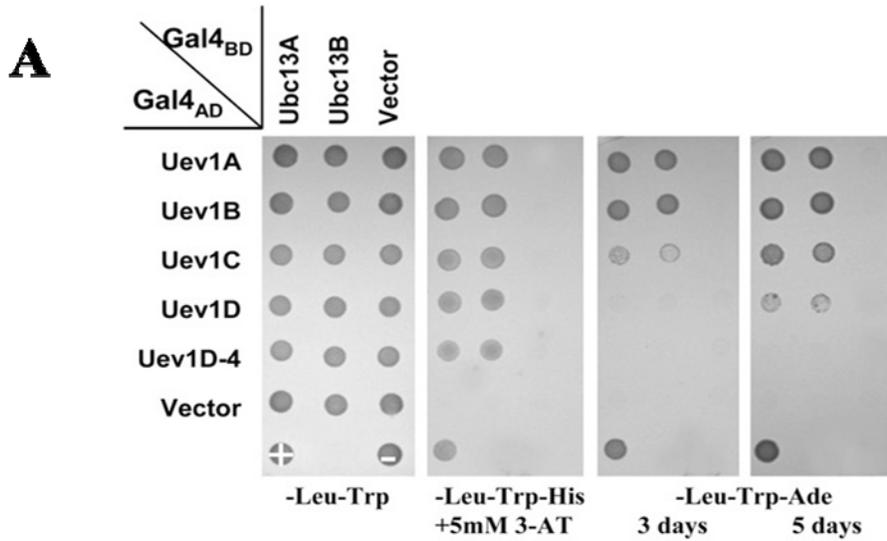
Figure 3-3 Physical interactions between Ubc13 and Uev1 in a yeast two-hybrid assay.

(A) The PJ69-4A transformants carrying one $Gal4_{AD}$ (from pGAD424) and one $Gal4_{BD}$ (from pGBT9) were replicated onto various plates as indicated and incubated for 3 d or as specified before being photographed. The result is representative of at least five independent transformants from each treatment.

(B) Physical interactions between AtUev1A/D, and Ubc13 from yeast or human in a yeast two-hybrid assay. Experimental conditions were the same as in (A). (C) Physical interactions between AtUev1B/C and Ubc13 from yeast or human in a yeast two-hybrid assay. Experimental conditions were the same as in (A).

To further confirm the physical interaction between AtUev1 and AtUbc13 *in vitro*, a glutathione S-transferase (GST)–affinity pull-down assay was conducted. As shown in Figure 3-4A, purified GST-Uev1A (lane 6) and GST-Uev1D (lane 7) are able to specifically interact with AtUbc13A. As a negative control, GST alone (lane 5) did not bind to AtUbc13A under the same experimental conditions. Similar results were also obtained with AtUev1B and AtUev1C (Figure 3-4B). Hence, all four AtUev1 proteins are able to form stable heterodimers with AtUbc13.
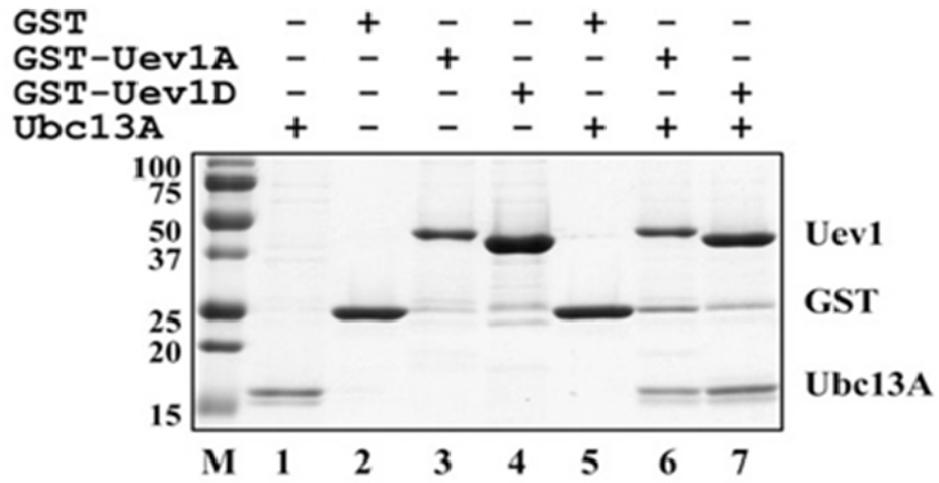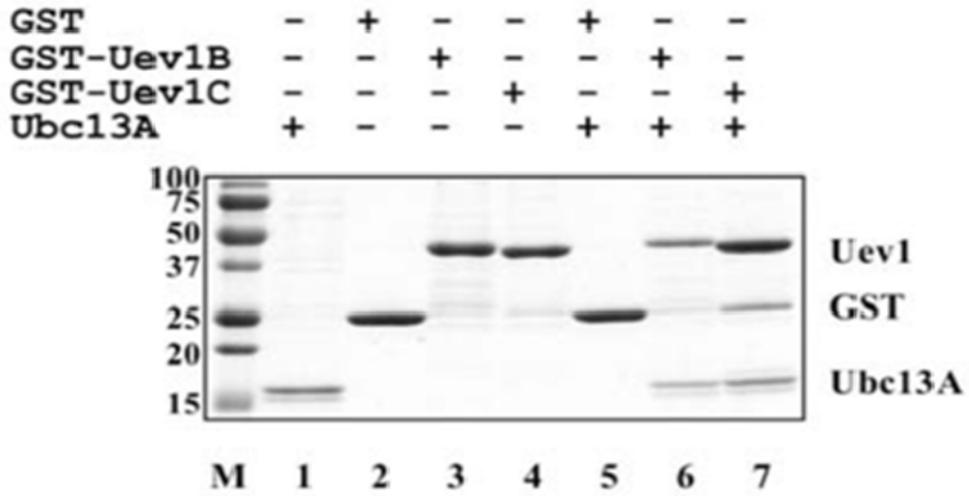
Figure 3-4 Protein interactions between Uev1A/D, Uev1B/C and Ubc13 by an affinity pulldown assay. Purified GST (lane 2 in A and B), GST-Uev1A, GST-Uev1B (lane 3 in A and B), or GST-Uev1D, GST-Uev1C (lane 4 in A and B) were added to GST microspin columns. Following incubation, the columns were spun and washed, and purified Ubc13A was added to the column. After reincubation and washing, the column contents were eluted with reduced glutathione, followed by SDS-PAGE gel analysis. Lanes 1 to 4 contain purified input proteins as indicated at top. Lanes 5, 6 and 7 show the eluent from the column preloaded with GST (lane 5) and GST-Uev1A/B (lane 6) and GST-Uev1D/C (lane 7). Note that spontaneous cleavage occurred in the four GST-Uev1 protein samples (lanes 3 and 4 in A and B).

3.2.3 Uev1 is required for Ubc13-mediated Lys63–linked polyubiquitination *in vitro*

It has been reported that yeast and human Ubc13s are bona fide E2 enzymes capable of forming active-site thioesters with Ub, and a Uev is absolutely required for Ub chain assembly. Furthermore, these chains are linked through Lys63 instead of the conventional Lys48 linkages (Hofmann and Pickart, 1999, 2001; McKenna et al., 2001) That the cloning and characterization of the *AtUBC13* genes was previously reported (Wen et al., 2006). With the cloning of the *UEV1* genes in this study, we were able to ask whether Ubc13 requires Uev1 for the assembly of Lys63– linked poly-Ub chains and this work was done by Dr. Landon Pastushok in Dr. Xiao's Lab. As shown in Figures 3-5A and 3-5B, Uev1A/1B and Uev1D/1C alone cannot generate free poly-Ub chains (lanes 2 and 6 in Figures 3-5A and 3-5B, respectively). Ubc13A with Uev1A/B (lane 3 in Figure 3-5A and 3-5B) and Uev1D/C (lane 7 in Figures 3-5A and 3-5B) can generate di- and tri-Ub chains. Furthermore, the poly-Ub chains generated are linked through Lys63, since poly-Ub conjugates were not detected when using a Ub-K63R mutant that lacks Lys63 (lanes 4 and 8 in Figure 3-5A and 3-5B), but were detected when using the Ub-K48R mutant that lacks the predominant Lys48 residue for conjugation but retains Lys63 (lanes 5 and 9 in Figure 3-5A and 3-5B).

A

Ubc13A	+	–	+	+	+	–	+	+	+
Uev1A	–	+	+	+	+	–	–	–	–
Uev1D	–	–	–	–	–	+	+	+	+
Ub	+	+	+	–	–	+	+	–	–
Ub–K63R	–	–	–	+	–	–	–	+	–
Ub–K48R	–	–	–	–	+	–	–	–	+

Ub₃
Ub₂
Ub

1 2 3 4 5 6 7 8 9

B

Ubc13A	+	–	+	+	+	–	+	+	+
Uev1B	–	+	+	+	+	–	–	–	–
Uev1C	–	–	–	–	–	+	+	+	+
Ub	+	+	+	–	–	+	+	–	–
Ub–K63R	–	–	–	+	–	–	–	+	–
Ub–K48R	–	–	–	–	+	–	–	–	+

Ub₃
Ub₂
Ub

1 2 3 4 5 6 7 8 9
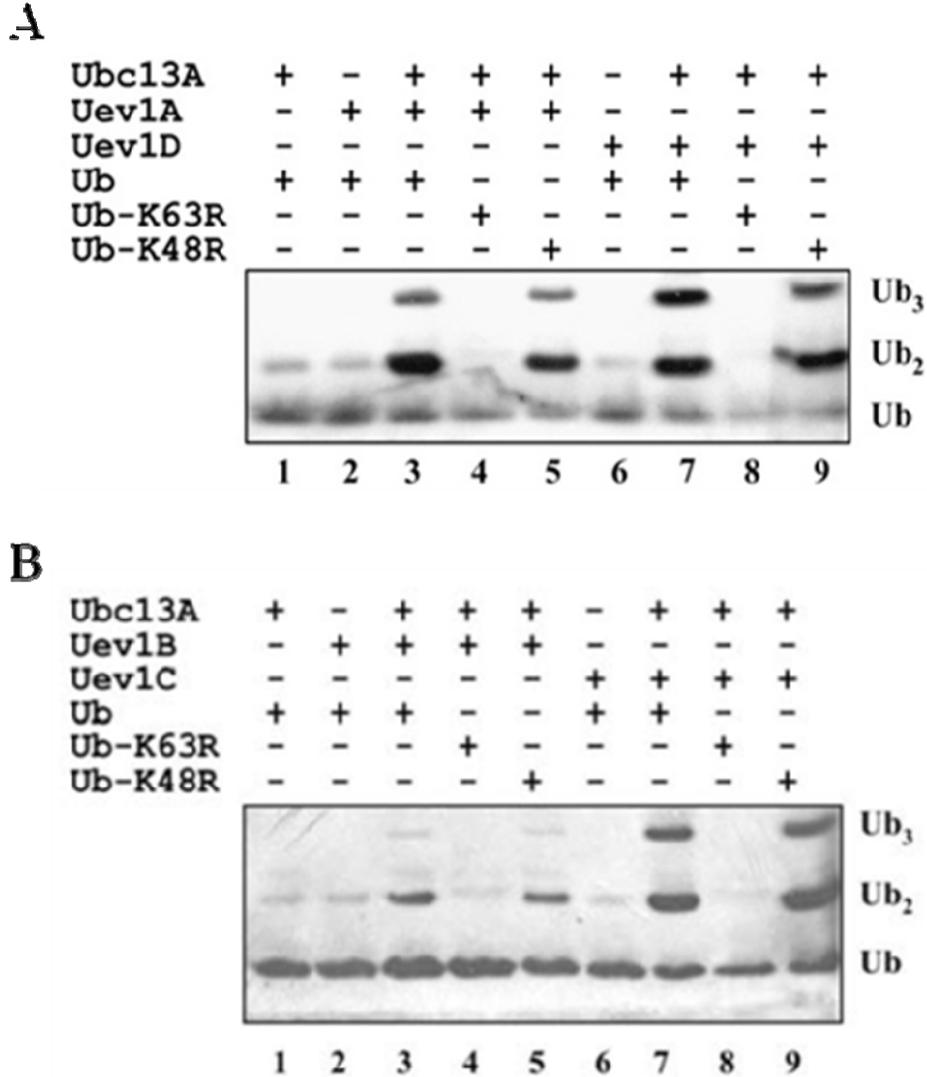
Figure 3-5 Ub conjugation by *Arabidopsis thaliana* Ubc13, Uev1A, Uev1D, Uev1B and Uev1C. An *in vitro* Ub conjugation assay was performed using purified proteins as indicated. Assay samples were subjected to SDS-PAGE, and a protein gel blot using an anti-Ub antibody was assayed to monitor poly-Ub formation. The low background of spontaneously formed di-Ub in the absence of E2 or Uev (lanes 1, 2, and 6 in A and B) is commonly observed in these reactions (McKenna et al., 2001).

3.2.4 *AtUEV1* genes functionally complement yeast *mms2* null mutants

Yeast *MMS2* is a member of the error-free DDT pathway and plays an important role in protecting yeast cells from mutagenesis and cell death caused by DNA-damaging agents (Broomfield et al., 1998). Therefore a yeast killing (work done by Lindsay Pelzer in Dr. Xiao's Lab) and spontaneous mutagenesis assays were performed to determine whether *AtUEV1* could functionally complement the error-free PRR defect in the yeast. Any one of the *AtUEV1* genes from the yeast two-hybrid plasmid rescued the *mms2* mutant from killing by MMS to a level comparable to that in wild type cells, whereas *mms2* mutant cells transformed with the vector alone did not acquire any MMS resistance. It is interesting that the *AtUEV1D-4* clone also provides protection to *mms2* cells, albeit at a slightly reduced level (Figure 3-6A). The complementation of yeast *mms2* relies on heterodimer formation between AtUev1 and yeast Ubc13. In order to assess *in vivo* complex formation and functions between *Arabidopsis thaliana* Uev1 and Ubc13, yeast *mms2ubc13* double mutant was created and co-transformed with *AtUEV1* and *AtUBC13*. When the double mutant cells were transformed with only *AtUBC13* or *AtUEV1*, the transformed cells did not display enhanced resistance to MMS (Figures 3-6B and 3-6C), indicating that both Ubc13 and a Uev are required for the DDT function. Interestingly, when combined with *AtUBC13*, *AtUEV1C* and *AtUEV1D* completely restored the MMS resistance to the wild type level, whereas *AtUEV1A* and *AtUEV1B* barely rescued the host cells (Figures 3-6B and 3-6C). This result is in sharp contrast with the observations that all *AtUEV1*s functioned equally well in the complementation of yeast *mms2* single mutant (Figure 3-6A) and that Uev1A/B displayed higher binding

capacity to Ubc13A/Ubc13B than those of Uev1C/D in yeast two-hybrid assays (Figure 3-3A). One of the most astonishing phenotypes of a yeast *mms2* (Broomfield et al., 1998) or *ubc13* (Brusky et al., 2000) mutant is its massive increase in spontaneous mutagenesis, indicating that these genes play an important role in protecting cells from genome instability. Indeed, in this experiment, the *mms2* mutant strain showed an increase of >20-fold in spontaneous mutagenesis compared with wild type cells (Table 3-1). When the same *mms2* mutant was transformed with a plasmid expressing an *AtUEV1*, the spontaneous mutation rate was reduced to a level similar to that of the wild type cells. Again, *AtUEV1C* and *AtUEV1D* appear to be more effective than *AtUEV1A* and *AtUEV1B* in limiting mutagenesis. Collectively, the results obtained from the yeast complementation experiments suggest that *AtUEV1* genes are able to replace the PRR function of yeast *MMS2* and that *AtUEV1C* and *AtUEV1D* are more efficient than *AtUEV1A* and *AtUEV1B* in such a function in *Arabidopsis thaliana*.

A

WT
mms2Δ
pGAD
pGAD-Uev1A
pGAD-Uev1B
pGAD-Uev1C
pGAD-Uev1D
pGAD-Uev1D-4

YPD   YPD + 0.025% MMS

B

WT
mms2Δ ubc13Δ
pGAD+pGBT-Ubc13A
pGAD-Uev1A+pGBT
pGAD-Uev1A+pGBT-Ubc13A
pGAD-Uev1D+pGBT
pGAD-Uev1D+pGBT-Ubc13A

YPD   YPD + 0.025% MMS

C

WT
mms2Δ ubc13Δ
pGAD+pGBT-Ubc13A
pGAD-Uev1B+pGBT
pGAD-Uev1B+pGBT-Ubc13A
pGAD-Uev1C+pGBT
pGAD-Uev1C+pGBT-Ubc13A

YPD   YPD + 0.025% MMS

76
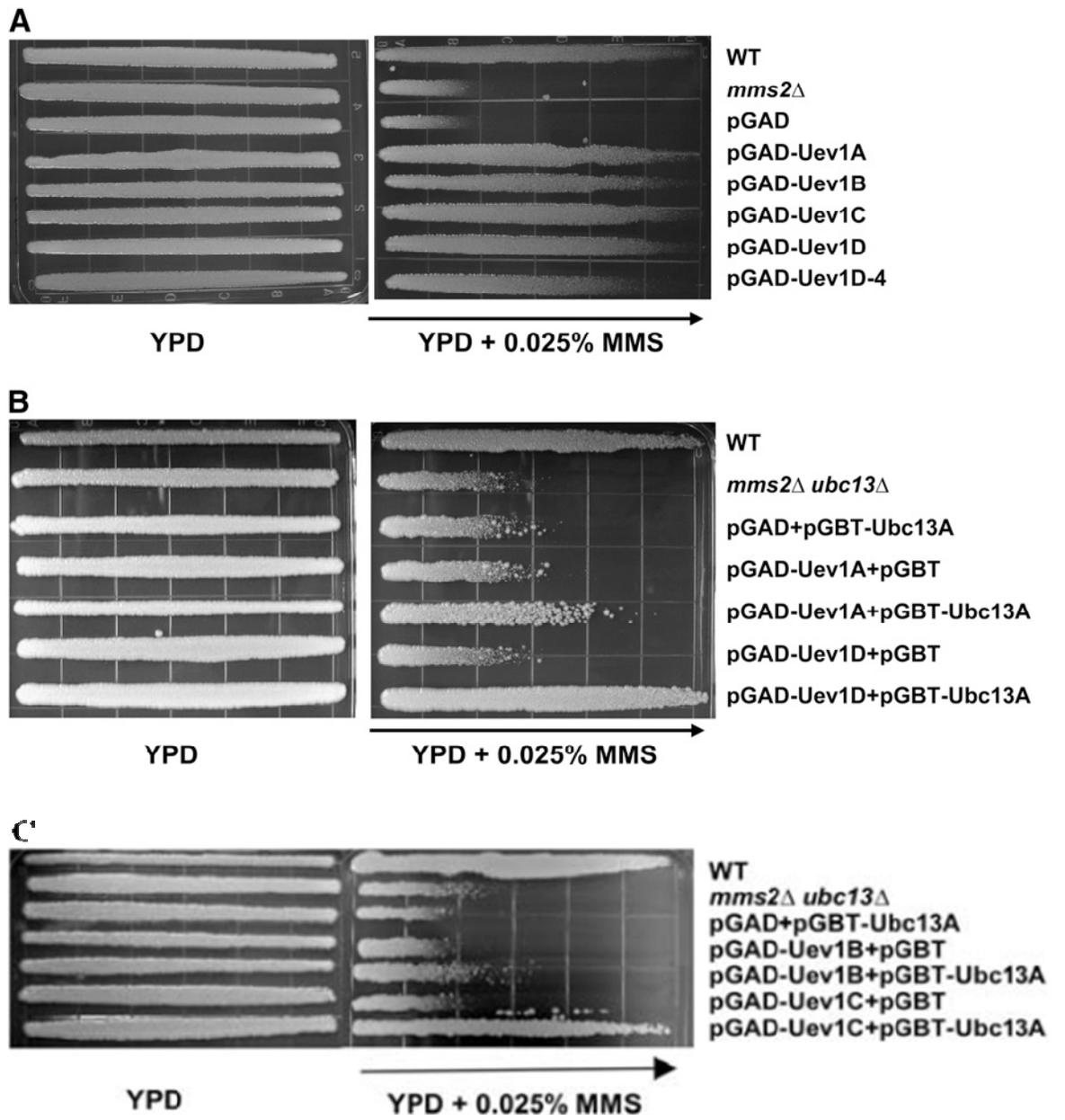
Figure 3-6 Complementations of yeast *mms2* mutants by *AtUEV1*

(A) Complementation of the *mms2* single mutant by *AtUEV1*. WXY942 (*mms2Δ*) transformants were grown overnight and printed onto YPD and YPD+0.025% MMS gradient plates. The plates were incubated at 30 °C for 2 d before being photographed. The arrow indicates higher MMS concentrations. Several transformants of each treatment were tested with the same result, and only one is shown here.

(B, C) Complementations of the *mms2 ubc13* double mutant (WXY955) by *AtUEV1A*, *AtUEV1D*, *AtUEV1B*, *AtUEV1C* and *AtUBC13*. Experimental conditions were the same as in (A).

Table 3-1   Effects of *AtUEV1* on the Spontaneous Mutation Rate of the

S. cerevisiae mms2 Mutant

Strain[a]	Key Alleles	Rate (X10^{-8})[b]	Fold[c]
DBY747	Wild type	3.2 ± 0.18	1.00
WXY642/pGAD424	mms2 Δ	70.2 ± 7.96	22.10
WXY642/*AtUEV1A*	mms2 Δ *AtUEV1A*	8.1 ± 0.16	2.53
WXY642/*AtUEV1B*	mms2 Δ *AtUEV1B*	7.1 ± 0.13	2.22
WXY642/*AtUEV1C*	mms2 Δ *AtUEV1C*	5.3 ± 0.98	1.66
WXY642/*AtUEV1D*	mms2 Δ *AtUEV1D*	4.9 ± 0.56	1.53

[a] All strains are isogenic derivatives of DBY747.

[b] The spontaneous mutation rates are the average of three independent experiments with standard deviations.

[c] Relative to the wild-type mutation rate.

3.2.5 *AtUEV1* expression in different tissues and under stresses

Since *UEV1* is presumed to be involved in DDT and the ubiquitination process is often involved in stress responses, the *UEV1* expression under various stress conditions have been analyzed. *Arabidopsis thaliana* cell suspension culture was subjected to treatments as indicated and total RNA was isolated for RNA gel blot hybridization. The results from samples of 24-h treatments are presented in Figure 3-7A. It appears that *UEV1* expression is decreased after treatment with MMS or H_2O_2 and increased after treatment with abscisic acid or mannitol, although for the latter two treatments, the transcript level of the control *UBQ11* was also higher. Since all four *UEV1* genes share >72% nucleotide sequence identity in their core coding region and all four predicted transcripts are similar in size, it is suspected that the *UEV1C* probe used for RNA gel blot hybridization actually detected all four *UEV1* transcripts. Given the fact that the two human Uev homologs (*UEV1A* and *hMMS2*) play distinct roles in cellular metabolism (Andersen et al., 2005) and the observation in this study that the two pairs of *UEV1* genes may function differently, it is important to assess the expression of individual *UEV1* genes, to fulfill this objective, the existing microarray data (available from www. Arabidopsis.org) for individual *UEV1* gene expression profiles have been analyzed and found no evidence of strong stress responses after treatment of *Arabidopsis thaliana* plants (Figure 3-7B). This analysis suggests that various environmental stresses used in this study have little effect on the expression of *UEV1* genes at the transcriptional level. The expression of *UEV1* genes in different tissues was also determined by RNA gel blot hybridization (Figure 3-7C) and by analyzing the microarray data (Figure 3-8A, this work

done by Dr. J. Antonio Torres-Acosta in Dr. Wang's Lab). While most tissues express variable levels of each *UEV1* transcript, *UEV1D* appears to show a higher level of expression than the other three *UEV1* genes in most tissues examined (Figure 3-8A). Greater differences in transcript levels of the *UEV1* genes were found in samples from pollen and geminating seeds. The microarray data indicated that 3 h after seed germination, the expression of *UEV1C* and *UEV1D* was much higher than that of *UEV1A* and *UEV1B* and that *UEV1D* was essentially the only *UEV1* transcript detected from pollen. To validate the microarray data, Dr. J. Antonio Torres-Acosta and I performed RT-PCR with various tissues, including germinating seeds and pollen. Under the conditions used, the amount of PCR product was not excessive and was deemed to reflect the amount of cDNA template. Representative results were shown in Figure 3-8B and summarized as follows. Firstly, all four *UEV1* genes were indeed expressed in most common tissues, such as root, shoot, leaf and stem. Secondly, only *UEV1D* transcript was detectable in pollen under our experimental conditions, consistent with the microarray data. Thirdly, 6 h after seed germination, all transcripts except for *UEV1B* were detected, while after 2 d of seed germination, only *UEV1A* and *UEV1D* transcripts were found, with *UEV1D* at a clearly higher level than *UEV1A*. Microarray data show little expression of *UEV1A* in 3-h germinating seeds, but we consistently observed *UEV1A* transcript by PT-PCR in the sample used. These differences may result from the conditions used in the microarray experiments and in this study.
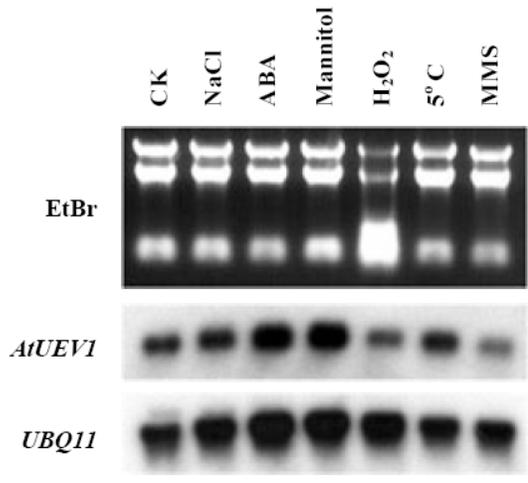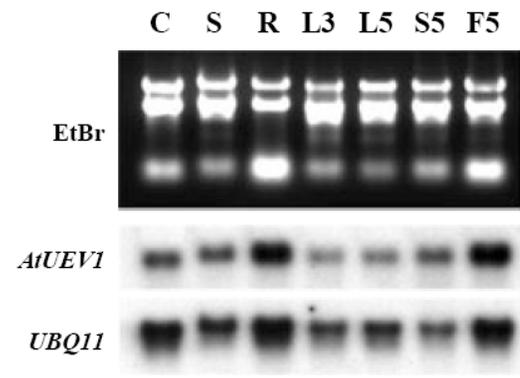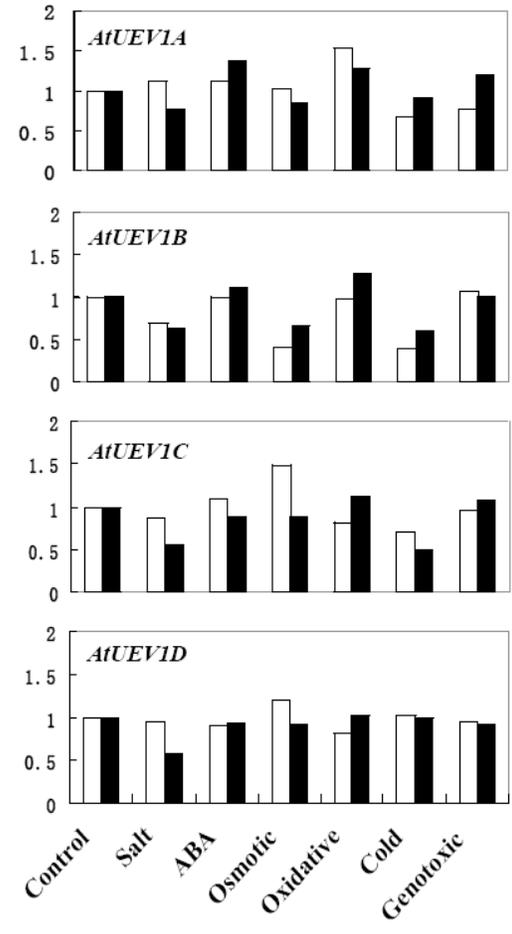
Figure 3-7 *AtUEV1* expression profiles

(A) Northern hybridization measuring *AtUEV1* transcript levels from cell suspension culture under 24-h stress. Each lane contains 15 μg of total RNA from different samples. The treatments were: CK, control; NaCl, 300 mM; ABA, 20uM (+)-abscisic acid; mannitol, 400 mM; H_2O_2, 20 mM; 5 ℃, low temperature; and MMS, 0.01%. Abnormal rRNA profile after H_2O_2 treatment was repeatedly observed.

(B) Graphic presentation of data extracted from microarray analyses in www.arabidopsis.org and expressed as relative levels to the untreated control. Tissue sources (except ABA): open bars, shoots; solid bars, roots. The conditions for the treatments and source of information (TAIR accession No.) were: NaCl, 150 mM (1007966888); ABA, 10 μM (1007964750); mannitol, 300 mM (1007966835) for osmotic stress; methyl viologen, 10 μM (1007966941) for oxidative stress; 5 ℃ (1007966553) for cold stress; and bleomycin (1.5 μg/ml) plus mitomycin (22 μg/ml) (1007966782) for genotoxic treatment. All treatments were for 24 h except for ABA treatments, which were seedlings treated for 1 h (open bars) and 3 h (solid bars).

(C) Measuring *UEV1* transcript levels from different tissues by Northern hybridization. Each lane contains 20 μg of total RNA from different tissues: C, cell suspension culture; S, shoot of 13-day seedlings; R, root of 13-day seedlings; L3, leaves of 3-week plants; L5, leaves of 5-week plants; S5, stems of 5-week plants; and F5, floral tissues of 5-week plants.
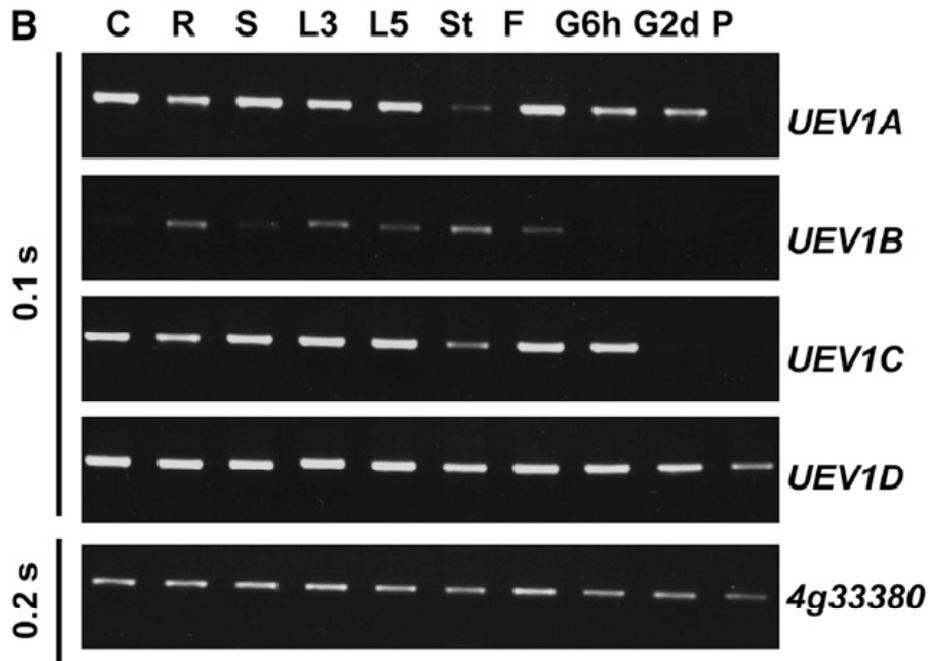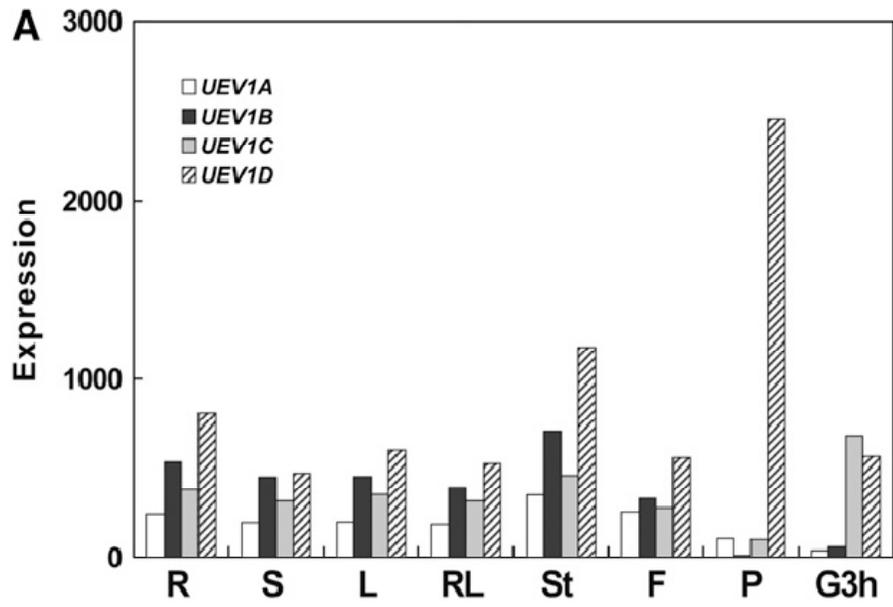
Figure 3-8 Tissue distribution of *UEV1* expression

(A) Relative expression of *UEV1* transcripts in different tissues was determined using data from the Arabidopsis NASCArrays microarray database (http://affymetrix.Arabidopsis.info/narrays/experimentbrowse.pl) (Craigon et al., 2004). R, roots of 17-d plants; S, shoots of 8-d seedlings; L, rosette leaf 2 of 17-d plants; RL, mature rosette leaves of 23-d plants; St, second internode of 21-d plants; F, stage 12 flowers of 21-d plants; P, mature pollen; G3h, seed germinating for 3 h. The original microarray data are from AtGenExpress: Expression Atlas of Arabidopsis Development (TAIR accession number 1006710873: ATGE_9, ATGE_12, ATGE_24, ATGE_27, ATGE_33, ATGE_73, and ATGE_96 samples) (Schmid et al., 2005), except for G3h data, which are from AtGenExpress: Expression Profiling of Early Germinating Seeds (TAIR accession number 1007966994: RIKEN-PRESTON2 sample).

(B) Expression of *UEV1* transcripts in different tissues analyzed by RT-PCR. The At4g33380 gene was assayed as an input control (Czechowski et al., 2005). The exposure time of the gels is shown at left (BioDoc-It System; UVP). C, cell suspension; R, roots of 13-d seedlings; S, shoots of 13-d seedlings; L3, leaves of 3-week plants; L5, leaves of 5-week plants; St, stems of 5-week plants; F, floral tissues of 5-week plants; G6h and G2d, seeds germinating on Petri dishes for 6 h and 2 d, respectively; P, pollen.

3.2.6 *Atuev1d* mutant plants are sensitive to the DNA damaging agent MMS

The analysis of *UEV1* expression as well as the observation that in combination with *UBC13*, *UEV1D* but not *UEV1A* or *UEV1B* could completely rescue the yeast *ubc13 mms2* double mutant, prompted us to focus our attention on *UEV1D*. We reasoned that *uev1d* mutant plants may display compromised tolerance to DNA damage in pollen and during seed germination. The *UEV1D* T-DNA insertion line SALK_064912 was obtained from the ABRC (www.arabidopsis.org), and the allele was named *uev1d-1*. Sequence analysis revealed that the T-DNA was inserted in the first intron of *UEV1D*, with the left border oriented toward the 3' end of the gene (Figure 3-9A). The gene-specific primers (SP1 and SP2) and a primer specific to the left border sequence (LB1) were used to confirm the insertion of T-DNA (Figure 3-9B). To further confirm that *UEV1D* expression was abolished by this T-DNA insertion, total RNA was extracted from seedlings of wild type and homozygous *uev1d-1* plants and analyzed by RT-PCR for the expression of four *UEV1* genes. As shown in Figure 3-9D, a fragment corresponding to the *UEV1D* ORF could be amplified from wild type plants but not from the *uev1d-1* line, while the expression of the other three *AtUEV1* genes remained unaltered. The homozygous *uev1d-1* plants did not display apparent morphological variations. In order to investigate the possible role of *UEV1D* in protecting cells from DNA damage, the effect of MMS on seed germination was analyzed, considering that *UEV1D* is strongly expressed during seed germination. Three control: wild type *Arabidopsis thaliana* ecotype Columbia, a T-DNA insertion line (SALK_042050) not affecting *UEV1* genes, and a wild type segregant line derived from the initial SALK_064912 seeds (1d-1WT) -

along with the homozygous *uev1d-1* T-DNA insertion line were examined. Three parameters related to seed germination were surveyed. Firstly, the percentage of seeds that germinated in the presence of various concentrations of MMS was scored after a 5-d incubation. Seeds from *uev1d-1* plants were much more sensitive to MMS treatment than any of the three control plants, and this response was dose-dependent (Figure 3-10A). By contrast, in the absence of MMS, the *uev1d-1* seeds did not show a noticeable difference from controls in the percentage of seed germination. Secondly, it was observed that the homozygous *uev1d-1* seedlings were dying relatively quickly in the presence of MMS and displayed bleached pale cotyledons rather than the normal green cotyledons. Thus, the percentage of germinated seeds with green cotyledons was scored after 13 d. The data clearly indicated that the *uev1d-1* line had reduced numbers of viable seedlings in the presence of MMS. In particular, in the presence of 0.01% MMS, 75 to 90% of control seedlings were viable, as judged by green seedlings, compared with <15% viable *uev1d-1* seedlings under the same growth condition (Figures 3-10B and 3-10C). Finally, the average fresh weight of 13-d *uev1d-1* mutant seedlings was reduced compared with that in control seedlings after MMS treatments. More specifically, with 0.005% MMS treatment, even though almost all *uev1d-1* seedlings remained green, they only had half the fresh weight of the wild type seedlings (Figure 3-10D).

To ensure that the above observations were specific to the T-DNA insertion at *UEV1D*, the second *UEV1D* T-DNA insertion line SALK_052144 was obtained from the ABRC, in which the T-DNA was inserted in the third exon of *UEV1D* (Figure 3-9A). The T-DNA insertion was confirmed by genomic PCR (Figure 3-9C). RT-PCR analysis demonstrated that the *UEV1D* mRNA was absent in the homozygous T-DNA line (Figure

3-9D) and thus the mutant is named *uev1d-2*. Phenotypic analyses showed that, like

uev1d-1, the *uev1d-2* mutant is hypersensitive to MMS treatment during seed germination

(Figures 3-10E and 3-10F). From these results, we conclude that *UEV1D* is required for

tolerance to DNA damage during seed germination.
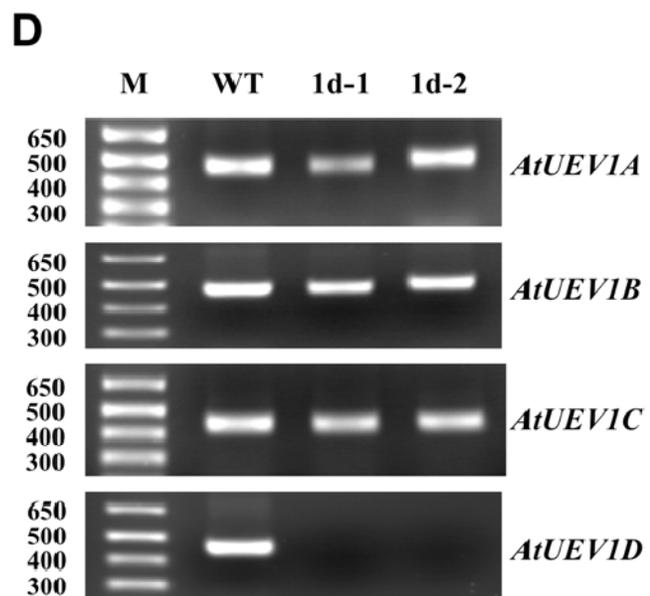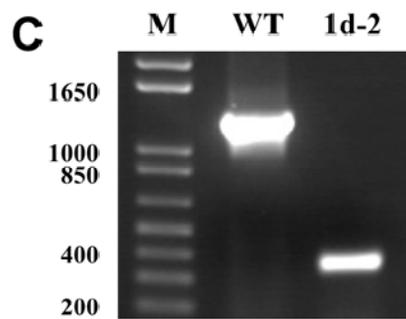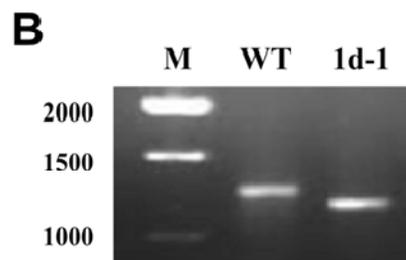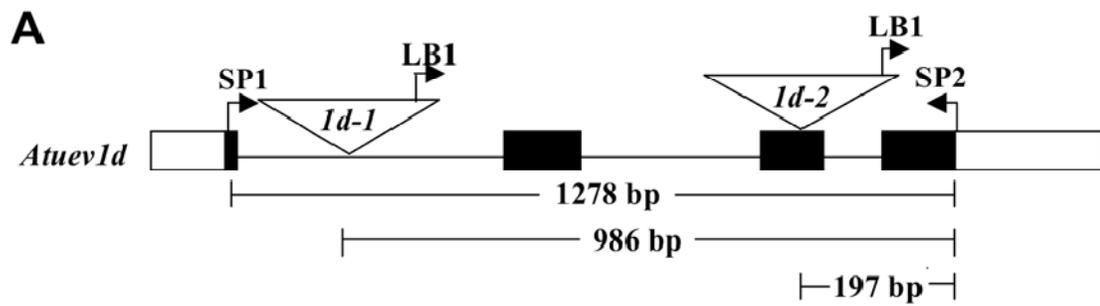
Figure 3-9 Confirmation of two *uev1d* T-DNA insertion mutants

(A) Genomic structure showing the positions of two T-DNA insertions in *UEV1D*. Open boxes, exons; closed boxes, *UEV1D* ORF; lines, introns. SP1, 5' gene-specific primer *AtUEV1D-1*; SP2, 3' gene-specific primer *AtUEV1D-2*; LB1, T-DNA left border primer.

(B) and (C) Genomic DNA PCR to confirm *uev1d-1* (1d-1) (B) and *uev1d-2* (1d-2) (C). The fragment was amplified using three primers (SP1, SP2, and LB1) in each reaction and genomic DNA from Columbia (WT), 1d-1 (B), or 1d-2 (C) as a template.

(D) RT-PCR detection of the *UEV1* transcripts. *UEV1* gene-specific primers were used for RT-PCR against total RNA extracted from Columbia (WT), *uev1d-1*, and *uev1d-2* lines. Total RNA was extracted from flowers.
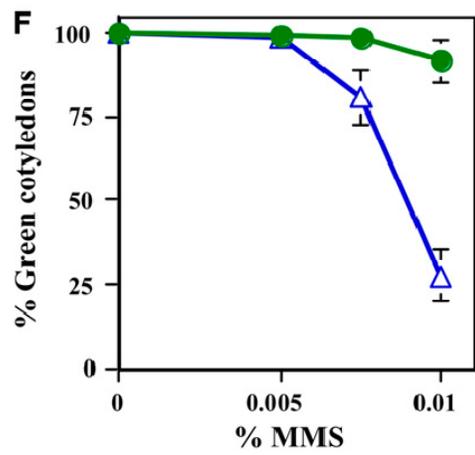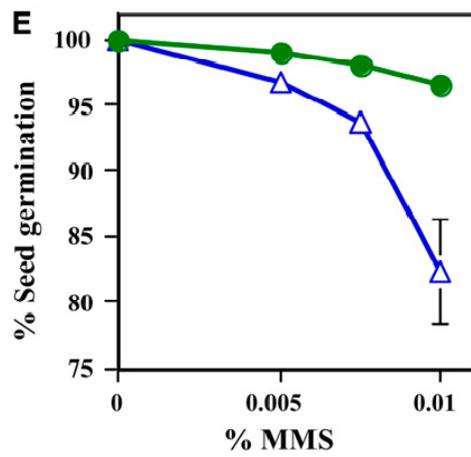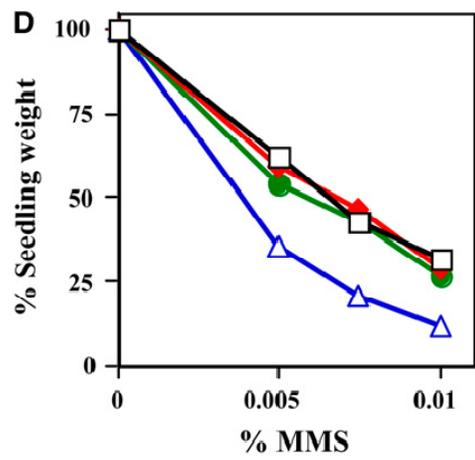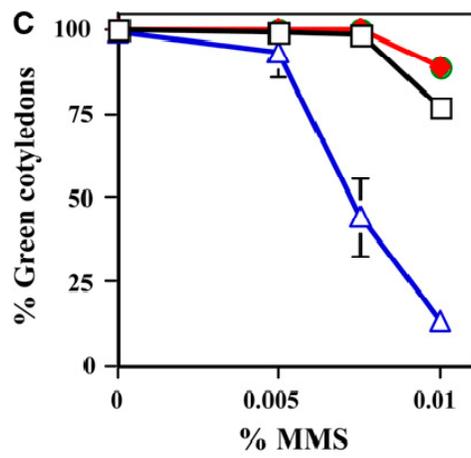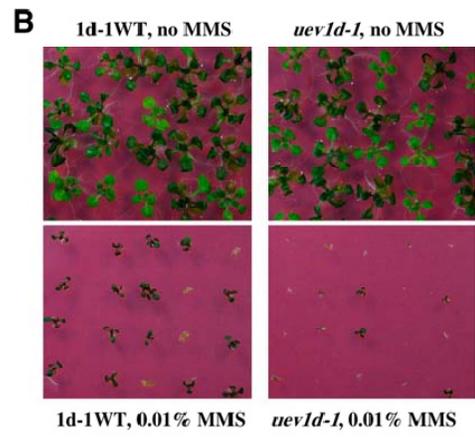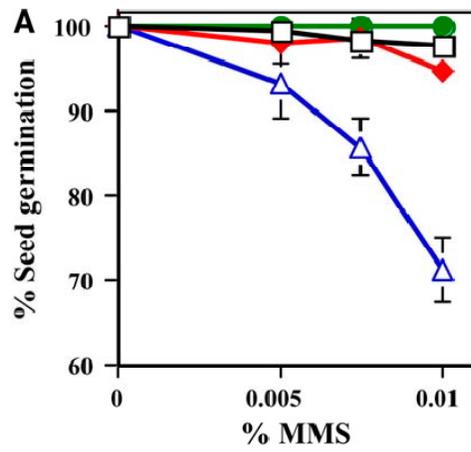
Figure 3-10 Phenotypic analysis of DNA damage response during seed germination

(A) to (D) The homozygous *uev1d-1* mutant (open triangles) is compared with three controls: Columbia (open squares), an unrelated T-DNA insertion line, SALK_042051 (closed diamonds), and a wild type segregant line from the same SALK_064912 seeds (1d-1WT; closed circles). Synchronized seeds were sown on half-strength Murashige and Skoog agar plates with or without MMS as indicated and incubated for the given period, and phenotypes were quantitatively assessed.

(A) Percentage of seed germination after 5 d seeding

(B) Representative photographs after 13 d seeding

(C) Percentage of seedlings with green cotyledons after 13 d seeding.

(D) Relative fresh weight of seedlings with green cotyledons after 13 d.

(E) and (F) The homozygous *uev1d-2* mutant (open triangles) is compared with 1d-2WT, a wild type segregant from the same T-DNA insertion line SALK_052144 (closed circles).

(E) Percentage of seed germination after 5 d seeding.

(F) Percentage of seedlings with green cotyledons after 13 d seeding.

All data are averages of three independent experiments with SD.

We also attempted to assess the role of *UEV1D* in pollen germination by measuring the percentage of pollen germination in the presence of MMS. As shown in Figure 3-11, inactivation of *UEV1D* resulted in a moderate but significant decrease in pollen germination. In the presence of 0.005% MMS, 33% of wild type pollens germinated, while only 20% of *uev1d-1* pollen germinated after 8 h of incubation, indicating that *UEV1D* also plays a critical role in protecting pollen from environmental DNA damage.

A

1d-1WT, no MMS   *uev1d-1*, no MMS

1d-1 WT, 0.005% MMS   *uev1d-1*, 0.005% MMS

B

93
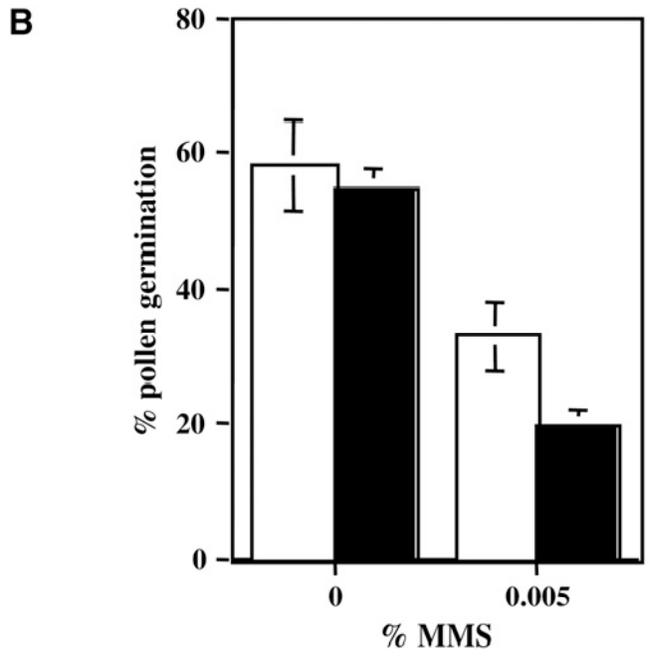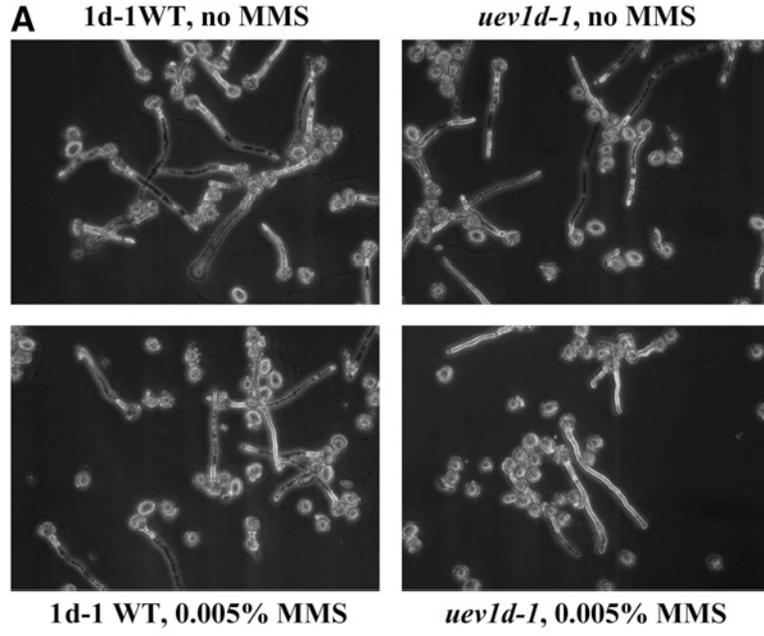
Figure 3-11 Phenotypic analysis of DNA damage response during *in vitro* pollen germination

(A) Representative in vitro pollen germination images of 1d-1WT and *uev1d-1* with or without MMS treatment as indicated.

(B) Summary of the pollen germination results. Data presented are averages of three independent experiments with SD. Open bars, 1d-1WT; closed bars, *uev1d-1*.

3.2.7 *Atuev1a* mutant plants do not display MMS sensitivity

Since *UEV1A* is the only other *UEV1* gene expressed during seed germination, we were interested in the phenotypes of this mutant plant. Unfortunately, a *uev1a* T-DNA insertion mutant line is not available from the ABRC; instead, we found a line (FLAG_128G02) with a T-DNA insertion at the fourth exon (Figure 3-12A) from the Institut Jean-Pierre Bourgin collection. We obtained this line, screened the segregants, and confirmed the homozygous *uev1a* mutant (*uev1a-1*) by both genomic PCR (Figure 3-12B) and RT-PCR (Figure 3-12C). Seed germination assays were performed under the same experimental conditions described above. *uev1a-1* mutant plants did not display enhanced MMS sensitivity in seed germination, percentage of cotyledon and fresh weight compared with its wild type segregants or with the parental strain Ws-4 (Figure 3-13). This result indicated that inactivation of *UEV1A* does not alter DDT during *Arabidopsis thaliana* seed germination.
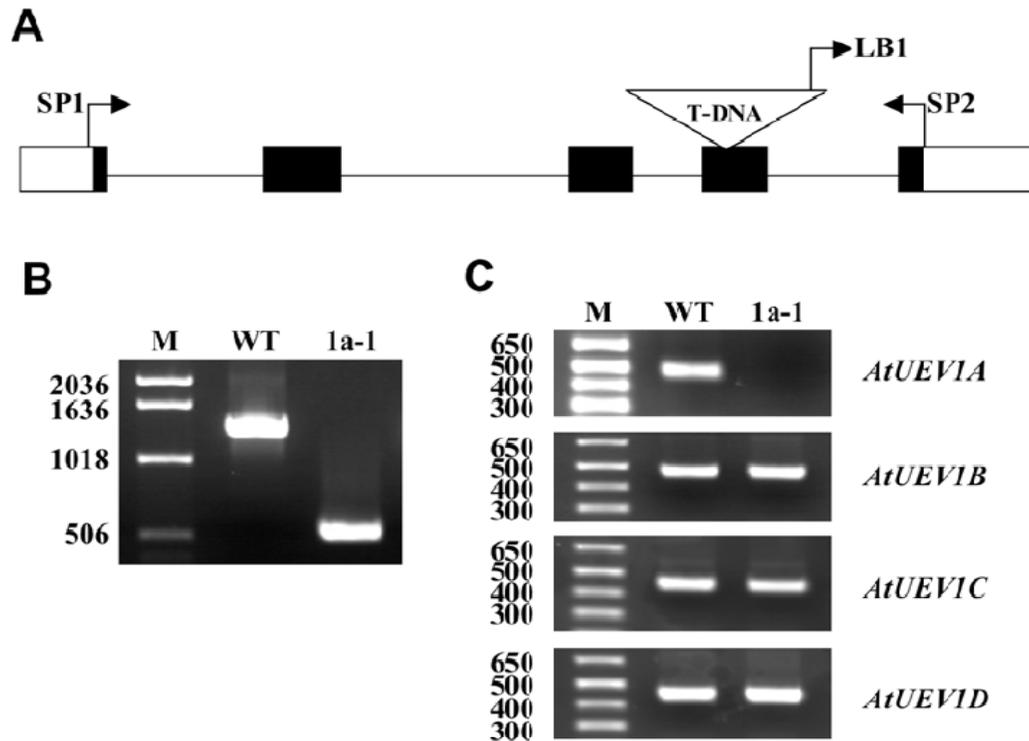
Figure 3-12 Confirmation of the *uev1a-1* T-DNA insertion mutant

(A) Genomic structure showing the positions of T-DNA insertions in *UEV1A*. Boxes represent exons, solid boxes represent *AtUEV1A* ORF and lines represents introns. SP1, 5' gene-specific primer AtUEV1A-1; SP2: 3' gene-specific primer AtUEV1A-2; LB1, T-DNA left border primer.

(B) Genomic DNA PCR to confirm *uev1a-1*. The fragment was amplified by using three primers (SP1, SP2 and LB1) in each reaction and genomic DNA from WS-4 (WT) or *uev1a-1* (1a-1) as a template. (C) RT-PCR detecting each of the *UEV1* transcripts. *AtUEV1* gene specific primers were used for an RT-PCR reaction against total RNA extracted from WS-4 (WT) and *uev1a-1* (1a-1) lines.

A

AtUev1a-WT   *Atuev1a*

0 ppm MMS

100 ppm MMS
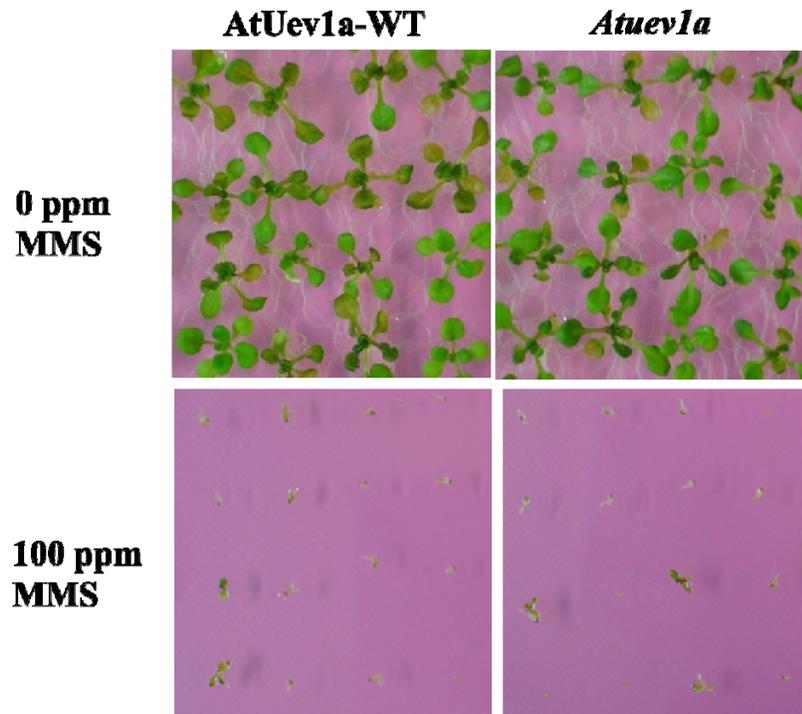
B
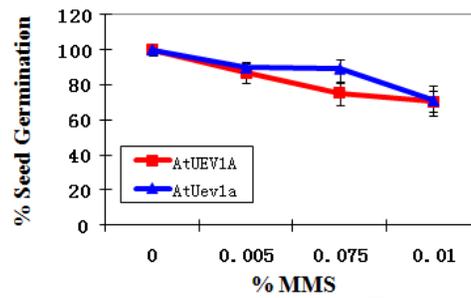
C
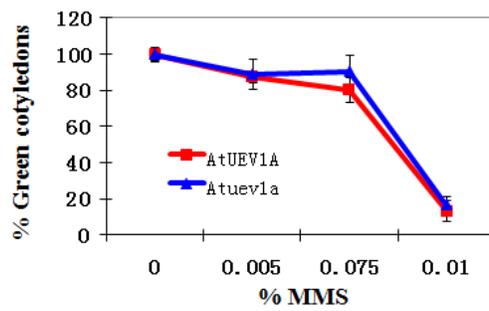
D
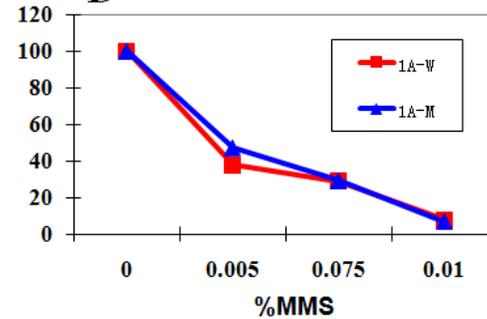
Figure 3-13 Phenotypic analysis of DNA damage response during seed germination

Synchronized seeds of the homozygous *Atuev1a* mutant (closed triangle), a wild type (WT, closed square) parental line, an unrelated T-DNA insertion line (1a-50, closed diamond) were sown on 1/2 MS agar plates with or without MMS as indicated, incubated for the given period and phenotypes were quantitatively assessed.

(A) Representative photographs after 13 d seeding.

(B) Percentage of seed germination after 5 d seeding.

(C) Percentage of seedlings with green cotyledons after 13 d seeding.

(D) Relative fresh weight of seedlings after 13 d seeding.

3.3 Discussion

3.3.1 *Arabidopsis thaliana* Uev1 promotes Lys63-linked polyubiquitination

Lys63-linked polyubiquitination of target proteins is considered to be a fundamentally different process from conventional Lys48-linked polyubiquitination that targets proteins for degradation via the 26S proteasome (Hochstrasser, 1996b; Pickart, 2001a). Instead, it is deemed analogous to other post-translational regulatory processes such as phosphorylation and sumoylation that alter the target protein activities. Lys63-linked polyubiquitination has been reported to be involved in several cellular processes including stress response (Arnason and Ellison, 1994), mitochondrial inheritance (Fisk and Yaffe, 1999), plasma membrane protein endocytosis (Galan and Haguenauer-Tsapis, 1997), ribosome function (Spence et al., 2000), innate immunity (Deng et al., 2000; Wang et al., 2001; Zhou et al., 2004), mitotic cell cycle checkpoint (Bothos et al., 2003), and DNA repair (Hoege et al., 2002; Hofmann and Pickart, 1999). The unique feature of Ubc13 compared to other Ubcs is its ability to form a stable complex with a Uev, which is homologous to other Ubcs but lacks the active Cys residue (Broomfield et al., 1998; Sancho et al., 1998). This family of Uevs engages a non-covalent interaction with Ub (McKenna et al., 2001) and orients this acceptor Ub to allow its Lys63 residue to be exposed to the C-terminus of donor Ub covalently bound to Ubc13 (McKenna et al., 2003; McKenna et al., 2001). It appears that in mammals, Uevs not only facilitate polyubiquitination but also serve as a regulatory subunit to promote ubiquitination of different targets (Andersen et al., 2005). In this study, we identified four *Arabidopsis thaliana* genes *UEV1A*, *UEV1B*, *UEV1C,* and *UEV1D*. Amino acid sequence alignments

with those of Uev proteins from six other eukaryotic organisms including human indicated 47 to 56% sequence identity and 65 to 75% sequence similarity between At Uev1s and those from other species. In addition, several critical residues such as Phe-13 and Ser-32 of hMms2 which are required for physical interaction with Ubc13 (Pastushok et al., 2005; Pastushok et al., 2007) and non-covalent interaction with Ub are all conserved in AtUev1s (Figure 3-1). In this study, we also demonstrated that all four Uev1 proteins can replace yeast MMS2 DDT functions in vivo (Figure 3-6), form a stable complex with AtUbc13 or with Ubc13 from yeast or human (Figures 3-3 and 3-4), and promote Ubc13-mediated Lys-63 polyubiquitination (Figure 3-5). The only known other *Arabidopsis thaliana* Uev so far is Cop10, which was identified as a negative regulator of photomorphogenesis and functioned in promoting target protein degradation (Suzuki et al., 2002)**.**

3.3.2 AtUev1D is involved in DNA damage tolerance

AtUEV1 is able to functionally complement the corresponding yeast mutant defective in DDT. However, we do not know whether AtUev1 plays the same role in *Arabidopsis thaliana*. Although four AtUevs have high nucleotide and amino acid sequence identities, we do not know whether all four AtUevs have the same function. A good example is human *UEV1A* which confers a similar DDT function in yeast but is exclusively involved in NF-κB activation instead of DNA repair in human (Andersen et al., 2005). In this study, we took advantage of the fact that *AtUEV1D* is the predominant *AtUEV1* gene expressed in germinating seeds and in pollen (Figure 3-8) characterized by the sensitivity of *Atuev1d* mutant plants to a DNA damaging agent in these tissues. Our

results clearly showed that in the presence of DNA damage agent, lack of AtUev1D activity compromised seed germination, seedling survival, and growth. To our knowledge, this is the first report of putative error-free DDT mutant phenotypes in a multicellular tissue of any organism, and the assays developed in this study can also be applied to other similar studies. Hence, this study, along with previous studies in yeast and mammalian cells, supports a notion that error-free DDT promoted by polyubiquitination via Ubc13-Uev is an evolutionarily conserved function throughout eukaryotes.

Despite its predominant expression among the four *AtUEV1* genes, inactivation of *AtUEV1D* caused only a very moderate but nevertheless significant compromise in pollen tube growth in the presence of DNA damage agent. This probably reflects the lack of cell division during pollen germination whereas DDT is expected to only operate on replicating DNA (Barbour and Xiao, 2003). It is of great interest to note that in contrast to many other plant species, it has been observed that DNA synthesis in the *Arabidopsis thaliana* sperm nuclei is initiated prior to anthesis and continues as the pollen tube develops (Friedman, 1999). Thus, the *Arabidopsis thaliana* sperm nuclei are essential in a "prolonged" S phase at the time of anthesis, in preparation for eventual double fertilization. Our observation that in the presence of replication-blocking lesions induced by MMS, pollen tubes from the *Atuev1d* mutant plants did not develop equally well as those from wild-type segregant lines is consistent with a notion that *AtUEV1D* plays a more active role than other *AtUEV1* genes when DNA synthesis occurs in the presence of DNA damage, which is essentially a DDT activity. We wish to stress that our analysis does not rule out the possibility that MMS-induced DNA lesions may inhibit

transcription, and MMS can also directly methylate and damage RNA (Friedberg et al., 2006b), which could contribute to the observed phenotypes, although Lys63 ubiquitination has not been linked to these processes.

In our opinion, this study provides an important major step towards understanding Ubc13-Uev mediated Lys63-polyubiquitination in general and mechanisms of DDT in particular in plants. Several questions remain to be addressed. Firstly, is *AtUEV1D* the only *AtUEV1* gene involved in error-free DDT? Secondly, is *AtUEV1D* also involved in other cellular processes? Thirdly, what are the other cellular processes that also require Ubc13-Uev mediated polyubiquitination? We feel that given the near identity in amino acid sequence and similar complementation phenotypes in yeast, AtUev1C is likely involved in the same cellular process (es) as AtUev1D. Indeed, the phenotypes of *Atuev1d* mutant plants may be considered to be moderate, which is due to either the backup or residual expression of other *AtUEV1* genes, or the nature of the error-free DDT defect in plants. One important aspect of future work will be to identify an *Atuev1c* null mutant, combine this mutation with *Atuev1d*, examine various tissues for a DDT, defect and relate the results to the *AtUEV1* expression profile. It is also interesting to note that the yeast *mms2-ubc13* or *rev1/rev3/rev7* single mutants are moderately sensitive to killing by DNA damaging agents, but the combination of any two mutations from different pathways results in strong synergistic interactions (Broomfield et al., 1998; Xiao et al., 1999b). It would be of great interest to see if the combination of *Atuev1d* and *Atrev* mutations also results in a synergistic sensitivity to DNA damage.

Although it remains possible that AtUev1A and AtUev1B are involved in DDT as well, we favour the argument that the AtUev1A/B pair is probably involved in other

cellular processes unrelated to DNA damage response. Indeed, although *AtUEV1A* is expressed during seed germination, inactivation of this gene does not result in compromised seed germination in the presence of MMS (Figure 3-13), which is in sharp contrast to the *Atuev1d* mutant lines. In this regard, it is interesting to note that in the presence of *AtUBC13*, the DDT activities of *AtUEV1A/B* are much lower than *AtUEV1C/D* in yeast cells, despite the fact that AtUev1A/B interacts with AtUbc13 and Ubc13 from other species very well and is able to fully complement the yeast *mms2* mutant when yeast Ubc13 is present. The above result also effectively rules out the possibility that partial complementation by *AtUEV1A/B* was due to their poor expression in yeast cells. Another interesting observation is that human Uev1A contains an additional N-terminal 25 amino acid residues and plays a distinct role from hMms2; it may be reverted to play a role in DDT when its N-terminal sequence is experimentally deleted (Andersen et al., 2005). Similarly, AtUev1A and AtUev1B contain a unique C-terminal tail that may be critical for their functions other than DDT. It is difficult at this stage to predict what type of activity it may be, given the fact that AtUev1 appears to have evolved independently of vertebrate Uev paralogs, that Drosophila *ubc13/bendless* confers a more different function than its mammalian counterpart, and that other reports have claimed additional Lys63-mediated cellular processes and some of them have also been linked to Ubc13-Uev (Bothos et al., 2003; Doss-Pepe et al., 2005; Laine et al., 2006). What we can predict though is that additional *Arabidopsis thaliana* Ubc13-Uev1 functions should be mediated by its Lys63-linked poly-Ub chains, and that different AtUev1 proteins may serve as cofactor and critical regulator in these processes. In this regard, future research may focus on the search for AtUbc13-Uev ubiquitination targets

103

through bioinformatics and proteomic approaches, as well as genomic approaches such as microarray analysis of *Atuev* mutants reported in this study.

CHAPTER FOUR

ANALYSIS AND FUNCTION CHARACTERIZATION OF

***ARABIDOPSIS THALIANA UBC13* GENES**

4.1 Introduction

Ubiquitynation is an essential process found in all eukaryotic cells, from unicellular yeast to human. It is involved in many cellular processes including ribosomal biogenesis (Finley et al., 1989), cell cycle progression (Wei et al., 2004), apoptosis (Zhang et al., 2004), mitochondrial inheritance (Fisk and Yaffe, 1999), transcriptional regulation (Kao et al., 2004a) and DNA repair. The conventional post-translational modification of target proteins with poly-Ub chains is via the Gly76-Lys48 linkage, which targets these proteins to 26S proteasomes for degradation. Proteins ubiquitylated through the non-conventional Gly76-Lys63 linkage regulates the functions of diverse proteins in a nonproteolytic manner (Pickart, 2001b). So far, Ubc13 is the only known E2 enzyme capable of catalyzing the Lys63-linked polyubiquitylation reaction, which also requires a Ubc/E2 variant (Uev) as a co-factor (Hofmann and Pickart, 1999; McKenna et al., 2001). In the budding yeast *Saccharomyces cerevisiae*, Ubc13 physically interacts with a Uev called Mms2 (Hofmann and Pickart, 1999), and promotes error-free DNA damage tolerance (also known as postreplication repair) (Broomfield et al., 1998) by polyubiquitylation of the proliferating cell nuclear antigen (PCNA) via Lys63-linked chains (Hoege et al., 2002). Ubc13 homologs have been found in many eukaryotic

organisms; however, functional analysis is limited due to the lack of an efficient means of targeted gene disruption in most multicellular eukaryotes and the intolerance of mammals to genomic instability. In this chapter, we report the isolation and initial functional characterization of *Arabidopsis thaliana* UBC13 genes

4.2 Results

4.2.1 *Arabidopsis thaliana UBC13* genes

To identify *Arabidopsis thaliana UBC13* genes, the human Ubc13 protein (hUbc13) was used to search the Arabidopsis protein database (through TAIR). Two highly similar proteins (E-values at 10^{-56} or better) were found. The cDNAs containing the open reading frame for the two genes were cloned by RT-PCR (done by Dr. Genyi Li in Dr. Wang' Lab). The two putative proteins were named AtUbc13A and AtUbc13B. The sequences of the putative AtUbc13 proteins, both with 153 amino acids, were aligned with Ubc13s from other organisms (Figure 4-1A). The AtUbc13 proteins differ in only two amino acids and both differences are conserved variations from AtUbc13A Asp to AtUbc13B Glu). Compared with Ubc13s from six other organisms, AtUbc13A has 78.6% amino acid sequence identity with hUbc13 and mUbc13, 65.5% identity with ScUbc13, 66% identity with SpUbc13, 78.4% identity with CeUbc13, 73.2% identity with DmUbc13a (Bendless) and 71% identity with DmUbc13b. Furthermore, critical residues for three functions as defined in hUbc13, namely the Cys87 in the active site for Ub thioester formation, the Met64 required for the interaction with a E3 (TRAF6) (Wooff et al., 2004), and three ''pocket'' residues (Glu55, Phe57 and Arg70) that determine binding specificity for Mms2 (Pastushok et al., 2005) are all conserved in AtUbc13s (Figure 4-

1A). Both *Arabidopsis thaliana UBC13* genes are located on chromosome 1 and our cDNA sequences agree completely with the predicted genomic structures and sequences for both genes on the ATIR database (the genomic locus ID numbers are AT1g78870 for *AtUBC13A* and AT1g16890 for *AtUBC13B*). The two ORFs share 90.5% nucleotide sequence identity with each other, and the genomic structures of *AtUBC13A* and *AtUBC13B* are highly conserved, with the same number of introns located at the same position relative to coding exons (Figure 4-1B), suggesting that *AtUBC13A* and *AtUBC13B* are derived from recent duplication. However, the lengths of the seven introns all differ between the two *AtUBC13* genes, with the first three introns differing by more than 50 nucleotides in length. The *AtUBC13* gene duplication is not unusual, since the analysis of the *Arabidopsis thaliana* genome indicated that more than 50% of its DNA sequences are duplicated. Interestingly, the promoter and downstream regions (2 kb each) of *AtUBC13A* and *AtUBC13B* do not share noticeable sequence similarity, and their flanking genes are not duplicated, indicating that *AtUBC13A* and *AtUBC13B* are derived from a segmental duplication instead of block duplication. We also compared the genomic structure of *AtUBC13* with *UBC13* genes from the fission yeast and human. As illustrated in Figure 4-1B, *hUBC13* contains three introns, two of which have identical intron/exon borders as *AtUBC13*. *Spubc13* shares one intron–exon border with both *hUBC13* and *AtUBC13*, and one only with *hUBC13*. These results further indicated that *UBC13* has evolved early in the eukaryotic kingdom and that at least some of its introns predate speciation among yeast, plant and mammal. Phylogenetic analysis (Figure 4-2) was also performed on AtUbc13s in relation to Ubc13s from above model organisms as well as with other plant species of known genomic sequence. This analysis revealed that

plant *UBC13* genes evolved from a common ancestor, which was duplicated and evolved

further within each species, and *UBC13* genes among plant species are closer in evolution

history than between plants and other species such as human and yeast.

A

B

Figure 4-1 Analysis of Ubc13 from different organisms

(A) Amino acid sequence alignment of *AtUBC13* gene products with Ubc13s from six other organisms. Identical residues shared by the majority of *Ubc13s* are highlighted. Critical residues for *Ubc13* functions are indicated with asterisks underneath the residue.

(B) Genomic organization of *S. pombe*, human and *Arabidopsis thaliana UBC13*. Filled boxes, exons; open boxes, untranslated region; solid lines, introns. Identical intron-exon locations between different *UBC13* orthologs relative to their coding sequences are indicated by a connection line. All intron–exon border locations between *AtUBC13A* and *AtUBC13B* are identical but the lengths and nucleotide sequences of the introns are different.
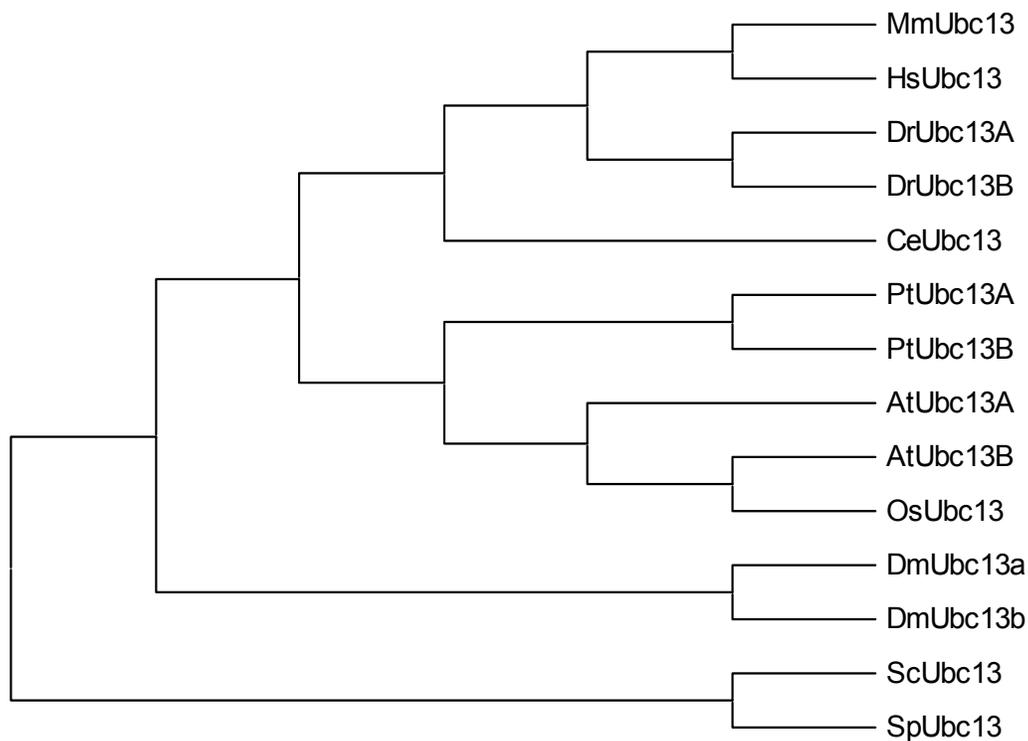
Figure 4-2 Phylogenetic analyses of hypothetical Ubc 13 family proteins from

different organisms

The similarity clustering was conducted by using MEGA version 3 (Tamura et al., 2007)

High similarity is indicated by the short branch length between any two sequences.

The prefixes for different species and the source of sequences (Gen-

Bank accession No) are: Sc, *S. cerevisiae* (X99443); Sp, *Schizosaccharomyces pombe*

(AF470232); Dm, *Drosophila melanogaster*; (DmUbc13a – Bendless=NP-511150;

DmUbc13b=NP-609715); Mm, *Mus musculus* (AY039837); At, *Arabidopsis thaliana*

(AtUbc13A=NP-565192; AtUbc13B=NP-564011); Ce, *Caenorhabditis elegans* (NP-

500272), Hs, Homo sapiens (D83004), Os, *Oryza sativa* (NP-001043834);

Pt, *Populus trichocarpa* (PtUbc13A =A9PA76, Pt Ubc13B = A9PBY5).

4.2.2 Physical interaction of AtUbc13 with yeast and human Mms2

Since the function of Ubc13 in Lys63-linked ubiquitylation requires a Uev as a cofactor. The protein-protein interaction between AtUbc13 with a Uev, in this case a Uev from yeast (yMms2) or human (hMms2), was analyzed in a yeast two-hybrid system (Fields and Song, 1989) (This work was done by Lindsay Newton in Dr. Xiao's Lab). The *AtUBC13A* and *AtUBC13B* ORFs were cloned in-frame into either a Gal4 DNA-binding domain vector pGBT9E or a Gal4 DNA-activation domain vector pGAD424E. As shown in Figure 4-3, co-expression of Gal4$_{AD}$-AtUbc13 with Gal4$_{BD}$-yMms2 or Gal4$_{BD}$-hMms2 in yeast cells led to strong expression of the endogenous P_{GAL1}-*HIS3* reporter gene, indicating that AtUbc13 interacts with yeast or human Mms2. This interaction is deemed to be specific between AtUbc13 and human Mms2, as neither protein alone expressed in the same yeast cell was able to activate the reporter gene. The interaction is also independent of the fusion orientation, as switching fusion partners resulted in the same AtUbc13 and Mms2-dependent interaction. Taken together, the above results indicate that both of the AtUbc13 proteins are capable of interacting with yeast or human Mms2 in the yeast two-hybrid system.

The physical interaction between AtUbc13 and heterologous Mms2 was further confirmed independently by a GST-affinity pull-down assay, as shown in Figure 4-4. In this experiment, AtUbc13A produced in bacterial cells was purified and the GST tag was cleaved. The purified AtUbc13A was added to a column bound with either GST or GST-hMms2. After incubation, washing and elution, AtUbc13A was found to be co-eluted

only with GST-hMms2, but not with GST alone. Hence, AtUbc13A is able to form a stable heterodimer with hMms2.

Gal4$_{AD}$	Gal4$_{BD}$	Control	+1 mM 3AT
AtUbc13a	yMms2		
AtUbc13b	yMms2		
--	yMms2		
AtUbc13a	--		
AtUbc13b	--		
AtUbc13a	hMms2		
AtUbc13b	hMms2		
--	hMms2		
hMms2	AtUbc13a		
hMms2	AtUbc13b		
--	AtUbc13a		
--	AtUbc13b		
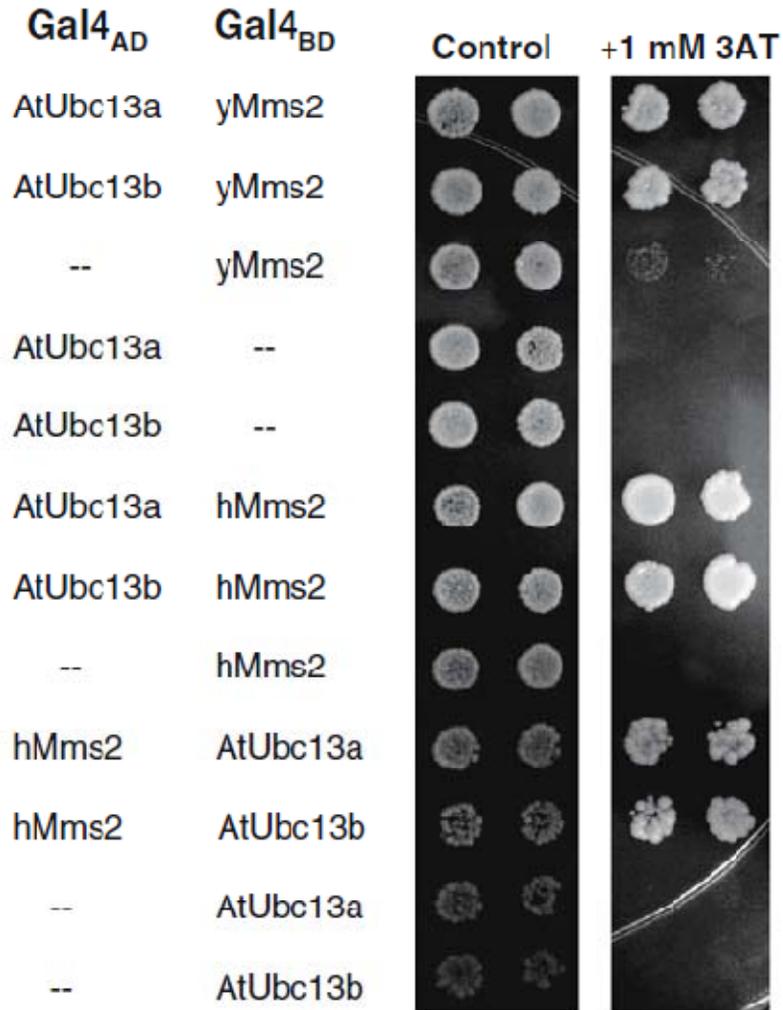
Figure 4-3 Interactions between AtUbc13 and Mms2 in a yeast two-hybrid assay

The PJ69-4A transformants (five independent colonies from each transformation) carrying one $Gal4_{AD}$ (from pGAD424E) and one $Gal4_{BD}$ (from pGBT9E) construct were replica on plated on SD-Trp-Leu (control) and SD-Trp-Leu-His plus various concentrations of 3-AT, and were incubated for 3 days at $30^{o}C$. The first column shows constructs in the $Gal4_{AD}$ vector, the second column constructs in the $Gal4_{BD}$ vector, the third column cell growth on the control SD-Trp-Leu plates and the fourth column

cell growth on the selective SD-Trp-Leu-His plus 3-AT plates. Two colonies from each treatment are shown. Other plates and colonies had the same results.
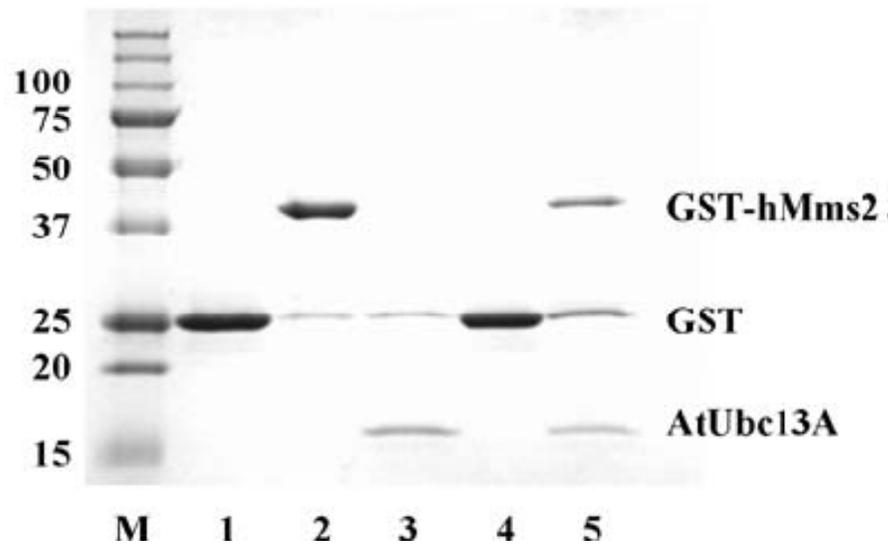
Figure 4-4 AtUbc13A Binds hMms2 in a GST Pull-down Assay

Purified GST or GST-hMms2 was added to microspin columns. Following incubation, columns were spun and washed, and the purified AtUbc13A was added. After further incubation and washing, the columns were eluted with reduced glutathione and subjected to SDS-PAGE gel analysis. Lanes 1 to 3 show the purified GST, GST-hMms2 and AtUbc13A used, respectively. Lanes 4 and 5 show the eluent from the column preloaded with GST (lane 4) and GST-hMms2 (lane 5). Note that the GST-hMms2 (lane 2) and AtUbc13A (lane 3) samples contain trace amount of free GST, which is also revealed after elution (lane 5).

4.2.3 *AtUBC13* functionally complements yeast *ubc13* null mutants

Yeast *UBC13* is a member of the error-free damage tolerance pathway (Brusky et al., 2000) and its product is able to promote Lys63-linked polyubiquitylation *in vitro* (Hofmann and Pickart, 2001) or *in vivo* (Hoege et al., 2002). In order to investigate whether AtUbc13s have the same function as yeast Ubc13, two types of experiments were carried out to determine whether AtUbc13 could functionally complement the error-free damage tolerance defect in the yeast *ubc13* null mutant. The yeast *ubc13* mutant displays an increased sensitivity to a variety of DNA-damaging agents including MMS (Brusky et al., 2000), which can be assessed by a gradient plate assay. Expression of either *AtUBC13A* or *AtUBC13B* from the yeast two-hybrid plasmid rescued the *ubc13* mutant to a level comparable to wild type cells; in contrast, the pGAD424E vector alone did not confer any MMS resistance to the *ubc13* mutant (Figure 4-5). Furthermore, the *ubc13* and *rev3* mutations are synergistic with respect to killing by DNA-damaging agents (Brusky et al., 2000). Indeed, the *ubc13 rev3* double mutant did not grow at all on a gradient plate containing 0.025% MMS, whereas expression of either *AtUBC13* gene was able to rescue its growth to a level comparable to the *rev3* single mutant (Figure 4-5).

One of the most astonishing phenotypes of an *mms2* (Broomfield et al., 1998) or *ubc13* (Brusky et al., 2000) mutant is its massive increase in spontaneous mutagenesis, indicating that these genes play an important role in protecting cells from genome instability. Indeed, in this experiment the *ubc13* mutant strain showed a nearly 30-fold increase in spontaneous mutagenesis when compared to wild type cells. When the *ubc13* mutant was transformed with a plasmid expressing *AtUBC13A* or *AtUBC13B*, the

spontaneous mutation rate was reduced to levels similar to that of the wild type cells (Table 4-1). The results from these two types of experiments showed clearly that *AtUBC13* genes are able to replace the DNA damage tolerance functions of yeast *UBC13*. Furthermore, since it is known that the *ubc13* mutation is defective in PCNA polyubiquitylation (Hoege et al., 2002), which is absolutely required for its error-free damage tolerance function, we can also infer that AtUbc13 is able to work with the yeast Mms2 *in vivo* to promote Lys63 polyubiquitylation of PCNA.
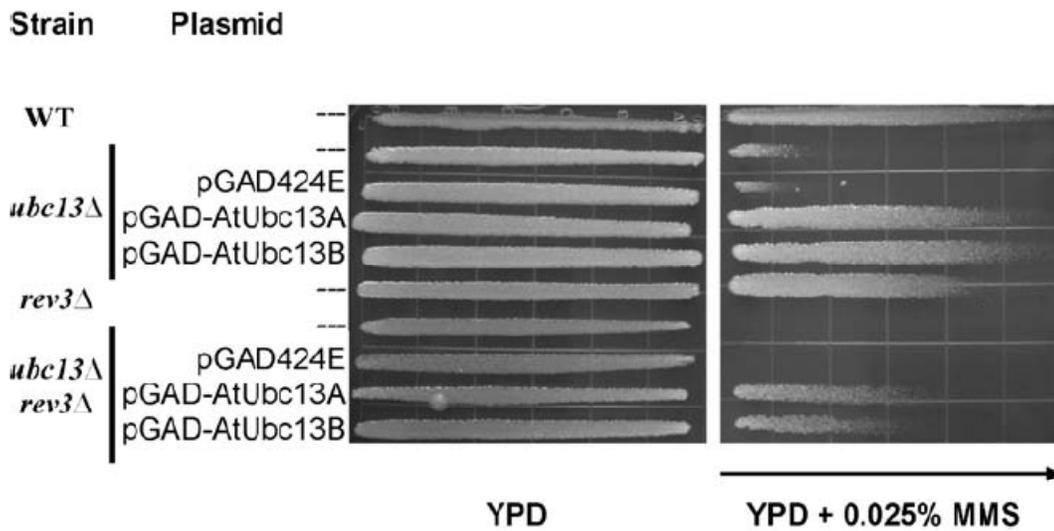
Figure 4-5 Functional complementation of the yeast *ubc13* mutant and *ubc13 rev3* double mutant by *AtUBC13*. The YPD control (left) and YPD+0.025% MMS gradient (right) plates were incubated at 30°C for 3 days. Arrow points to gradually increasing MMS concentrations. Yeast strains used: HK578-10D (wild type), WXY904 (*ubc13Δ*), WXY1233 (*rev3Δ*) and WXY921 (*ubc13Δ rev3Δ*).

Table 4-1   Effects of *AtUBC13* on the Spontaneous mutation rates of *S. cerevisiae*

** *ubc13* mutants**

Strain[a]	Key Alleles	Rate (X10^{-8})[b]	Fold[c]
DBY747	Wild type	4.95 ± 0.24	1.00
WXY849	*ubc13Δ*	132.3± 18.9	26.73
WXY849/*AtUBC3A*	*ubc13Δ AtUBC13A*	9.81 ± 2.88	1.98
WXY849/*AtUBC13B*	*ubc13Δ AtUBC13B*	12.89 ± 2.96	2.6

a All strains are isogenic derivatives of DBY747.

b The spontaneous mutation rates are the average of three independent experiments with standard deviations.

c Relative to the wild type mutation rate.

4.2.4 *AtUBC13* expression in different tissues and under stresses

To determine *AtUBC13* expression in *Arabidopsis thaliana* plants, tissue samples were taken from 2-, 5- and 9-week-old *Arabidopsis thaliana* plants, and total RNA was isolated (RNAs isolated and the blotted membrane provided by Dr. Hong Wang). Results from Northern analysis showed that *AtUBC13* transcripts were detected in all tissues analyzed, although at a relatively low level (Figure 4-6A). This observation indicated a relatively uniform expression of *AtUBC13*. The observation on the relatively low level of *AtUBC13* transcript is also supported by an analysis of microarray data available from TAIR www.arabidopsis.org.

Yeast *UBC13* expression is induced when cells are treated with different DNA-damaging agents. To determine whether *AtUBC13* responds to various abiotic stresses, we analyzed *AtUBC13* expression in cell suspension following treatments with NaCl, abscisic acid (ABA), mannitol, H_2O_2, low temperature or MMS. The Northern results from samples of 12-h treatments were presented in Figure 4-6B. The data indicated that none of the above treatments induced overall *AtUBC13* transcript level. The treatment of low temperature appeared to decrease the *AtUBC13* transcript level. As a comparison, the transcript of *UBQ11* showed a moderate level of increase. We searched the microarray expression data from www.arabidopsis.org. The microarray data from similar treatments of *Arabidopsis thaliana* plants (Figure 4-6C) indicated a persistent level of *AtUBC13* transcripts under various conditions. Hence, *AtUBC13* expression appears to be constant under those conditions examined. We also used Expression Browser through the Botany ArrayResource (Toufighi et al., 2005) to perform ''electronic Northerns'', and the results suggested that under stress conditions, the expression level of *AtUBC13* did not show

obvious variation following treatments with different conditions. Due to the high degree of sequence similarity between the two *AtUBC13* genes, neither Northern hybridization nor microarray analysis is able to distinguish individual *AtUBC13* gene expression. Since *AtUBC13A* and *AtUBC13B* do not share noticeable promoter sequence similarity, one cannot rule out the possibility that under certain stress conditions, one of the *AtUBC13* genes is induced whereas the other is decreased accordingly. Thus, we performed semi-quantitative RT-PCR using a pair of primers specific for *AtUBC13A* or *AtUBC13B*, and another pair of primers for *UBQ11* as an internal control (Figure 4-6D). This result was in agreement with Northern and microarray data and indicated that the two *AtUBC13* genes are not differentially regulated under the conditions tested.
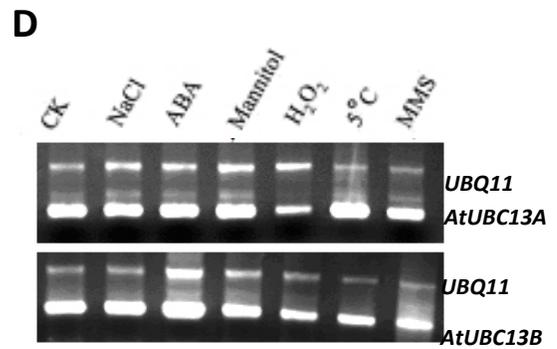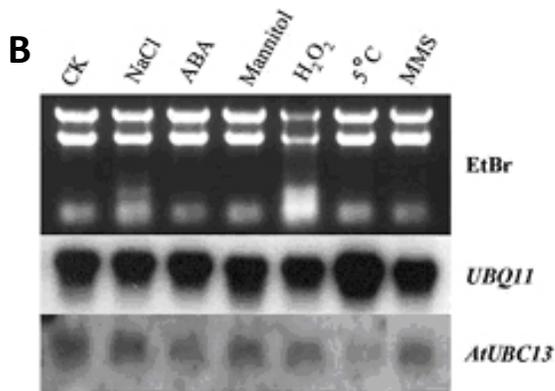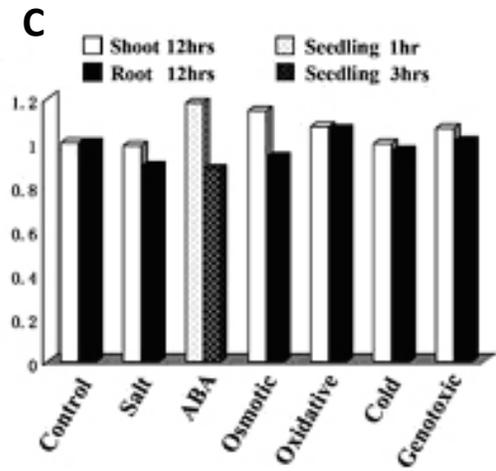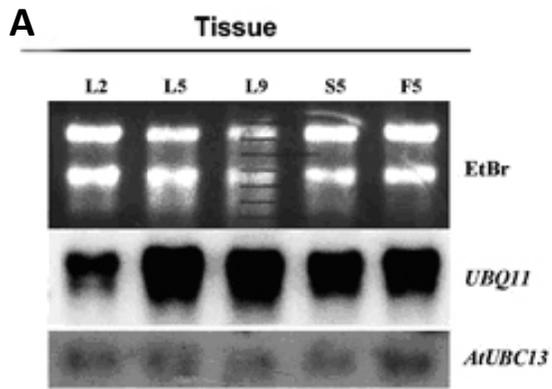
Figure 4-6 Expression of *AtUBC13* Genes

(A) Expression of *AtUBC13* transcripts by Northern hybridization. Each lane contains 5 ug of total RNA from different tissues. L2, leaves of 2-week -old seedlings; L5, leaves of 5-week-old plants; L9, leaves of 9-week-old plants; S5, stems of 5-week-old plants; F5, floral tissues of 5-week-old plants.

(B) Expression of *AtUBC13* transcripts in cell suspension treated with different stress conditions for 12 h and analyzed by Northern hybridization. Each lane contains 10 ug of total RNA from different samples. The conditions used were: control, 300 mM NaCl, 20 M (+)-abscisic acid (ABA), 400 mM mannitol, 20 mM H_2O_2, low temperature (5°C), and 100 ppm MMS.

(C) Graphic presentation of data extracted from microarray analyses in www.arabidopsis.org and expressed as relative levels to the untreated control. Tissue source: open bars, shoots; solid bars, roots; striped bars, seedling.

(D) Expression of *AtUBC13* transcripts in cell suspension treated with different stress conditions for 6 h and assessed by quantitative RT-PCR.

4.2.5 Roles of *Arabidopsis thaliana UBC13* in plant development

4.2.5.1 Confirmation of the *Atubc13a* T-DNA insertion mutant

By searching the website www.arabidopsis.org, one T-DNA insertion line of *Atubc13a*, WISCDSLOX323H12, which would truncate C-terminal 12 amino acids, was found. The Genomic structure displaying the position of the T-DNA insertion is shown in Figure 4-7A with the putative T-DNA insertion site indicated. In order to determine whether deletion of 12 amino acids of AtUbc13A affects its function, two experiments, yeast two hybrid assay and functional complementation, were carried out. The results showed that the truncated AtUbc13A protein was still able to interact with AtUev1A to the same extent as full length AtUbc13A (Figure 4-8A). However, unlike the AtUbc13A, the truncated AtUbc13A-Δ12aa (named *Atubc13a-1*) was unable to functionally complement the yeast *ubc13* null mutant for resistance to DNA damage induced by MMS; the level of resistance provided by *Atubc13a-1*is no better than that of vector alone (Figures 4-8B). Thus we ordered seeds of this line and performed the genomic DNA PCR using gene specific primers SP1 and SP2 as well as another pair of gene specific primers SP1 and SP3 (Figure 4-7A). Genomic PCR confirmed the expected location of T-DNA insertion (Figure 4-7B). Furthermore, to ask whether the truncated *Atubc13a-1*allele still produces mRNA, we performed RT-PCR using total RNA from wild type and homozygous mutant plants. The results showed that only wild type plants can produce the full length *AtUBC13A* mRNA. However, when SP1 and SP3 primers were used for RT-PCR, the transcript of expected size was detected from both wild type and the mutant

plants (Figure 4-7C), suggesting that truncated *Atubc13a-1*allele is capable of producing a truncated transcript. Hence, we named this T-DNA insertion mutation *Atubc13a-1*.
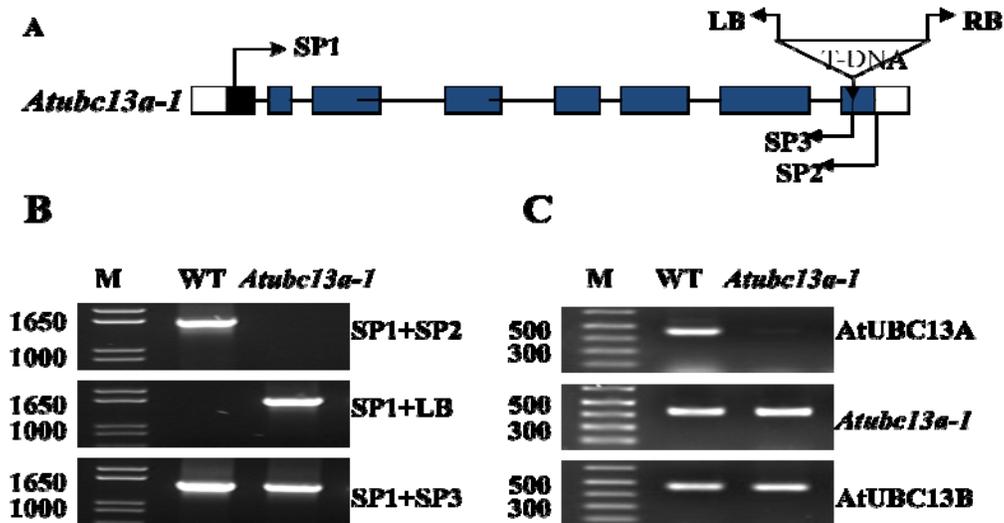
Figure 4-7 Confirmation of the *Atubc13a* T-DNA insertion mutant

(A) Genomic structure showing the positions of the T-DNA insertion. Filled boxes represent exons, while connecting lines represent introns. T-DNA is inserted in the last exon. SP1, 5' gene specific primer; SP2, SP3: 3' gene specific primers; LB, T-DNA left border primer.

(B) Genomic DNA PCR results. The fragment in WT line was amplified by using primers SP1 and SP2. The *Atubc13a-1* was amplified by primers SP1 and LB, while a truncated fragment of *AtUBC13A* could be amplified from both wild type and the mutant line by using primers SP1 and SP3.

(C) RT-PCR. In wild type plant, two *AtUBC13* genes were amplified by using gene specific primers of *AtUBC13A*; while in the mutant *Atubc13a-1* plant, *AtUBC13A* gene

was disrupted, and the other gene *AtUBC13B* was amplified by using gene specific primers of *AtUBC13B*.

A

Gal4AD	Gal4BD	-Leu-Trp	-His	3AT	-Ade
pGAD424	AtUbc13A				
pGAD424	Atubc13a-1				
AtUev1A	pGBT9				
AtUev1A	AtUbc13A				
AtUev1A	Atubc13a-1				

B

pGBT-AtUbc13A
pGBT-Atubc13a-1
pGBT9
ubc13
WT

YPD   YPD+0.025%MMS
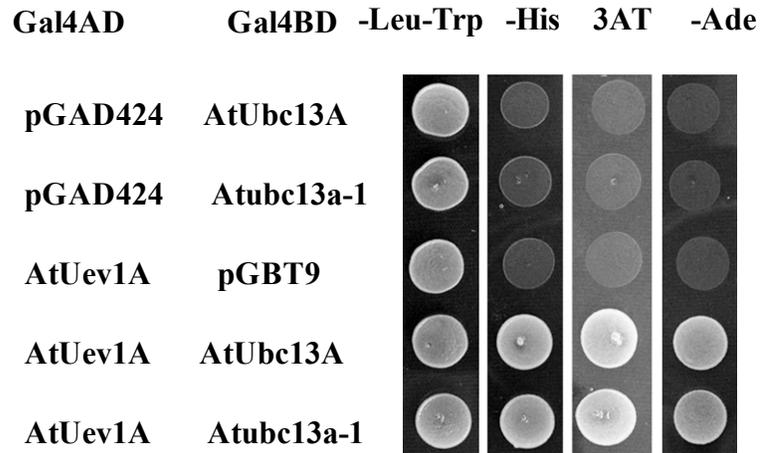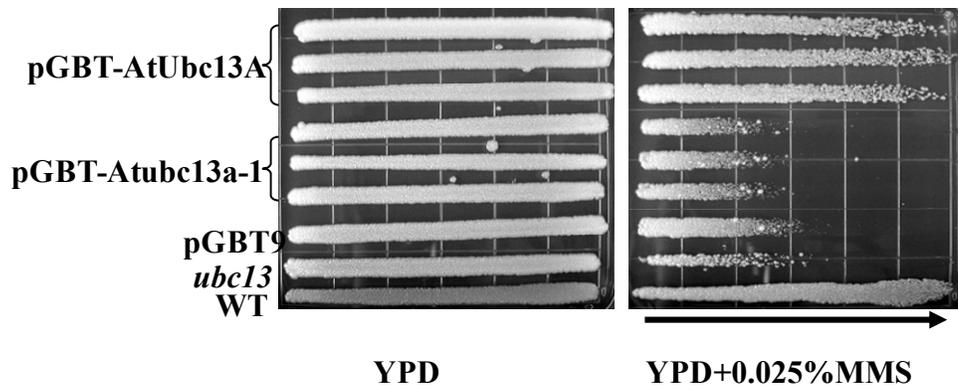
Figure 4-8 Characterization of the *Atubc13a-1* mutant in yeast cells

(A) Physical interactions between truncated *Atubc13a-1* and AtUev1A in a yeast two-hybrid assay. AD: constructs in the Gal4 activation domain vector pDAD424. BD: constructs in the Gal4 DNA-binding domain vector pGBT9. The transformants carrying one AD construct and one BD construct were plated on: non-selective SD-Leu-Trp (first panel), SD-His-Leu-Trp (second panel), SD-His-Leu-Trp+3 mM 3-AT (third panel) or SD-Ade-Leu-Trp (forth panel). All plates were incubated for three days before taking photograph.

(B) Functional complementation analysis of the yeast *ubc13* mutant by *AtUBC13A* and *Atubc13a-1 (Δ12aa)*. The YPD control (left) and YPD + 0.025% MMS gradient (right) plates were incubated at 30°C for 3 days. All strains grow well on the YPD plate without MMS; on YPD + 0.025% MMS plate. *AtUBC13A* rescues the corresponding mutants to the wild type level while *Atubc13a-1* did not rescue the yeast *ubc13* mutant. The arrow points towards the higher MMS concentration.

4.2.5.2. Confirmation of the *Atubc13b* T-DNA insertion mutant

The T-DNA insertion line of *AtUBC13B*, SALK_043781 was obtained. Genomic DNA PCR result showed that the T-DNA insertion was located in the first intron. This result is different from that published in the website www.arabidopsis.org. The T-DNA insertion position and orientation are shown in Figure 4-9A. In order to obtain the homozygous T-DNA insertion mutant, primers LB and SP1 were used to amplify mutant *Atubc13b* genomic DNA by PCR, the fragment was much smaller than that amplified from wild type genomic DNA by using gene specific primers SP1 and SP2 (4-9B). To further confirm this mutant, RT-PCR was also performed, which indicated that the mutant line was unable to produce the full-length coding transcript while *AtUBC13A* expression remains unaffected (Figure 4-9C). We herein name this *AtUBC13B* T-DNA insertion mutation *Atubc13b-1*.
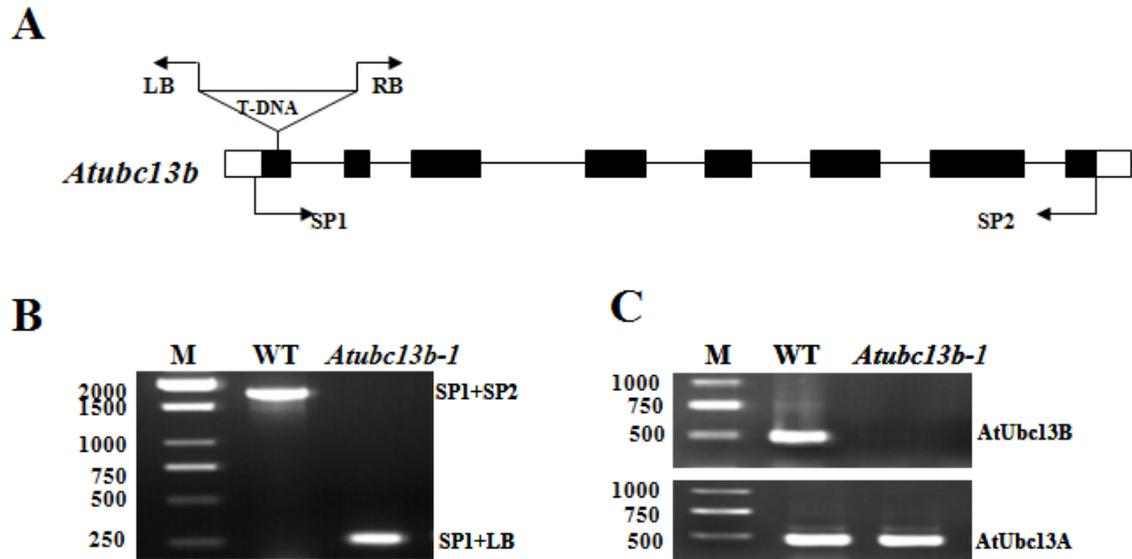
Figure 4-9 Confirmation of the *Atubc13b-1* T-DNA insertion mutant

(A) Genomic structure of the *AtUBC13B* gene showing the position of T-DNA insertion.

Filled boxes represent exons, and lines represent introns. T-DNA is inserted in the first

intron. SP1: 5' gene specific primer; SP2: 3' gene specific primer. LB: T-DNA left

border primer.

(B) Genomic DNA PCR results. Three primers (SP1, SP2 and LB) were mixed to amplify

the full length and truncated *AtUBC13B* genes.

(C) RT-PCR results. In wild type plant, both *AtUBC13* genes were amplified; while in the

homolozygous mutant *Atubc13b-1* plant, *AtUBC13B* gene was disrupted, and another

AtUBC13 gene (*AtUBC13A*) was amplified as an internal control.

4.2.5.3 Cross *Atubc13a* and *Atubc13b* mutants

The position of *AtUBC13A* (At1g78870) in the physical map is 29655349 - 29657410 bp, while *AtUBC13B* (At1g16890) is 5776339 - 5778448 bp. These two genes are located in the same chromosome but in different arms. The physical distance of these two genes is about 23.9 Mbp, and the genetic distance is more than 25 cM. Hence recombinant progenies are expected to be readily obtained.

The cross between mutant *Atubc13a-1* and *Atubc13b-1* was performed and the first generation (F1) was obtained. The F1 seeds were planted into the soil. Four weeks later, genomic DNA was isolated from the F1 plants and the genomic DNA PCR was carried out. Because the genotype of all F1 plants is heterozygous (AaBb), PCR bands representing both wild type and the mutant alleles are expected when two gene specific primers and the left border primer of T-DNA were mixed together to amplify the genomic DNA, with one band amplified by the gene specific primer, and another by LB and one of the gene-specific primers depending on the orientation of the T-DNA. When primes SP1, SP2 of *AtUBC13B* and LB were used, the PCR results were as predicted (Figures 4-10A). SP1 and SP2 of *AtUBC13B* amplified the full-length *AtUBC13B* gene, and LB with SP1 amplified the Atubc13b-1 allele. However, when primers SP1, SP2 of *AtUBC13A* and LB were used, only one band came out and the size of the band was the same as that of *AtUBC13A* (Figure 4-10B). Careful analysis of the insertion site revealed that the size of the amplified Atubc13a-1 is 1582 bp (1560 bp Atubc13a-1 plus 22 bp LB Primer), while the size of the full length *AtUBC13A* is 1595 bp, with only 13 bp difference between the two bands, which is very difficult to distinguish. Therefore, I carried out two separate

PCR by using different pairs of primers, and the results were as expected, and shown in

Figures 4-10C and 4-10D. The seeds of the F1 plants were obtained, and planted to get

F2 double mutant plants.
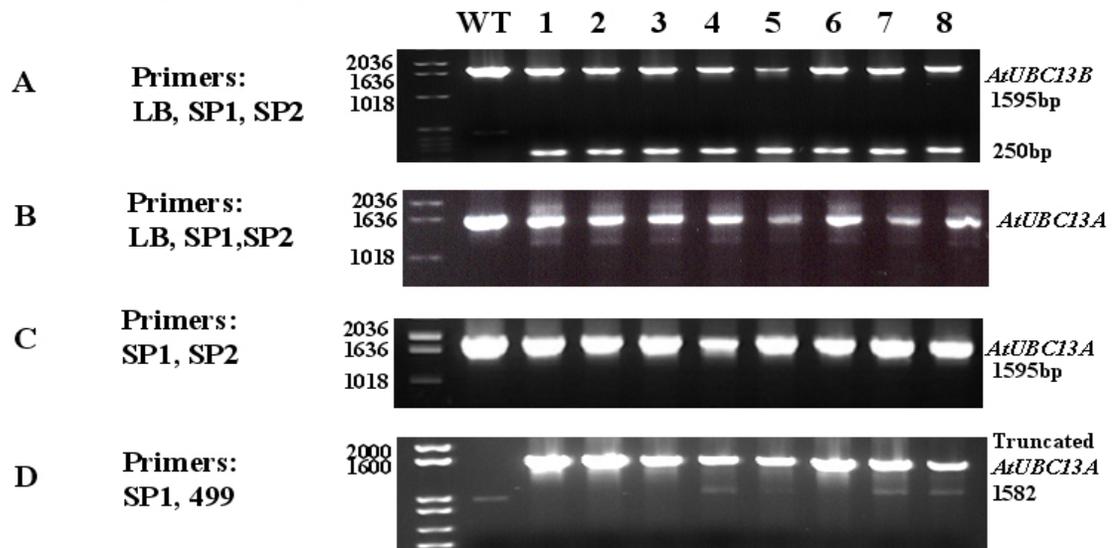
Figure 4-10 Confirmation of F1 heterozygote from the *Atubc13a-1* and *Atubc13b-1* cross

(A)Three primers were mixed to amplify *AtUBC13B* and *Atubc13b-1*.

(B) Three primers were mixed to amplify *AtUBC13A* and *Atubc13a-1*.

(C) Gene specific primers of *AtUBC13A* were used to amplify *AtUBC13A*.

(D) Left border primer LB and one of the gene specific primers SP1 were used to amplify

the *Atubc13a-1* allele.

4.2.5.4 Screening F2 generation plants to obtain *Atubc13a Atubc13b* double mutants

Six hundred F2 generation seeds were sterilized and plated onto the 1/2 MS media plates. Each plate contained about 50 seeds. After five days, seed germination was investigated. According to Mendel's Law of Independent Segregation, the F2 generation will have 9:3:3:1 ratio, or 1/16 homozygous double mutants. In theory, six hundred seeds will produce 38 double mutant plants. Because the *Ubc13* knockout mice are embryonic lethal (Yamamoto et al., 2006a; Yamamoto et al., 2006b), the ratio may not follow the anticipated segregation if the double mutant seeds do not develop or germinate well. Hence, I paid special attention to poorly growing seedlings. Our results showed that among the 600 seeds, 11 seeds did not germinate and another 11 seedlings died after germination. For further characterization, 15 large-size, 30 mid-size and 30 small-size F2 plants were transferred into soil in pots. After two weeks, genomic DNA PCR was carried out to screen the double mutant plants. Total 75 plants (15 large-size, 30 mid-size and 30 small-size) were screened by genomic DNA PCR using different primer pairs. As described previously, when *AtUBC13B* primers SP1, SP2 and LB were used, SP1 and SP2 of *AtUBC13B* amplified the wild type *AtUBC13B* gene, and LB and SP1 amplified the *Atubc13b-1 allele*. Similarly, *AtUBC13A* primers SP1 and SP2 amplified the full length wild type *AtUBC13A* gene while LB primer 499 and SP1 amplified the *Atubc13a-1* allele. The F2 generation had total nine genotypes. The genomic PCR and some RT-PCR results of nine genotypes are shown in Figure 4-11. Among 75 screened F2 generation plants, 6 plants were AABB, 7 were AABb, 6 were AAbb, 5 were AaBB, 20 were AaBb, 11 were Aabb, 4 were aaBB, 11 were aaBb and 5 were aabb. This result was not exactly

comparable with the Mendel's Law of Independent Segregation, because plants were selected based on their size rather than randomly. Among the five homozygous double mutant plants, four of them were small in size and one was medium in size.
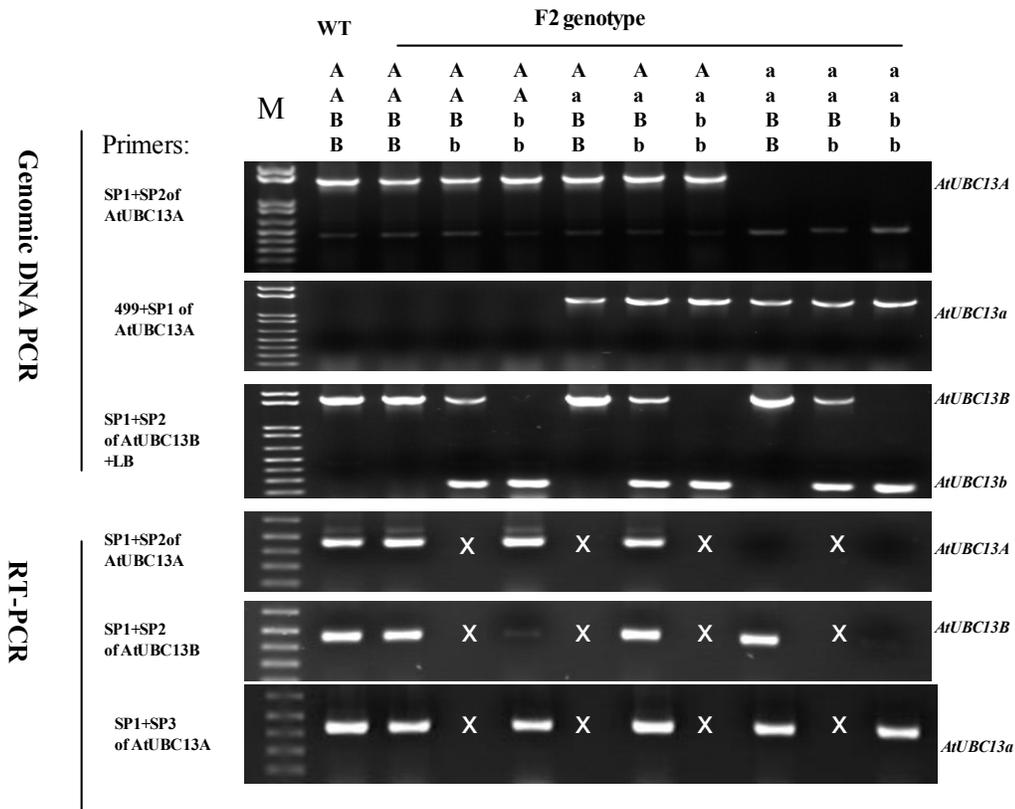
Figure 4-11 Genomic PCR and selected RT-PCR for all nine F2 genotypes from the *Atubc13a-1* and *Atubc13b-1* cross

Top legend indicates genotypes of F2 diploid plants. *AtUBC13*: A, *AtUBC13A*; a, *Atubc13a*-1; B , *AtUBC13B;* and b, *Atubc13b-1*. The top three panels are from genomic DNA PCRs using various primers as indicated to detect the wild type and mutant alleles from each AtUBC13 gene. The bottom three panels are from RT-PCRs, with the first two showing the detection of full-length coding transcripts of *AtUBC13A* and *AtUBC13B*, and the bottom panel showing the detection of a truncated *AtUBC13A* transcript common to both wild type and the Atubc13a-1 allele. X: Not determined because we will not focus on these genotypes.

134

4.2.5.5 Expression of *AtUBC13* in double mutant plants

Our previous RT-PCR results showed that although the full length *AtUBC13A* is disrupted in the *Atubc13a-1* allele, it is still able to transcribe a truncated mRNA (Figure 4-7C). To determine whether this transcript is capable of producing a stable protein and whether there is another homologous Ubc13 in *Arabidopsis thaliana*, a 4E11 monoclonal antibody against human Ubc13 raised in the Xiao laboratory (Andersen et al., 2008) was used in Western blot (WB) analysis. A previous experiment had shown that this antibody detected purified AtUbc13A protein and the endogenous AtUbc13 in wild type plants (data not shown). This is not surprising given the high degree of Ubc13 protein sequence conservation among different eukaryotic kingdoms (Figure 4-1). Indeed, as shown in Figure 4-12, 4E11 detected a predominant 17 kDa band of expected size (lane 1). In contrast, this band is completely absent in the two *Atubc13* double mutant lines (lanes 4 and 5). This observation allows us to conclude that the *Atubc13a-1* is a null allele and that *Arabidopsis thaliana* contains only two *UBC13* genes. Thus, the phenotypes of the *Atubc13* double mutant (see subsequent sections) are likely due to the absence of AtUbc13 proteins. Interestingly, each *Atubc13a* and *Atubc13b* homozygous single mutant line displayed reduced total Ubc13 level (lanes 2 and 3). This result demonstrated that: 1) The truncated AtUbc13 gene can be transcribed to mRNA and can not further be translated into protein; 2) This truncated protein can interact with AtUev1 in the yeast two hybrid assay but lose its function (Figure 4-2A and B); 3) It supports a notion that *AtUBC13* are housekeeping genes and that their expression is ubiquitous and is not regulated by exogenous stimulation.
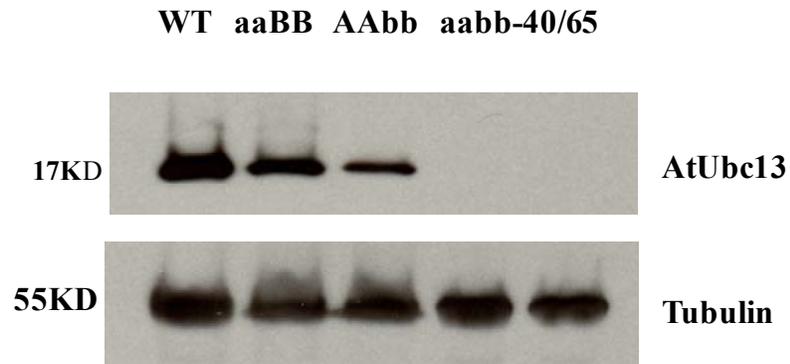
Figure 4-12 Western blot analysis of plant Ubc13 proteins

Protein levels of the wild type, *Atubc13* single and the *Atubc13a-1 Atubc13b-1* double mutant plants. Proteins were extracted from 13-day old seedlings and used in Western blot analysis with an antibody against hUbc13. An anti-tubulin antibody was used as an internal control.

4.2.5.6 Phenotypic characterization of *Atubc13* double mutant plants

We obtained five double mutant plants among 75 F2 plants examined. The common feature of these double mutant plants was that their leaves displayed yellow spots. The yellow spots started on the bottom leaves and gradually spread to the newer ones. After several weeks, the yellow spots expanded in size, joined each other and eventually caused the entire leaves yellow.

4.2.5.6.1 Phenotypes of plants growing in plates

To further investigate the phenotype of the double mutant plants, seedlings of wild type, two single mutants (aaBB and AAbb) and two double mutant lines (aabb-40 and aabb-65) were confirmed by genomic PCR and their phenotypes characterized. Seeds from the above lines were sterilized and plated onto the ½ MS media plates. After three-day incubation at $4\,^{o}C$ in the dark, the plates were placed in a $20\,^{o}C$ growth chamber. The differences displayed by the double mutant plants were observed. Generally speaking, the double mutant plants were greatly delayed in seed germination, as well as cotyledon and true leaf development. The phenotypes of the seedlings were shown in Figure 4-13. The detailed observations are as follows:

1) The radicals of wild type and single mutant plants appeared on the second day after seeding, while double mutant occurred on the third day.

2) Cotyledons of most wild type and single mutant seeds appeared on the third day while only a few cotyledons of double mutant seeds appeared on the fourth day.

3) The true leaves of wild type and single mutant seedlings appeared on the eighth

day, while the true leaves of a few double mutant seedlings appeared on the tenth day.

4) The phenotypes of wild type, single and double mutant seedlings of 5-day-old, 10-day-old, 15 -day-old, 21-day-old and 28-day-old are shown on Figure 4-13.
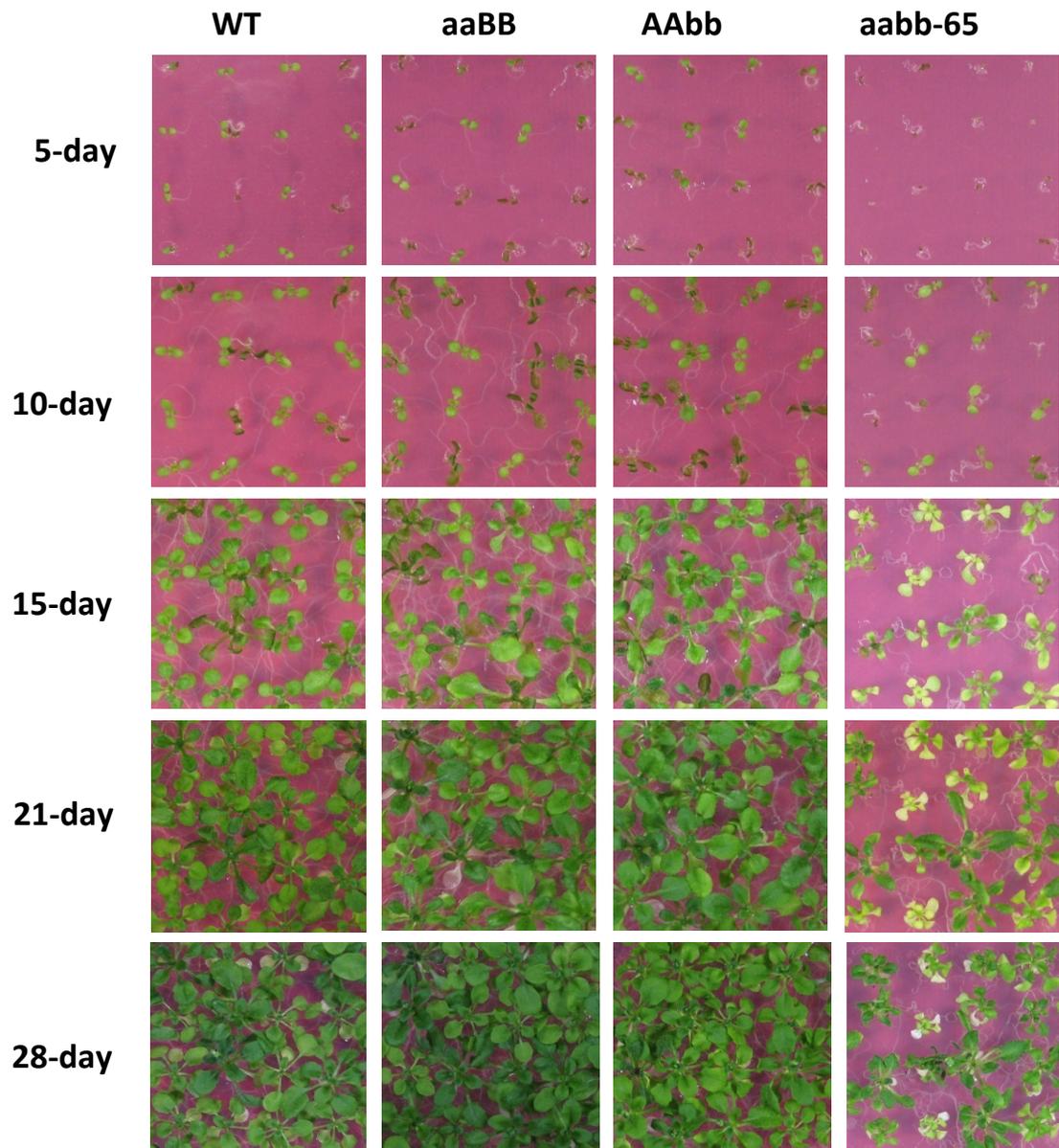
Figure 4-13 Growth and morphology of wild type, *Atubc13* single mutant and double mutant plants at different times after seeding

WT: wild type; aaBB: *Atubc13a* mutant; AAbb: *Atubc13b* mutant; aabb-65: the *Atubc13* double mutant. The double mutant plants did not develop evenly: most of them were small and had light-colored leaves and delayed seed germination as well as cotyledon and true leaf development.

4.2.5.6.2 Phenotype of roots on plates

We observed that the *Atubc13* double mutant displayed a mutant root phenotype (e.g. shorter root). However, the effect was difficult to measure with the normal plates when roots grew into the agar. Thus, the root phenotype was analyzed using seedlings growing vertically on plates. Seeds were sterilized and incubated at 4 °C in the dark for three days. Thirteen seeds were placed on each of the square plates containing 50 ml of ½ MS. The plates were placed vertically in a growth chamber.

Compared to the roots of wild type and single mutants, roots of the double mutant were shorter and grew in a zig-zag manner. The root lengths were measured at 5th day after incubation; the appearance of 5-day-old seedlings is shown in Figure 4-14A and the data on root length are shown in Figure 4-14B. Furthermore, lateral roots began to appear in most wild type and single mutant plants on the 8th day, while lateral roots were visible in few double mutant seedlings (Figure 4-15A). The number of lateral roots for the wild type and single mutants was about 3 times that of the *ubc13* double mutant (Figure 4-15B).
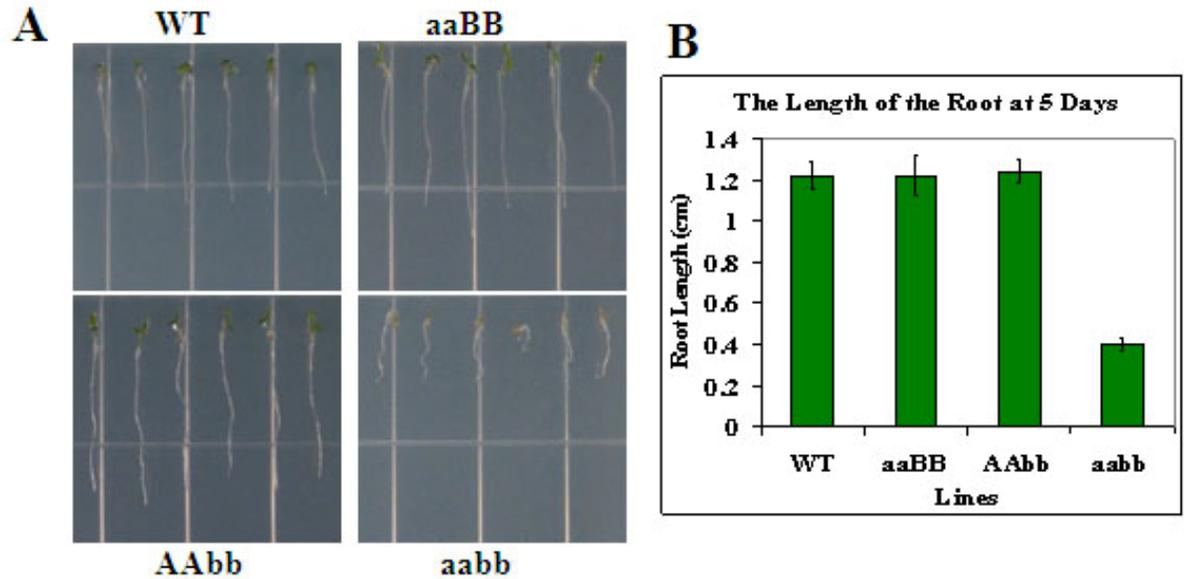
Figure 4-14 Root growth of the wild type, two single mutants and double mutant seedlings under the light condition

(A) Representative images on 5-day-old roots of wild type and mutant plants.

(B) Root length of 5-day seedlings growing on plates. Each result is from three independent plates and in each plate there were about 11-14 seedlings. Error bars indicate standard deviations.

A

WT   aaBB

AAbb   aabb-65

B

The Number of 12-day Lateral Roots
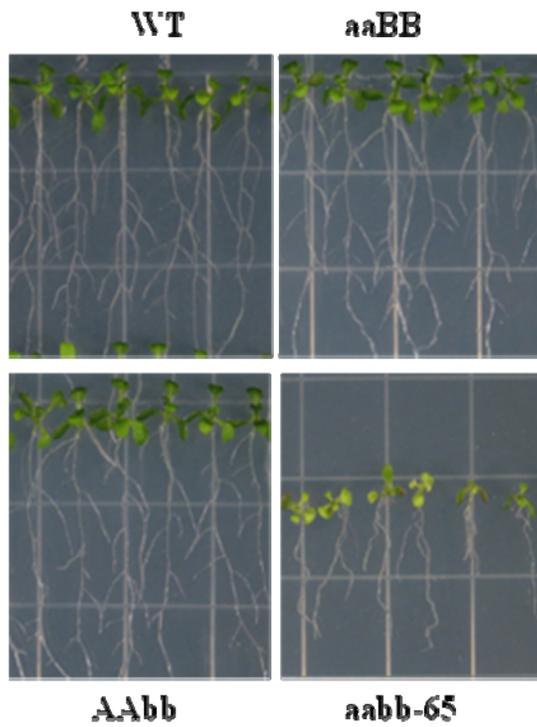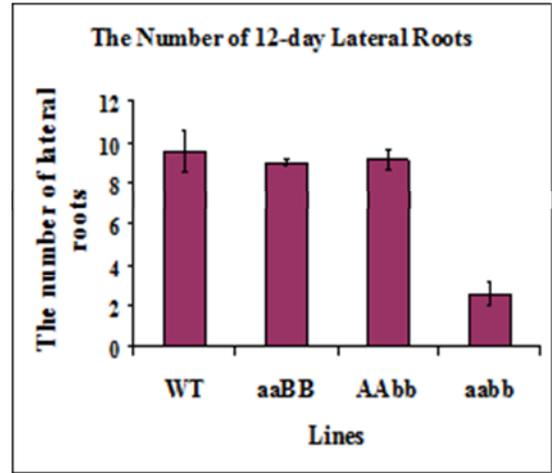
Figure 4-15 Effects of Ubc13 mutation on lateral root development

(A) Representative root images of 12-day-old seedlings.

(B) Number of lateral roots of 12-day-old wild type and mutant seedlings. Each result is from three independent plates and in each plate there were about 11-14 seedlings. Error bars indicate standard deviations.

4.2.5.6.3 Phenotype of double mutant in pots

To further study the phenotype of the double mutant, seeds from the wild type, single mutants and double mutant were directly sown into soil in pots. Seed germination and plant growth were monitored. For seed germination, most of the double mutant seeds did not germinate very well and it took about 2 or 3 days longer) to germinate compared to wild type. At 35 days after seeding, the double mutant plants displayed a small size with rosette leaves bearing a thinner and flatter leaf blade, as well as lighter color compared to the wild type plants. Leaf serrations were more prominent in the double mutant plants than in wild type and single mutant plants (Figure 4-16).
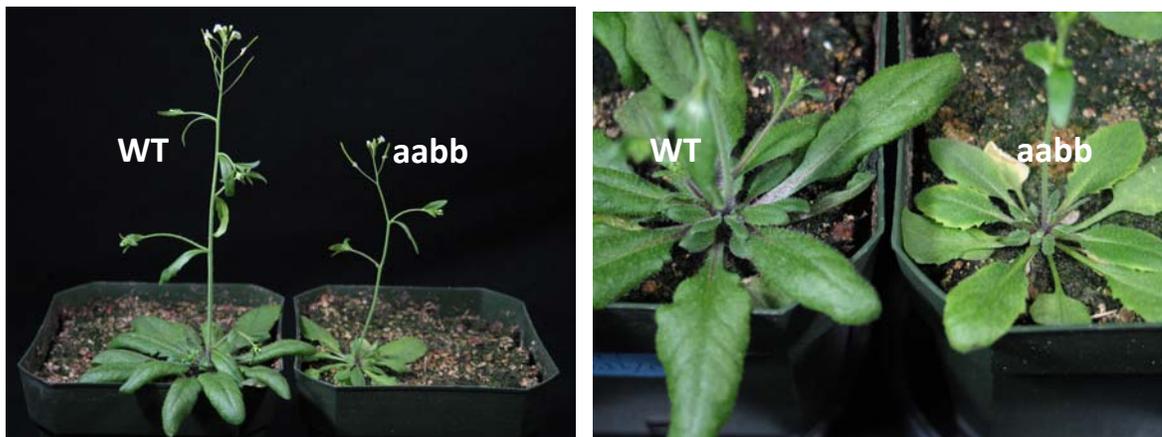
Figure 4-16 Wild type and double mutant plants 35 days after seeding

Compared to wild type, the double mutant plant has overall smaller size. The leaves are thinner and flatter as well as lighter in color.

4.3 Discussion

4.3.1 *Arabidopsis thaliana* **Ubc13-mediated Lys63-linked polyubiquitination is involved in DNA damage tolerance**

Lys63-linked polyubiquitylation of target proteins is involved in signal transduction other than proteins degradation (Pickart, 2001a).. The ultimate goal of our investigation is to uncover cellular activities of Ubc13-mediated Lys63-linked polyubiquitylation in plants. Although Ubc13 alone is able to form a thiol-ester bond with Ub, the formation of Lys63-linked Ub chain requires Uev as a binding partner (Hofmann and Pickart, 1999; McKenna et al., 2001). In this study, we examined the physical interaction between AtUbc13s and Uevs from other species by two different assays and demonstrated that AtUbc13s are able to form a stable complex with Uevs from *Arabidopsis thaliana* as well as yeast and human Mms2. Although neither assay employed was quantitative, our data indicate that the cross-species Ubc13-Uev interaction is as strong as yeast and human intra-species Ubc13-Uev interactions. It is inferred that plants also utilize Ubc13-mediated Lys63-linked polyubiquitination as a means of gene regulation in one or more cellular pathways. It appears that Ubc13-mediated DNA damage tolerance function is conserved from yeast to mammals (Andersen et al., 2005). Thus, in this study it was determined whether *AtUBC13* genes were able to functionally replace the corresponding yeast gene's cellular activity. Indeed, expression of AtUbc13 in the null yeast *ubc13* mutant fully restored the wild type *UBC13* activity, including resistance to DNA damaging agents and suppression of spontaneous mutagenesis. Since these are characteristic DNA damage tolerance phenotypes, these results suggest that

AtUBC13 may play the same role in its own host cells. Future functional analyses may prove that *AtUBC13* genes play crucial roles in maintaining genome stability in plants like their counterparts in other eukaryotes.

Data presented in this thesis indicate that *Arabidopsis thaliana* contains two highly conserved and likely duplicated *UBC13* genes encoding nearly identical proteins. AtUbc13 is evolutionarily conserved with Ubc13 from all other eukaryotic organisms, from yeast to human, with a minimum of 66% sequence identity and the conservation of all known functional sequence motifs. Furthermore, even certain intron–exon borders for *UBC13*s from distant organisms are also conserved, indicating that *UBC13* is likely an ancient gene with housekeeping functions. Indeed, *AtUBC13* appears to be expressed at a relatively equal level in all tissues examined. In comparison, the *UBC13* transcript level in human tissues fluctuates dramatically; for example, it is extremely high in heart, skeletal muscle, and testis and relatively low in other tissues examined (Yamaguchi et al., 1996). The difference of *AtUBC13* and *hUBC13* in tissue distribution suggests that Ubc13 may have different functions in different organisms. It should be noted that the Northern hybridization using *AtUBC13A* ORF as a probe is unable to distinguish between *AtUBC13A* and *AtUBC13B* transcripts; hence, in this experiment, total *AtUBC13* transcripts were measured and we cannot rule out the possibility that *AtUBC13A* and *AtUBC13B* have differential expression patterns, given that their promoter sequences appear to be rather different. Ubiquitination in general and Ubc13-mediated polyubiquitination in particular appear to be primarily involved in environmental stress responses. In yeast, *UBC13* expression is DNA damage-inducible (Brusky et al., 2000). In mammalian cells, the Ubc13-Uev complex functions in TRAF6-mediated stress response

pathways following activation by proinflammatory cytokines (Deng et al., 2000; Wang et al., 2001), as well as bacterial and viral infections (Zhou et al., 2004; Andersen et al., 2005). It was found that both *AtUBC13* transcript levels remain relatively constant under stresses such as high salt, osmotic pressure, cold temperature, hormone, and DNA damage. This result can be interpreted in several ways. Firstly, *AtUBC13* may be induced by reagents not included in my experiments, or by treatment conditions different from those described in this study. Secondly, *AtUBC13* transcripts may be constant while the gene product is subjected to post-translational regulation. Thirdly, *AtUBC13* may be adapted to housekeeping functions because its expression is very stable in different tissues and stress conditions tested. Lastly, the AtUbc13 protein level may be unaffected, but its activity is altered by its binding partners such as Uev, which is absolutely required for Ubc13-mediated Lys63-linked polyubiquitination (Hofmann and Pickart, 1999; McKenna et al., 2001) and may direct Ubc13 to different cellular functions (Andersen et al., 2005).

4.3.2 Functions of Lys63-linked polyubiquitination in plants

Among ubiquitin conjugating enzymes (E2s or Ubcs), Ubc13 is unique because it can promote Lys63-linked polyubiquitination, which is believed to serve in cellular signalling. In yeast and mammalian cells, Ubc13-mediated Lys63-linked polyubiquitination has been shown to function in DNA damage tolerance and NF-κB activation as well as some other less defined pathways including stress response (Arnason and Ellison, 1994), mitochondrial inheritance (Fisk and Yaffe, 1999), plasma membrane protein endocytosis (Galan and Haguenauer-Tsapis, 1997), ribosome function (Spence et

al., 2000), innate immunity (Deng et al., 2000; Wang et al., 2001; Zhou et al., 2004), and mitotic cell cycle checkpoint (Bothos et al., 2003). In *Arabidopsis thaliana*, Ubc13 and E3 RGLG-mediated Lys63-linked polyubiquitination plays a role in regulating apical dominance (Yin et al., 2007). The present studies showed that *Arabidopsis thaliana* Ubc13 forms a complex with Uev1D, promotes Lys63-linked polyubiquitination and is involved in DNA damage response Wen et al., 2008). To date these are the only two known reports concerning the Lys63-linked polyubiquitination in plants. The essential role of Ubc13 in mammals is implied by the mouse embryonic lethality from *Ubc13* deletion, which hampers its further genetic analysis. *Arabidopsis thaliana* contains two highly conserved *UBC13* genes. We created and surprisingly found that mutant plants with both *UBC13* genes inactivated are still viable and fertile. Nevertheless the homozygous double mutant plants display a number of altered phenotypes compared with wild-type or single mutants. The double mutant plants were delayed in seed germination, as well as cotyledon and true leaf development. In particular, the *ubc13* null mutant developed shorter and distorted roots. In addition, the number of lateral roots is also reduced significantly. It is well known that auxin plays an important role in root hair and lateral root formation. In plants, lateral root (LR) formation is essential for the root architecture. LRs originate from the pericycle which is located in the parent roots. When there is no auxin signal in the pericycle cells, the ARF:Aux/IAA dimer transcription is repressed, and auxin-inducible genes can be expressed (Leyser, 2006). When auxin signal is present in the pericycle cells, it is captured and lateral root can be initiated (Leyser, 2006). The phenotypes *Arabidopsis thaliana ubc13* displayed implicate that Ubc13 mediated Lys63-linked polyubquitination plays pleiotropic roles in plants. Based on our

data, we propose that the specific E2-E3 interaction between Ubc13 and unknown E3s promotes Lys63-linked polyubiquitination of a number of yet unidentified target proteins that is required to mediate different cellular processes in plants.

CHAPTER FIVE

CONCLUSIONS AND FUTURE DIRECTIONS

5.1 Summary and conclusions

In this study, we cloned and functionally characterized two *Arabidopsis thaliana* *UBC13* genes *AtUBC13A* and *AtUBC13B* and four *UEV1* genes *AtUEV1A*, *AtUEV1B*, *AtUEV1C,* and *AtUEV1D*. These genes appear to express ubiquitously in most tissues and are not induced by various conditions tested. Biochemical, biological, and genetic studies of these genes indicate that certain AtUbc13-AtUev1 complexes promote Lys63 linked polyubiquitination and play important roles in plant development and DNA damage tolerance. Several conclusions are drawn from this study: 1) Ubc13 and Uev1 are highly evolutionarily conserved from yeast, human to plants; 2) AtUbc13 and AtUev1 form a stable complex and mediate Lys63–linked polyubiquitination; 3) AtUbc13 and AtUev1 can functionally complement yeast *ubc13* and *mms2* null mutants, respectively, in the error-free pathway of PRR; 4) AtUbc13-AtUev1D mediated polyubiquitination is involved in error-free DNA tolerance pathway in plants; 5) AtUbc13 double mutants are viable and fertile but display altered phenotypes, indicating that Ubc13-mediated Lys63-linked polyubquitination is involved in other development pathway.

5.2 Future directions

5.2.1 Functional studies of AtUbc13 using RNA interference

RNA interference (RNAi) is a phenomenon of gene silencing at the mRNA level. It offers a quick and easy way to down-regulate the expression of a gene or a group of highly related genes. In order to provide independent evidence that the phenotype of the double mutant plants is the result of *AtUBC13* down-regulation and to understand the relationship between the phenotype and the level of AtUbc13 protein, AtUbc13 RNAi construct was prepared, and a set of lines with different levels of AtUbc13 protein (WT, single mutants, and RNAi lines) have been obtained. The RNAi plants with AtUbc13 protein levels between single mutants and the double mutant will be used to examine the relationship between the level of AtUbc13 and tolerance to DNA damage in plants. One of criteria for selecting the lines is that they are similar to the wild type plant in seed germination and seedling growth when the analysis is conducted. These lines will be used to determine the tolerance to DNA damage induced by MMS and UV. Detection of mono- and poly-ubiquitinated PCNA in wild type and the above mutant plants through an immuno-precipitation method will be conducted.

5.2.2 Characterization and functional studies of *Atubc13* double mutant plants

Atubc13 double mutant plants will be analyzed to fully characterize their phenotypes. Previous observations were conducted at various stages of plant growth and development. Further analyses will include the responses of the double mutant to biotic or abiotic stresses and particularly to hormonal treatments. The altered phenotypes will be

carefully examined and the underlying molecular mechanisms will be further investigated.

5.3 Identification of possible E3 ligases

Ubiquitination is accomplished via a cascade of enzymatic steps which include Ub, E1, E2, and E3 (Hochstrasser 1996). Ubc13 is the only known E2 enzyme and has the capability to catalyze Lys63-linked poly-Ub in yeast and mammalian cells, acting as a novel signal in DNA repair (Hofmann and Pickart 1999) and NF-kB activation (Deng, Wang et al. 2000).

In yeast and human, the known E3s that interact with Ubc13 are Rad5, Rad18, Shprh, Traf6, Traf2, Chfr, Chip, Rnf8, Brca1, Bard1, and Parkin. The common feature of these E3s proteins is that they all have a ring finger domain, a specialized type of Zn-finger of 40-60 residues that binds two atoms of zinc, and this domain mediates protein-protein interaction. From this study, it is known that AtUbc13 with AtUev forms a complex promoting Lys63 poly-Ub chain, functioning DNA repair pathway. But we do not know what the E3s in Arabidopsis interact with AtUbc13 or AtUev1s, therefore, identifying the E3 in *Arabidopsis thaliana* will help us to better understand the functions of Ubc13–Uev complex.

REFERENCES

Adhikari, A., Xu, M., and Chen, Z.J. (2007). Ubiquitin-mediated activation of TAK1 and IKK. Oncogene *26*, 3214-3226.

Alberts, B. (2002). Molecular Biology of the Cell.

Andersen, P.L., Xu, F., and Xiao, W. (2008). Eukaryotic DNA damage tolerance and translesion synthesis through covalent modifications of PCNA. Cell Res *18*, 162-173.

Andersen, P.L., Zhou, H., Pastushok, L., Moraes, T., McKenna, S., Ziola, B., Ellison, M.J., Dixit, V.M., and Xiao, W. (2005). Distinct regulation of Ubc13 functions by the two ubiquitin-conjugating enzyme variants Mms2 and Uev1A. J Cell Biol *170*, 745-755.

Arnason, T., and Ellison, M.J. (1994). Stress resistance in Saccharomyces cerevisiae is strongly correlated with assembly of a novel type of multiubiquitin chain. Mol Cell Biol *14*, 7876-7883.

Asada, K. (1999). [Responses to active oxygens, strong and weak lights, an overview]. Tanpakushitsu Kakusan Koso *44*, 2230-2231.

Baboshina, O.V., and Haas, A.L. (1996). Novel multiubiquitin chain linkages catalyzed by the conjugating enzymes E2EPF and RAD6 are recognized by 26 S proteasome subunit 5. J Biol Chem *271*, 2823-2831.

Bakowska, J.C., Jupille, H., Fatheddin, P., Puertollano, R., and Blackstone, C. (2007). Troyer syndrome protein spartin is mono-ubiquitinated and functions in EGF receptor trafficking. Mol Biol Cell *18*, 1683-1692.

Balajee, A.S., and Bohr, V.A. (2000). Genomic heterogeneity of nucleotide excision repair. Gene *250*, 15-30.

Ballare, C.L., Rousseau, M.C., Searles, P.S., Zaller, J.G., Giordano, C.V., Robson, T.M., Caldwell, M.M., Sala, O.E., and Scopel, A.L. (2001). Impacts of solar ultraviolet-B radiation on terrestrial ecosystems of Tierra del Fuego (southern Argentina). An overview of recent progress. J Photochem Photobiol B *62*, 67-77.

Barbour, L., and Xiao, W. (2003). Regulation of alternative replication bypass pathways at stalled replication forks and its effects on genome stability: a yeast model. Mutat Res *532*, 137-155.

Bemark, M., Khamlichi, A.A., Davies, S.L., and Neuberger, M.S. (2000). Disruption of mouse polymerase zeta (Rev3) leads to embryonic lethality and impairs blastocyst development in vitro. Curr Biol *10*, 1213-1216.

Bennetzen, J.L. (2001). Arabidopsis arrives. Nat Genet *27*, 3-5.

Bicknell, K.A., and Brooks, G. (2008). Reprogramming the cell cycle machinery to treat cardiovascular disease. Curr Opin Pharmacol *8*, 193-201.

Bienko, M., Green, C.M., Crosetto, N., Rudolf, F., Zapart, G., Coull, B., Kannouche, P., Wider, G., Peter, M., Lehmann, A.R.*, et al.* (2005). Ubiquitin-binding domains in Y-family polymerases regulate translesion synthesis. Science *310*, 1821-1824.

Blanc, G., Hokamp, K., and Wolfe, K.H. (2003). A recent polyploidy superimposed on older large-scale duplications in the Arabidopsis genome. Genome Res *13*, 137-144.

Boesch, P., Ibrahim, N., Paulus, F., Cosset, A., Tarasenko, V., and Dietrich, A. (2009). Plant mitochondria possess a short-patch base excision DNA repair pathway. Nucleic Acids Res *37*, 5690-5700.

Bonifacino, J.S., and Traub, L.M. (2003). Signals for sorting of transmembrane proteins to endosomes and lysosomes. Annu Rev Biochem *72*, 395-447.

Bonura, T., and Smith, K.C. (1975). Quantitative evidence for enzymatically-indeced DNA double-strand breaks as lethal lesions in UV irradiated pol+ and polA1 strains of E. coli K-12. Photochem Photobiol *22*, 243-248.

Bothos, J., Summers, M.K., Venere, M., Scolnick, D.M., and Halazonetis, T.D. (2003). The Chfr mitotic checkpoint protein functions with Ubc13-Mms2 to form Lys63-linked polyubiquitin chains. Oncogene *22*, 7101-7107.

Bowman, J.L. (1993). Arabidopsis: an Atlas of Mophology and Development (Berlin & New York, Springer-Verlag).

Bradford, M. (1976). A Rapid and Sensitive Method for the Quantitation of Microgram Quantities of Protein Utilizing the Principle of Protein-Dye Binding. Anal Biochem, 248-254.

Briggs, S.D., Xiao, T., Sun, Z.W., Caldwell, J.A., Shabanowitz, J., Hunt, D.F., Allis, C.D., and Strahl, B.D. (2002). Gene silencing: trans-histone regulatory pathway in chromatin. Nature *418*, 498.

Britt, A.B. (1996). Dna Damage And Repair In Plants. Annu Rev Plant Physiol Plant Mol Biol *47*, 75-100.

Britt, A.B. (1999). Molecular genetics of DNA repair in higher plants. Trends Plant Sci *4*, 20-25.

Broomfield, S., Chow, B.L., and Xiao, W. (1998). MMS2, encoding a ubiquitin-conjugating-enzyme-like protein, is a member of the yeast error-free postreplication repair pathway. Proc Natl Acad Sci U S A *95*, 5678-5683.

Broomfield, S., Hryciw, T., and Xiao, W. (2001). DNA postreplication repair and mutagenesis in Saccharomyces cerevisiae. Mutat Res *486*, 167-184.
Brusky, J., Zhu, Y., and Xiao, W. (2000). UBC13, a DNA-damage-inducible gene, is a member of the error-free postreplication repair pathway in Saccharomyces cerevisiae. Curr Genet *37*, 168-174.

Callis, J., Carpenter, T., Sun, C.W., and Vierstra, R.D. (1995). Structure and evolution of genes encoding polyubiquitin and ubiquitin-like proteins in Arabidopsis thaliana ecotype Columbia. Genetics *139*, 921-939.

Chen, I.P., Mannuss, A., Orel, N., Heitzeberg, F., and Puchta, H. (2008). A homolog of ScRAD5 is involved in DNA repair and homologous recombination in Arabidopsis. Plant Physiol *146*, 1786-1796.

Cook, J.C., and Chock, P.B. (1992). Isoforms of mammalian ubiquitin-activating enzyme. J Biol Chem *267*, 24315-24321.

Cook, W.J., Jeffrey, L.C., Carson, M., Chen, Z., and Pickart, C.M. (1992). Structure of a diubiquitin conjugate and a model for interaction with ubiquitin conjugating enzyme (E2). J Biol Chem *267*, 16467-16471.

Curtis, M.J., and Hays, J.B. (2007). Tolerance of dividing cells to replication stress in UVB-irradiated Arabidopsis roots: requirements for DNA translesion polymerases eta and zeta. DNA Repair (Amst) *6*, 1341-1358.

Czechowski, T., Stitt, M., Altmann, T., Udvardi, M.K., and Scheible, W.R. (2005). Genome-wide identification and testing of superior reference genes for transcript normalization in Arabidopsis. Plant Physiol *139*, 5-17.

Dany, A.L., Douki, T., Triantaphylides, C., and Cadet, J. (2001). Repair of the main UV-induced thymine dimeric lesions within Arabidopsis thaliana DNA: evidence for the major involvement of photoreactivation pathways. J Photochem Photobiol B *65*, 127-135.

Deng, L., Wang, C., Spencer, E., Yang, L., Braun, A., You, J., Slaughter, C., Pickart, C., and Chen, Z.J. (2000). Activation of the IkappaB kinase complex by TRAF6 requires a dimeric ubiquitin-conjugating enzyme complex and a unique polyubiquitin chain. Cell *103*, 351-361.

Di Fiore, P.P., Polo, S., and Hofmann, K. (2003). When ubiquitin meets ubiquitin receptors: a signalling connection. Nat Rev Mol Cell Biol *4*, 491-497.

Dikic, I. (2003). Mechanisms controlling EGF receptor endocytosis and degradation. Biochem Soc Trans *31*, 1178-1181.

Doherty, A.J., and Jackson, S.P. (2001). DNA repair: how Ku makes ends meet. Curr Biol *11*, R920-924.

Dorval, V., and Fraser, P.E. (2007). SUMO on the road to neurodegeneration. Biochim Biophys Acta *1773*, 694-706.

Doss-Pepe, E.W., Chen, L., and Madura, K. (2005). {alpha}-Synuclein and Parkin Contribute to the Assembly of Ubiquitin Lysine 63-linked Multiubiquitin Chains. J Biol Chem *280*, 16619-16624.

Eddins, M.J., Carlile, C.M., Gomez, K.M., Pickart, C.M., and Wolberger, C. (2006). Mms2-Ubc13 covalently bound to ubiquitin reveals the structural basis of linkage-specific polyubiquitin chain formation. Nat Struct Mol Biol *13*, 915-920.

Edwards, K., Johnstone, C., and Thompson, C. (1991). A simple and rapid method for the preparation of plant genomic DNA for PCR analysis. Nucleic Acids Res *19*, 1349.

Esposito, G., Texido, G., Betz, U.A., Gu, H., Muller, W., Klein, U., and Rajewsky, K. (2000). Mice reconstituted with DNA polymerase beta-deficient fetal liver cells are able to mount a T cell-dependent immune response and mutate their Ig genes normally. Proc Natl Acad Sci U S A *97*, 1166-1171.

Eytan, E., Ganoth, D., Armon, T., and Hershko, A. (1989). ATP-dependent incorporation of 20S protease into the 26S complex that degrades proteins conjugated to ubiquitin. Proc Natl Acad Sci U S A *86*, 7751-7755.

Fan, L.M., Wang, Y.F., Wang, H., and Wu, W.H. (2001). In vitro Arabidopsis pollen germination and characterization of the inward potassium currents in Arabidopsis pollen grain protoplasts. J Exp Bot *52*, 1603-1614.

Fei, H., Zhang, R., Pharis, R.P., and Sawhney, V.K. (2004). Pleiotropic effects of the male sterile33 (ms33) mutation in Arabidopsis are associated with modifications in endogenous gibberellins, indole-3-acetic acid and abscisic acid. Planta *219*, 649-660.

Feldmann, E., Schmiemann, V., Goedecke, W., Reichenberger, S., and Pfeiffer, P. (2000). DNA double-strand break repair in cell-free extracts from Ku80-deficient cells: implications for Ku serving as an alignment factor in non-homologous DNA end joining. Nucleic Acids Res *28*, 2585-2596.

Fields, S., and Song, O. (1989). A novel genetic system to detect protein-protein interactions. Nature *340*, 245-246.

Finley, D., Bartel, B., and Varshavsky, A. (1989). The tails of ubiquitin precursors are ribosomal proteins whose fusion to ubiquitin facilitates ribosome biogenesis. Nature *338*, 394-401.

Fisk, H.A., and Yaffe, M.P. (1999). A role for ubiquitination in mitochondrial inheritance in Saccharomyces cerevisiae. J Cell Biol *145*, 1199-1208.

Fortini, P., Parlanti, E., Sidorkina, O.M., Laval, J., and Dogliotti, E. (1999). The type of DNA glycosylase determines the base excision repair pathway in mammalian cells. J Biol Chem *274*, 15230-15236.

Franko, J., Ashley, C., and Xiao, W. (2001). Molecular cloning and functional characterization of two murine cDNAs which encode Ubc variants involved in DNA repair and mutagenesis. Biochim Biophys Acta *1519*, 70-77.

Friedberg, E.C. (2005). Suffering in silence: the tolerance of DNA damage. Nat Rev Mol Cell Biol *6*, 943-953.

Friedberg, E.C., Aguilera, A., Gellert, M., Hanawalt, P.C., Hays, J.B., Lehmann, A.R., Lindahl, T., Lowndes, N., Sarasin, A., and Wood, R.D. (2006a). DNA repair: from molecular mechanism to human disease. DNA Repair (Amst) *5*, 986-996.

Friedberg, E.C., Walker, G.C., Wolfram, S., Wood, R.D., Schultz, R.A., and Ellenberger, T. (2006b). DNA Repair and Mutagenesis, 2nd Edition (Washington, D.C., ASM Press).

Friedman, W.E. (1999). Expression of the cell cycle in sperm of Arabidopsis: implications for understanding patterns of gametogenesis and fertilization in plants and other eukaryotes. Development *126*, 1065-1075.

Galan, J.M., and Haguenauer-Tsapis, R. (1997). Ubiquitin lys63 is involved in ubiquitination of a yeast plasma membrane protein. Embo J *16*, 5847-5854.

Garber, K. (2002). Cancer research. Taking garbage in, tossing cancer out? Science *295*, 612-613.

Garcia-Ortiz, M.V., Ariza, R.R., Hoffman, P.D., Hays, J.B., and Roldan-Arjona, T. (2004). Arabidopsis thaliana AtPOLK encodes a DinB-like DNA polymerase that extends mispaired primer termini and is highly expressed in a variety of tissues. Plant J *39*, 84-97.

Garg, P., and Burgers, P.M. (2005). DNA polymerases that propagate the eukaryotic DNA replication fork. Crit Rev Biochem Mol Biol *40*, 115-128.

Gaudeul, M., and Till-Bottraud, I. (2004). Reproductive ecology of the endangered Alpine species Eryngium alpinum L. (Apiaceae): phenology, gene dispersal and reproductive success. Ann Bot (Lond) *93*, 711-721.

Glickman, M.H., and Ciechanover, A. (2002). The ubiquitin-proteasome proteolytic pathway: destruction for the sake of construction. Physiol Rev *82*, 373-428.

Goosen, N., and Moolenaar, G.F. (2008). Repair of UV damage in bacteria. DNA Repair (Amst) *7*, 353-379.

Gray, W.M., del Pozo, J.C., Walker, L., Hobbie, L., Risseeuw, E., Banks, T., Crosby, W.L., Yang, M., Ma, H., and Estelle, M. (1999). Identification of an SCF ubiquitin-ligase complex required for auxin response in Arabidopsis thaliana. Genes Dev *13*, 1678-1691.

Gray, W.M., Muskett, P.R., Chuang, H.W., and Parker, J.E. (2003). Arabidopsis SGT1b is required for SCF(TIR1)-mediated auxin response. Plant Cell *15*, 1310-1319.

Grilley, M., Holmes, J., Yashar, B., and Modrich, P. (1990). Mechanisms of DNA-mismatch correction. Mutat Res *236*, 253-267.

Grilley, M., Welsh, K.M., Su, S.S., and Modrich, P. (1989). Isolation and characterization of the Escherichia coli mutL gene product. J Biol Chem *264*, 1000-1004.

Grossman, S.R., Deato, M.E., Brignone, C., Chan, H.M., Kung, A.L., Tagami, H., Nakatani, Y., and Livingston, D.M. (2003). Polyubiquitination of p53 by a ubiquitin ligase activity of p300. Science *300*, 342-344.

Gupta-Rossi, N., Six, E., LeBail, O., Logeat, F., Chastagner, P., Olry, A., Israel, A., and Brou, C. (2004). Monoubiquitination and endocytosis direct gamma-secretase cleavage of activated Notch receptor. J Cell Biol *166*, 73-83.

Haber, J.E., and Heyer, W.D. (2001). The fuss about Mus81. Cell *107*, 551-554.
Haglund, K., Di Fiore, P.P., and Dikic, I. (2003a). Distinct monoubiquitin signals in receptor endocytosis. Trends Biochem Sci *28*, 598-603.

Haglund, K., Sigismund, S., Polo, S., Szymkiewicz, I., Di Fiore, P.P., and Dikic, I. (2003b). Multiple monoubiquitination of RTKs is sufficient for their endocytosis and degradation. Nat Cell Biol *5*, 461-466.

Hall, T.A. (1999). BioEdit: a user-friendly biological sequence slignment editor and analysis program for Windows 95/98/
NT. Nucl Acids Symp, 95–98.

Handley-Gearhart, P.M., Stephen, A.G., Trausch-Azar, J.S., Ciechanover, A., and Schwartz, A.L. (1994). Human ubiquitin-activating enzyme, E1. Indication of potential

nuclear and cytoplasmic subpopulations using epitope-tagged cDNA constructs. J Biol Chem *269*, 33171-33178.

Hardtke, C.S., Okamoto, H., Stoop-Myer, C., and Deng, X.W. (2002). Biochemical evidence for ubiquitin ligase activity of the Arabidopsis COP1 interacting protein 8 (CIP8). Plant J *30*, 385-394.

Harper, J.W. (2002). A phosphorylation-driven ubiquitination switch for cell-cycle control. Trends Cell Biol *12*, 104-107.

Hatakeyama, S., and Nakayama, K.I. (2003). U-box proteins as a new family of ubiquitin ligases. Biochem Biophys Res Commun *302*, 635-645.

Hays, J.B. (2002). Arabidopsis thaliana, a versatile model system for study of eukaryotic genome-maintenance functions. DNA Repair (Amst) *1*, 579-600.

Hellmann, H., and Estelle, M. (2002). Plant development: regulation by protein degradation. Science *297*, 793-797.

Hershko, A., and Ciechanover, A. (1998). The ubiquitin system. Annu Rev Biochem *67*, 425-479.

Hershko, A., Ciechanover, A., Heller, H., Haas, A.L., and Rose, I.A. (1980). Proposed role of ATP in protein breakdown: conjugation of protein with multiple chains of the polypeptide of ATP-dependent proteolysis. Proc Natl Acad Sci U S A *77*, 1783-1786.

Hicke, L. (2001). Protein regulation by monoubiquitin. Nat Rev Mol Cell Biol *2*, 195-201.

Hickson, I.D., Arthur, H.M., Bramhill, D., and Emmerson, P.T. (1983). The E. coli uvrD gene product is DNA helicase II. Mol Gen Genet *190*, 265-270.

Hill, J., Donald, K.A., and Griffiths, D.E. (1991). DMSO-enhanced whole cell yeast transformation. Nucleic Acids Res *19*, 5791.

Hochstrasser, M. (1996a). Protein degradation or regulation: Ub the judge. Cell *84*, 813-815.

Hochstrasser, M. (1996b). Ubiquitin-dependent protein degradation. Annu Rev Genet *30*, 405-439.

Hoege, C., Pfander, B., Moldovan, G.L., Pyrowolakis, G., and Jentsch, S. (2002). RAD6-dependent DNA repair is linked to modification of PCNA by ubiquitin and SUMO. Nature *419*, 135-141.

Hofmann, R.M., and Pickart, C.M. (1999). Noncanonical MMS2-encoded ubiquitin-conjugating enzyme functions in assembly of novel polyubiquitin chains for DNA repair. Cell *96*, 645-653.

Hofmann, R.M., and Pickart, C.M. (2001). In vitro assembly and recognition of Lys-63 polyubiquitin chains. J Biol Chem *276*, 27936-27943.

Hwang, C.S., Shemorry, A., and Varshavsky, A. (2010). N-terminal acetylation of cellular proteins creates specific degradation signals. Science *327*, 973-977.

Ikeda, H., and Kerppola, T.K. (2008). Lysosomal localization of ubiquitinated Jun requires multiple determinants in a lysine-27-linked polyubiquitin conjugate. Mol Biol Cell *19*, 4588-4601.

Initiative, T.A.G. (2000). Analysis of the genome sequence of the flowering plant Arabidopsis thaliana. Nature *408*, 796-815.

Iyer, R.R., Pluciennik, A., Burdett, V., and Modrich, P.L. (2006). DNA mismatch repair: functions and mechanisms. Chem Rev *106*, 302-323.

James, P., Halladay, J., and Craig, E.A. (1996). Genomic libraries and a host strain designed for highly efficient two-hybrid selection in yeast. Genetics *144*, 1425-1436.

Jentsch, S. (1992). The ubiquitin-conjugation system. Annu Rev Genet *26*, 179-207.

Jentsch, S., McGrath, J.P., and Varshavsky, A. (1987). The yeast DNA repair gene RAD6 encodes a ubiquitin-conjugating enzyme. Nature *329*, 131-134.

Johnson, E.S., Ma, P.C., Ota, I.M., and Varshavsky, A. (1995). A proteolytic pathway that recognizes ubiquitin as a degradation signal. J Biol Chem *270*, 17442-17456.

Jones, J.M., Gellert, M., and Yang, W. (2001). A Ku bridge over broken DNA. Structure *9*, 881-884.

Kalderon, D. (1996). Protein degradation: de-ubiquitinate to decide your fate. Curr Biol *6*, 662-665.

Kannouche, P.L., Wing, J., and Lehmann, A.R. (2004). Interaction of human DNA polymerase eta with monoubiquitinated PCNA: a possible mechanism for the polymerase switch in response to DNA damage. Mol Cell *14*, 491-500.

Kao, C.F., Hillyer, C., Tsukuda, T., Henry, K., Berger, S., and Osley, M.A. (2004a). Rad6 plays a role in transcriptional activation through ubiquitylation of histone H2B. Genes Dev *18*, 184-195.

Kao, C.Y., Chen, Y., Thai, P., Wachi, S., Huang, F., Kim, C., Harper, R.W., and Wu, R. (2004b). IL-17 markedly up-regulates beta-defensin-2 expression in human airway epithelium via JAK and NF-kappaB signaling pathways. J Immunol *173*, 3482-3491.

Kao, T.H., and Tsukamoto, T. (2004). The molecular and genetic bases of S-RNase-based self-incompatibility. Plant Cell *16 Suppl*, S72-83.

Karsai, A., Muller, S., Platz, S., and Hauser, M.T. (2002). Evaluation of a homemade SYBR green I reaction mixture for real-time PCR quantification of gene expression. Biotechniques *32*, 790-792, 794-796.

Kim, B.O., Liu, Y., Ruan, Y., Xu, Z.C., Schantz, L., and He, J.J. (2003). Neuropathologies in transgenic mice expressing human immunodeficiency virus type 1 Tat protein under the regulation of the astrocyte-specific glial fibrillary acidic protein promoter and doxycycline. Am J Pathol *162*, 1693-1707.

Kimura, S., Tahira, Y., Ishibashi, T., Mori, Y., Mori, T., Hashimoto, J., and Sakaguchi, K. (2004). DNA repair in higher plants; photoreactivation is the major DNA repair pathway in non-proliferating cells while excision repair (nucleotide excision repair and base excision repair) is active in proliferating cells. Nucleic Acids Res *32*, 2760-2767.

Klungland, A., and Lindahl, T. (1997). Second pathway for completion of human DNA base excision-repair: reconstitution with purified proteins and requirement for DNase IV (FEN1). Embo J *16*, 3341-3348.

Knasmuller, S., Mersch-Sundermann, V., Kevekordes, S., Darroudi, F., Huber, W.W., Hoelzl, C., Bichler, J., and Majer, B.J. (2004). Use of human-derived liver cell lines for the detection of environmental and dietary genotoxicants; current state of knowledge. Toxicology *198*, 315-328.

Kolodner, R.D., and Marsischky, G.T. (1999). Eukaryotic DNA mismatch repair. Curr Opin Genet Dev *9*, 89-96.

Koonin, E.V., Senkevich, T.G., and Dolja, V.V. (2006). The ancient Virus World and evolution of cells. Biol Direct *1*, 29.

Kraft, E., Stone, S.L., Ma, L., Su, N., Gao, Y., Lau, O.S., Deng, X.W., and Callis, J. (2005). Genome analysis and functional characterization of the E2 and RING-type E3 ligase ubiquitination enzymes of Arabidopsis. Plant Physiol *139*, 1597-1611.

Krokan, H.E., Standal, R., and Slupphaug, G. (1997). DNA glycosylases in the base excision repair of DNA. Biochem J *325 (Pt 1)*, 1-16.

Kuhlbrodt, K., Mouysset, J., and Hoppe, T. (2005). Orchestra for assembly and fate of polyubiquitin chains. Essays Biochem *41*, 1-14.

Kunz, B.A., and Xiao, W. (2007). DNA damage tolerance in plants via translesion synthesis. Genes, Genomes & Genomics *1*, 89-99.

Laine, A., Topisirovic, I., Zhai, D., Reed, J.C., Borden, K.L., and Ronai, Z. (2006). Regulation of p53 localization and activity by Ubc13. Mol Cell Biol *26*, 8901-8913.

Leyser, O. (2006). Dynamic integration of auxin transport and signalling. Curr Biol *16*, R424-433.

Liang, F., and Jasin, M. (1996). Ku80-deficient cells exhibit excess degradation of extrachromosomal DNA. J Biol Chem *271*, 14405-14411.

Lindahl, T., Sedgwick, B., Sekiguchi, M., and Nakabeppu, Y. (1988). Regulation and expression of the adaptive response to alkylating agents. Annu Rev Biochem *57*, 133-157.

London, M.K., Keck, B.I., Ramos, P.C., and Dohmen, R.J. (2004). Regulatory mechanisms controlling biogenesis of ubiquitin and the proteasome. FEBS Lett *567*, 259-264.

Luca, F.C., and Ruderman, J.V. (1989). Control of programmed cyclin destruction in a cell-free system. J Cell Biol *109*, 1895-1909.

Luft, F.C. (2009). Preliminary comments on proteasome inhibition and cardiovascular disease. J Mol Med *87*, 749-751.

Maniatis, T., Fritsch, E. F. & Sambrook, J. (1982). *Molecular Cloning, A Laboratory Manual*.

Marinus, M.G., and Morris, N.R. (1975). Pleiotropic effects of a DNA adenine methylation mutation (dam-3) in Escherichia coli K12. Mutat Res *28*, 15-26.

Marti, T.M., Kunz, C., and Fleck, O. (2002). DNA mismatch repair and mutation avoidance pathways. J Cell Physiol *191*, 28-41.

McGrath, J.P., Jentsch, S., and Varshavsky, A. (1991). UBA 1: an essential yeast gene encoding ubiquitin-activating enzyme. Embo J *10*, 227-236.

McKenna, S., Moraes, T., Pastushok, L., Ptak, C., Xiao, W., Spyracopoulos, L., and Ellison, M.J. (2003). An NMR-based model of the ubiquitin-bound human ubiquitin conjugation complex Mms2.Ubc13. The structural basis for lysine 63 chain catalysis. J Biol Chem *278*, 13151-13158.

McKenna, S., Spyracopoulos, L., Moraes, T., Pastushok, L., Ptak, C., Xiao, W., and Ellison, M.J. (2001). Noncovalent interaction between ubiquitin and the human DNA

repair protein Mms2 is required for Ubc13-mediated polyubiquitination. J Biol Chem *276*, 40120-40126.

Meinnel, T., Peynot, P., and Giglione, C. (2005). Processed N-termini of mature proteins in higher eukaryotes and their major contribution to dynamic proteomics. Biochimie *87*, 701-712.

Mellon, I., and Hanawalt, P.C. (1989). Induction of the Escherichia coli lactose operon selectively increases repair of its transcribed DNA strand. Nature *342*, 95-98.

Modrich, P., and Lahue, R. (1996). Mismatch repair in replication fidelity, genetic recombination, and cancer biology. Annu Rev Biochem *65*, 101-133.

Morris, J.R., and Solomon, E. (2004). BRCA1 : BARD1 induces the formation of conjugated ubiquitin structures, dependent on K6 of ubiquitin, in cells during DNA replication and repair. Hum Mol Genet *13*, 807-817.

Mosesson, Y., Shtiegman, K., Katz, M., Zwang, Y., Vereb, G., Szollosi, J., and Yarden, Y. (2003). Endocytosis of receptor tyrosine kinases is driven by monoubiquitylation, not polyubiquitylation. J Biol Chem *278*, 21323-21326.

Muller, C.W., and Harrison, S.C. (1995). The structure of the NF-kappa B p50:DNA-complex: a starting point for analyzing the Rel family. FEBS Lett *369*, 113-117.

Myung, K., and Kolodner, R.D. (2003). Induction of genome instability by DNA damage in Saccharomyces cerevisiae. DNA Repair (Amst) *2*, 243-258.

Okumura, F., Hatakeyama, S., Matsumoto, M., Kamura, T., and Nakayama, K.I. (2004). Functional regulation of FEZ1 by the U-box-type ubiquitin ligase E4B contributes to neuritogenesis. J Biol Chem *279*, 53533-53543.

Orr-Weaver, T.L., and Szostak, J.W. (1983). Yeast recombination: the association between double-strand gap repair and crossing-over. Proc Natl Acad Sci U S A *80*, 4417-4421.

Ozkaynak, E., Finley, D., Solomon, M.J., and Varshavsky, A. (1987). The yeast ubiquitin genes: a family of natural gene fusions. Embo J *6*, 1429-1439.

Pang, Q., and Hays, J.B. (1991). UV-B-Inducible and Temperature-Sensitive Photoreactivation of Cyclobutane Pyrimidine Dimers in Arabidopsis thaliana. Plant Physiol *95*, 536-543.

Papouli, E., Chen, S., Davies, A.A., Huttner, D., Krejci, L., Sung, P., and Ulrich, H.D. (2005). Crosstalk between SUMO and ubiquitin on PCNA is mediated by recruitment of the helicase Srs2p. Mol Cell *19*, 123-133.

Paques, F., and Haber, J.E. (1999). Multiple pathways of recombination induced by double-strand breaks in Saccharomyces cerevisiae. Microbiol Mol Biol Rev *63*, 349-404.

Parker, B.O., and Marinus, M.G. (1992). Repair of DNA heteroduplexes containing small heterologous sequences in Escherichia coli. Proc Natl Acad Sci U S A *89*, 1730-1734.

Pastushok, L., Moraes, T.F., Ellison, M.J., and Xiao, W. (2005). A single Mms2 "key" residue insertion into a Ubc13 pocket determines the interface specificity of a human Lys63 ubiquitin conjugation complex. J Biol Chem *280*, 17891-17900.

Pastushok, L., Spyracopoulos, L., and Xiao, W. (2007). Two Mms2 residues cooperatively interact with ubiquitin and are critical for Lys63 polyubiquitination in vitro and in vivo. FEBS Lett *581*, 5343-5348.

Pastushok, L., and Xiao, W. (2004). DNA postreplication repair modulated by ubiquitination and sumoylation. Adv Protein Chem *69*, 279-306.

Pellicer, A., Robins, D., Wold, B., Sweet, R., Jackson, J., Lowy, I., Roberts, J.M., Sim, G.K., Silverstein, S., and Axel, R. (1980). Altering genotype and phenotype by DNA-mediated gene transfer. Science *209*, 1414-1422.

Peng, J., Schwartz, D., Elias, J.E., Thoreen, C.C., Cheng, D., Marsischky, G., Roelofs, J., Finley, D., and Gygi, S.P. (2003). A proteomics approach to understanding protein ubiquitination. Nat Biotechnol *21*, 921-926.

Perucho, M., Hanahan, D., and Wigler, M. (1980). Genetic and physical linkage of exogenous sequences in transformed cells. Cell *22*, 309-317.

Peters, J.M., Franke, W.W., and Kleinschmidt, J.A. (1994). Distinct 19 S and 20 S subcomplexes of the 26 S proteasome and their distribution in the nucleus and the cytoplasm. J Biol Chem *269*, 7709-7718.

Pfander, B., Moldovan, G.L., Sacher, M., Hoege, C., and Jentsch, S. (2005). SUMO-modified PCNA recruits Srs2 to prevent recombination during S phase. Nature *436*, 428-433.

Pfeiffer, P. (1998). The mutagenic potential of DNA double-strand break repair. Toxicol Lett *96-97*, 119-129.

Pfeiffer, P., Goedecke, W., and Obe, G. (2000). Mechanisms of DNA double-strand break repair and their potential to induce chromosomal aberrations. Mutagenesis *15*, 289-302.

Phillips, E.N., Gebow, D., and Liber, H.L. (1997). Spectra of X-ray-induced and spontaneous intragenic HPRT mutations in closely related human cells differentially expressing the p53 tumor suppressor gene. Radiat Res *147*, 138-147.

Pickart, C.M. (2001a). Mechanisms underlying ubiquitination. Annu Rev Biochem *70*, 503-533.

Pickart, C.M. (2001b). Ubiquitin enters the new millennium. Mol Cell *8*, 499-504.

Pickart, C.M. (2002). DNA repair: right on target with ubiquitin. Nature *419*, 120-121.

Pickart, C.M., and Fushman, D. (2004). Polyubiquitin chains: polymeric protein signals. Curr Opin Chem Biol *8*, 610-616.

Prolla, T.A., Pang, Q., Alani, E., Kolodner, R.D., and Liskay, R.M. (1994). MLH1, PMS1, and MSH2 interactions during the initiation of DNA mismatch repair in yeast. Science *265*, 1091-1093.

Qiao, H., Wang, F., Zhao, L., Zhou, J., Lai, Z., Zhang, Y., Robbins, T.P., and Xue, Y. (2004). The F-box protein AhSLF-S2 controls the pollen function of S-RNase-based self-incompatibility. Plant Cell *16*, 2307-2322.

Randahl, H., Elliott, G.C., and Linn, S. (1988). DNA-repair reactions by purified HeLa DNA polymerases and exonucleases. J Biol Chem *263*, 12228-12234.

Rasmussen, S.R., Larsen, M.R., and Rasmussen, S.E. (1991). Covalent immobilization of DNA onto polystyrene microwells: the molecules are only bound at the 5' end. Anal Biochem *198*, 138-142.

Reenan, R.A., and Kolodner, R.D. (1992). Isolation and characterization of two Saccharomyces cerevisiae genes encoding homologs of the bacterial HexA and MutS mismatch repair proteins. Genetics *132*, 963-973.

Robson, C.N., Hall, A., Harris, A.L., and Hickson, I.D. (1988). Bleomycin and X-ray-hypersensitive Chinese hamster ovary cell mutants: genetic analysis and cross-resistance to neocarzinostatin. Mutat Res *193*, 157-165.

Rodriguez-Rojas, L.X., Garcia-Cruz, D., Mendoza-Topete, R., Barba, L.B., Barrios, M.T., Patino-Garcia, B., Lopez-Cardona, M.G., Nuno-Arana, I., Garcia-Ortiz, J.E., and Cantu, J.M. (2004). Familial iridogoniodysgenesis and skeletal anomalies: a probable new autosomal recessive disorder. Clin Genet *66*, 23-29.

Rogers, S., Wells, R., and Rechsteiner, M. (1986). Amino acid sequences common to rapidly degraded proteins: the PEST hypothesis. Science *234*, 364-368.

Rousseaux, M.C., Ballare, C.L., Giordano, C.V., Scopel, A.L., Zima, A.M., Szwarcberg-Bracchitta, M., Searles, P.S., Caldwell, M.M., and Diaz, S.B. (1999). Ozone depletion and UVB radiation: impact on plant DNA damage in southern South America. Proc Natl Acad Sci U S A *96*, 15310-15315.

Saeki, Y., Kudo, T., Sone, T., Kikuchi, Y., Yokosawa, H., Toh-e, A., and Tanaka, K. (2009). Lysine 63-linked polyubiquitin chain may serve as a targeting signal for the 26S proteasome. EMBO J *28*, 359-371.

Saffran, W.A., Ahmed, S., Bellevue, S., Pereira, G., Patrick, T., Sanchez, W., Thomas, S., Alberti, M., and Hearst, J.E. (2004). DNA repair defects channel interstrand DNA cross-links into alternate recombinational and error-prone repair pathways. J Biol Chem *279*, 36462-36469.

Sakamoto, A., Lan, V.T., Hase, Y., Shikazono, N., Matsunaga, T., and Tanaka, A. (2003). Disruption of the AtREV3 gene causes hypersensitivity to ultraviolet B light and gamma-rays in Arabidopsis: implication of the presence of a translesion synthesis mechanism in plants. Plant Cell *15*, 2042-2057.

Sancho, E., Vila, M.R., Sanchez-Pulido, L., Lozano, J.J., Paciucci, R., Nadal, M., Fox, M., Harvey, C., Bercovich, B., Loukili, N.*, et al.* (1998). Role of UEV-1, an inactive variant of the E2 ubiquitin-conjugating enzymes, in in vitro differentiation and cell cycle behavior of HT-29-M6 intestinal mucosecretory cells. Mol Cell Biol *18*, 576-589.

Santiago, M.J., Alejandre-Duran, E., and Ruiz-Rubio, M. (2006). Analysis of UV-induced mutation spectra in Escherichia coli by DNA polymerase eta from Arabidopsis thaliana. Mutat Res *601*, 51-60.

Santopietro, R., Shabalova, I., Petrovichev, N., Kozachenko, V., Zakharova, T., Pajanidi, J., Podistov, J., Chemeris, G., Sozaeva, L., Lipova, E.*, et al.* (2006). Cell cycle regulators p105, p107, Rb2/p130, E2F4, p21CIP1/WAF1, cyclin A in predicting cervical intraepithelial neoplasia, high-risk human papillomavirus infections and their outcome in women screened in three new independent states of the former Soviet Union. Cancer Epidemiol Biomarkers Prev *15*, 1250-1256.

Scheffner, M., Huibregtse, J.M., Vierstra, R.D., and Howley, P.M. (1993). The HPV-16 E6 and E6-AP complex functions as a ubiquitin-protein ligase in the ubiquitination of p53. Cell *75*, 495-505.

Schmitz-Hoerner, R., and Weissenbock, G. (2003). Contribution of phenolic compounds to the UV-B screening capacity of developing barley primary leaves in relation to DNA damage and repair under elevated UV-B levels. Phytochemistry *64*, 243-255.

Schrammeijer, B., Risseeuw, E., Pansegrau, W., Regensburg-Tuink, T.J., Crosby, W.L., and Hooykaas, P.J. (2001). Interaction of the virulence protein VirF of Agrobacterium tumefaciens with plant homologs of the yeast Skp1 protein. Curr Biol *11*, 258-262.

Schubert, U., Anton, L.C., Gibbs, J., Norbury, C.C., Yewdell, J.W., and Bennink, J.R. (2000). Rapid degradation of a large fraction of newly synthesized proteins by proteasomes. Nature *404*, 770-774.

Sekiguchi, M., and Tsuzuki, T. (2002). Oxidative nucleotide damage: consequences and prevention. Oncogene *21*, 8895-8904.

Shi, C.S., and Kehrl, J.H. (2003). Tumor necrosis factor (TNF)-induced germinal center kinase-related (GCKR) and stress-activated protein kinase (SAPK) activation depends upon the E2/E3 complex Ubc13-Uev1A/TNF receptor-associated factor 2 (TRAF2). J Biol Chem *278*, 15429-15434.

Shinohara, A., and Ogawa, T. (1995). Homologous recombination and the roles of double-strand breaks. Trends Biochem Sci *20*, 387-391.

Sidorenko, V.S., and Zharkov, D.O. (2008). [The role of glycosylases of the base excision DNA repair in pathogenesis of hereditary and infectious human diseases]. Mol Biol (Mosk) *42*, 891-903.

Smerdon, M.J., and Thoma, F. (1990). Site-specific DNA repair at the nucleosome level in a yeast minichromosome. Cell *61*, 675-684.

Smyth, D.R., Bowman, J.L., and Meyerowitz, E.M. (1990). Early flower development in Arabidopsis. Plant Cell *2*, 755-767.

Spence, J., Gali, R.R., Dittmar, G., Sherman, F., Karin, M., and Finley, D. (2000). Cell cycle-regulated modification of the ribosome by a variant multiubiquitin chain. Cell *102*, 67-76.

Stahl, A., Nilsson, S., Lundberg, P., Bhushan, S., Biverstahl, H., Moberg, P., Morisset, M., Vener, A., Maler, L., Langel, U.*, et al.* (2005). Two novel targeting peptide degrading proteases, PrePs, in mitochondria and chloroplasts, so similar and still different. J Mol Biol *349*, 847-860.

Stelter, P., and Ulrich, H.D. (2003). Control of spontaneous and damage-induced mutagenesis by SUMO and ubiquitin conjugation. Nature *425*, 188-191.

Sullivan, J.C., Kalaitzidis, D., Gilmore, T.D., and Finnerty, J.R. (2007). Rel homology domain-containing transcription factors in the cnidarian Nematostella vectensis. Dev Genes Evol *217*, 63-72.

Sullivan, M.L., Carpenter, T.B., and Vierstra, R.D. (1994). Homologues of wheat ubiquitin-conjugating enzymes--TaUBC1 and TaUBC4 are encoded by small multigene families in Arabidopsis thaliana. Plant Mol Biol *24*, 651-661.

Suzuki, G., Yanagawa, Y., Kwok, S.F., Matsui, M., and Deng, X.W. (2002). Arabidopsis COP10 is a ubiquitin-conjugating enzyme variant that acts together with COP1 and the COP9 signalosome in repressing photomorphogenesis. Genes Dev *16*, 554-559.

Sweder, K.S., and Hanawalt, P.C. (1992). Preferential repair of cyclobutane pyrimidine dimers in the transcribed strand of a gene in yeast chromosomes and plasmids is dependent on transcription. Proc Natl Acad Sci U S A *89*, 10696-10700.

Takahashi, S., Sakamoto, A., Sato, S., Kato, T., Tabata, S., and Tanaka, A. (2005). Roles of Arabidopsis AtREV1 and AtREV7 in translesion synthesis. Plant Physiol *138*, 870-881.

Tamura, K., Dudley, J., Nei, M., and Kumar, S. (2007). MEGA4: Molecular Evolutionary Genetics Analysis (MEGA) software version 4.0. Mol Biol Evol *24*, 1596-1599.

Tenno, T., Fujiwara, K., Tochio, H., Iwai, K., Morita, E.H., Hayashi, H., Murata, S., Hiroaki, H., Sato, M., Tanaka, K.*, et al.* (2004). Structural basis for distinct roles of Lys63- and Lys48-linked polyubiquitin chains. Genes Cells *9*, 865-875.

Toufighi, K., Brady, S.M., Austin, R., Ly, E., and Provart, N.J. (2005). The Botany Array Resource: e-Northerns, Expression Angling, and promoter analyses. Plant J *43*, 153-163.

Tsui, C., Raguraj, A., and Pickart, C.M. (2005). Ubiquitin binding site of the ubiquitin E2 variant (UEV) protein Mms2 is required for DNA damage tolerance in the yeast RAD6 pathway. J Biol Chem *280*, 19829-19835.

Tuteja, N., Singh, M.B., Misra, M.K., Bhalla, P.L., and Tuteja, R. (2001). Molecular mechanisms of DNA damage and repair: progress in plants. Crit Rev Biochem Mol Biol *36*, 337-397.

Ulrich, H.D., and Jentsch, S. (2000). Two RING finger proteins mediate cooperation between ubiquitin-conjugating enzymes in DNA repair. Embo J *19*, 3388-3397.

Varadan, R., Walker, O., Pickart, C., and Fushman, D. (2002). Structural properties of polyubiquitin chains in solution. J Mol Biol *324*, 637-647.

Varshavsky, A., Bachmair, A., and Finley, D. (1987). The N-end rule of selective protein turnover: mechanistic aspects and functional implications. Biochem Soc Trans *15*, 815-816.

Vicient, C.M., and Delseny, M. (1999). Isolation of total RNA from Arabidopsis thaliana seeds. Anal Biochem *268*, 412-413.

Vierstra, R.D. (2003). The ubiquitin/26S proteasome pathway, the complex last chapter in the life of many plant proteins. Trends Plant Sci *8*, 135-142.

Villalobo, E., Morin, L., Moch, C., Lescasse, R., Hanna, M., Xiao, W., and Baroin-Tourancheau, A. (2002). A homologue of CROC-1 in a ciliated protist (Sterkiella histriomuscorum) testifies to the ancient origin of the ubiquitin-conjugating enzyme variant family. Mol Biol Evol *19*, 39-48.

Vodermaier, H.C. (2004). APC/C and SCF: controlling each other and the cell cycle. Curr Biol *14*, R787-796.

Volk, S., Wang, M., and Pickart, C.M. (2005). Chemical and genetic strategies for manipulating polyubiquitin chain structure. Methods Enzymol *399*, 3-20.

Wang, C., Deng, L., Hong, M., Akkaraju, G.R., Inoue, J., and Chen, Z.J. (2001). TAK1 is a ubiquitin-dependent kinase of MKK and IKK. Nature *412*, 346-351.

Wang, H., Qi, Q., Schorr, P., Cutler, A.J., Crosby, W.L., and Fowke, L.C. (1998). ICK1, a cyclin-dependent protein kinase inhibitor from Arabidopsis thaliana interacts with both Cdc2a and CycD3, and its expression is induced by abscisic acid. Plant J *15*, 501-510.

Wang, Z., and Rossman, T.G. (1994). Isolation of DNA fragments from agarose gel by centrifugation. Nucleic Acids Res *22*, 2862-2863.

Ward, J.F. (1988). DNA damage produced by ionizing radiation in mammalian cells: identities, mechanisms of formation, and reparability. Prog Nucleic Acid Res Mol Biol *35*, 95-125.

Wegener, E., and Krappmann, D. (2008). Dynamic protein complexes regulate NF-kappaB signaling. Handb Exp Pharmacol, 237-259.

Wei, W., Ayad, N.G., Wan, Y., Zhang, G.J., Kirschner, M.W., and Kaelin, W.G., Jr. (2004). Degradation of the SCF component Skp2 in cell-cycle phase G1 by the anaphase-promoting complex. Nature *428*, 194-198.

Weissman, A.M. (2001). Themes and variations on ubiquitylation. Nat Rev Mol Cell Biol *2*, 169-178.

Wen, R., Newton, L., Li, G., Wang, H., and Xiao, W. (2006). Arabidopsis thaliana UBC13: implication of error-free DNA damage tolerance and Lys63-linked polyubiquitylation in plants. Plant Mol Biol *61*, 241-253.

Wen, R., Torres-Acosta, J.A., Pastushok, L., Lai, X., Pelzer, L., Wang, H., and Xiao, W. (2008). Arabidopsis UEV1D promotes Lysine-63-linked polyubiquitination and is involved in DNA damage response. Plant Cell *20*, 213-227.

Wester, U., Boldemann, C., Jansson, B., and Ullen, H. (1999). Population UV-dose and skin area--do sunbeds rival the sun? Health Phys *77*, 436-440.

Wilkinson, K.D. (2000). Ubiquitination and deubiquitination: targeting of proteins for degradation by the proteasome. Semin Cell Dev Biol *11*, 141-148.

Williamson, M.S., Game, J.C., and Fogel, S. (1985). Meiotic gene conversion mutants in Saccharomyces cerevisiae. I. Isolation and characterization of pms1-1 and pms1-2. Genetics *110*, 609-646.

Wilson, D.M., 3rd, and Thompson, L.H. (1997). Life without DNA repair. Proc Natl Acad Sci U S A *94*, 12754-12757.

Wittschieben, J., Shivji, M.K., Lalani, E., Jacobs, M.A., Marini, F., Gearhart, P.J., Rosewell, I., Stamp, G., and Wood, R.D. (2000). Disruption of the developmentally regulated Rev3l gene causes embryonic lethality. Curr Biol *10*, 1217-1220.

Wooff, J., Pastushok, L., Hanna, M., Fu, Y., and Xiao, W. (2004). The TRAF6 RING finger domain mediates physical interaction with Ubc13. FEBS Lett *566*, 229-233.

Xiao, B., Singh, S.P., Nanduri, B., Awasthi, Y.C., Zimniak, P., and Ji, X. (1999a). Crystal structure of a murine glutathione S-transferase in complex with a glutathione conjugate of 4-hydroxynon-2-enal in one subunit and glutathione in the other: evidence of signaling across the dimer interface. Biochemistry *38*, 11887-11894.

Xiao, W., Chow, B.L., Broomfield, S., and Hanna, M. (2000). The Saccharomyces cerevisiae RAD6 group is composed of an error-prone and two error-free postreplication repair pathways. Genetics *155*, 1633-1641.

Xiao, W., Chow, B.L., Fontanie, T., Ma, L., Bacchetti, S., Hryciw, T., and Broomfield, S. (1999b). Genetic interactions between error-prone and error-free postreplication repair pathways in Saccharomyces cerevisiae. Mutat Res *435*, 1-11.

Xiao, W., Lin, S.L., Broomfield, S., Chow, B.L., and Wei, Y.F. (1998). The products of the yeast MMS2 and two human homologs (hMMS2 and CROC-1) define a structurally and functionally conserved Ubc-like protein family. Nucleic Acids Res *26*, 3908-3914.

Xiao, W., and Samson, L. (1993). In vivo evidence for endogenous DNA alkylation damage as a source of spontaneous mutation in eukaryotic cells. Proc Natl Acad Sci U S A *90*, 2117-2121.

Xie, Q., Guo, H.S., Dallman, G., Fang, S., Weissman, A.M., and Chua, N.H. (2002). SINAT5 promotes ubiquitin-related degradation of NAC1 to attenuate auxin signals. Nature *419*, 167-170.

Xu, P., Duong, D.M., Seyfried, N.T., Cheng, D., Xie, Y., Robert, J., Rush, J., Hochstrasser, M., Finley, D., and Peng, J. (2009). Quantitative proteomics reveals the function of unconventional ubiquitin chains in proteasomal degradation. Cell *137*, 133-145.

Yamamoto, M., Okamoto, T., Takeda, K., Sato, S., Sanjo, H., Uematsu, S., Saitoh, T., Yamamoto, N., Sakurai, H., Ishii, K.J.*, et al.* (2006a). Key function for the Ubc13 E2 ubiquitin-conjugating enzyme in immune receptor signaling. Nat Immunol *7*, 962-970.

Yamamoto, M., Sato, S., Saitoh, T., Sakurai, H., Uematsu, S., Kawai, T., Ishii, K.J., Takeuchi, O., and Akira, S. (2006b). Cutting Edge: Pivotal function of Ubc13 in thymocyte TCR signaling. J Immunol *177*, 7520-7524.

Yin, X.J., Volk, S., Ljung, K., Mehlmer, N., Dolezal, K., Ditengou, F., Hanano, S., Davis, S.J., Schmelzer, E., Sandberg, G.*, et al.* (2007). Ubiquitin lysine 63 chain forming ligases regulate apical dominance in Arabidopsis. Plant Cell *19*, 1898-1911.

Zhang, H.G., Wang, J., Yang, X., Hsu, H.C., and Mountz, J.D. (2004). Regulation of apoptosis proteins in cancer cells by ubiquitin. Oncogene *23*, 2009-2015.

Zhang, J., Johnston, G., Stebler, B., and Keller, E.T. (2001). Hydrogen peroxide activates NFkappaB and the interleukin-6 promoter through NFkappaB-inducing kinase. Antioxid Redox Signal *3*, 493-504.

Zhao, D., Yu, Q., Chen, M., and Ma, H. (2001). The ASK1 gene regulates B function gene expression in cooperation with UFO and LEAFY in Arabidopsis. Development *128*, 2735-2746.

Zhou, H., Wertz, I., O'Rourke, K., Ultsch, M., Seshagiri, S., Eby, M., Xiao, W., and Dixit, V.M. (2004). Bcl10 activates the NF-kappaB pathway through ubiquitination of NEMO. Nature *427*, 167-171.

Zwirn, P., Stary, S., Luschnig, C., and Bachmair, A. (1997). Arabidopsis thaliana RAD6 homolog AtUBC2 complements UV sensitivity, but not N-end rule degradation deficiency, of Saccharomyces cerevisiae rad6 mutants. Curr Genet *32*, 309-314.